Alma Mater Studiorum · Università di Bologna

Scuola di Scienze
Dipartimento di Fisica e Astronomia
Corso di Laurea in Fisica

A Maximum Entropy Approach to Disturbed Ecosystems

Relatore:
Prof. Armando Bazzani

Presentata da:
Silvia Montagnani

Anno Accademico 2021/2022

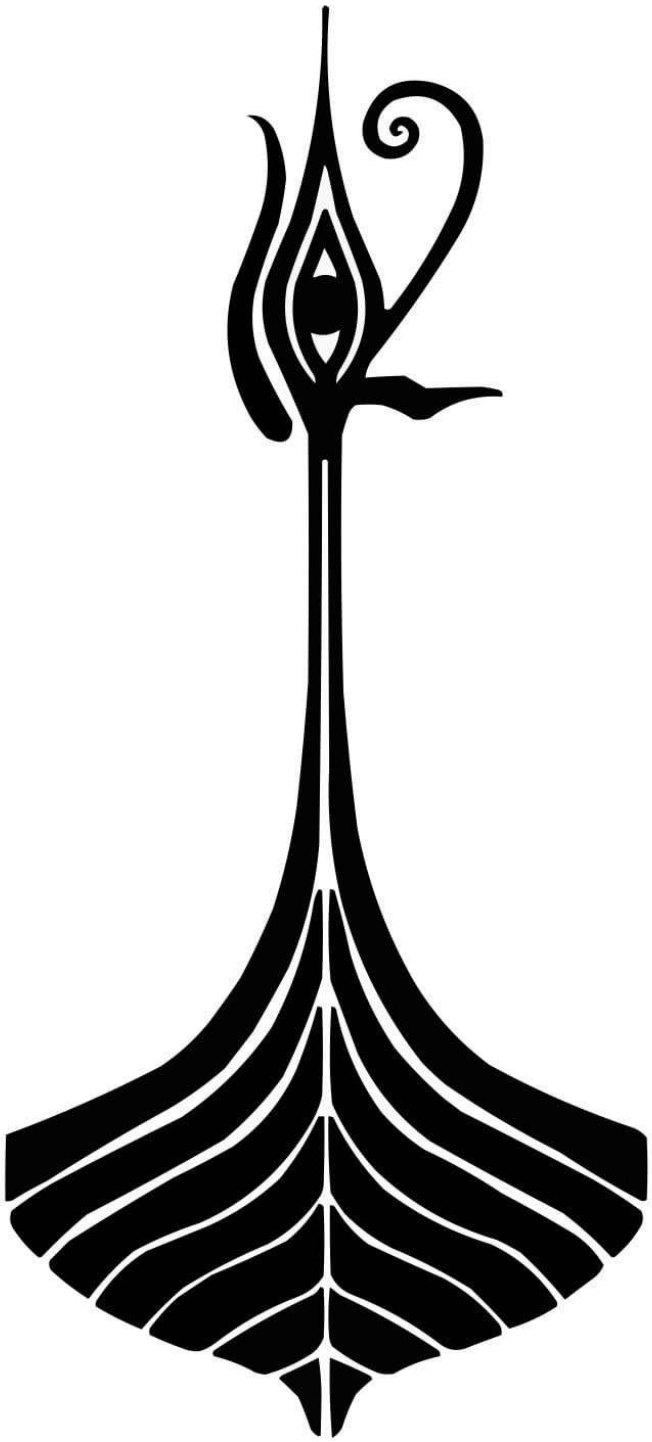

The force that through the green fuse drives the flower,
Drives my green age; that blasts the roots of trees
is my destroyer.
And I am dumb to tell the crooked rose
My youth is bent by the same wintry fever.

The force that drives the water through the rocks
Drives my red blood; that dries the mouthing streams
Turns mine to wax.
And I am dumb to mouth unto my veins
How at the mountain spring the same mouth sucks.

The hand that whirls the water in the pool
Stirs the quicksand; that ropes the blowing wind
Hauls my shroud sail.
And I am dumb to tell the hanging man
How of my clay is made the hangman's lime.

And I am dumb to tell the lover's tomb
How at my sheet goes the same crooked worm.

Dylan Thomas

To the Isua Greenstone Belt,

May your trace never vanish.

Abstract

The current climate crisis requires a comprehensive understanding of biodiversity to acknowledge how ecosystems' responses to anthropogenic disturbances may result in feedback that can either mitigate or exacerbate global warming.
Although ecosystems are dynamic and macroecological patterns change drastically in response to disturbance, dynamic macroecology has received insufficient attention and theoretical formalisation.
In this context, the maximum entropy principle (MaxEnt) could provide an effective inference procedure to study ecosystems.
Since the improper usage of entropy outside its scope often leads to misconceptions, the opening chapter will clarify its meaning by following its evolution from classical thermodynamics to information theory.
The second chapter introduces the study of ecosystems from a physicist's viewpoint. In particular, the MaxEnt Theory of Ecology (METE) will be the cornerstone of the discussion. METE predicts the shapes of macroecological metrics in relatively static ecosystems using constraints imposed by static state variables. However, in disturbed ecosystems with macroscale state variables that change rapidly over time, its predictions tend to fail.
In the final chapter, DynaMETE is therefore presented as an extension of METE from static to dynamic. By predicting how macroecological patterns are likely to change in response to perturbations, DynaMETE can contribute to a better understanding of disturbed ecosystems' fate and the improvement of conservation and management of carbon sinks, like forests.
Targeted strategies in ecosystem management are now indispensable to enhance the interdependence of human well-being and the health of ecosystems, thus avoiding climate change tipping points.

Sommario

L'attuale crisi climatica richiede uno studio esaustivo della diversità biologica per comprendere come le risposte degli ecosistemi alla forzante antropogenica possano risultare in feedback capaci di mitigare o di aggravare il riscaldamento globale.
Nonostante gli ecosistemi siano dinamici e i modelli macroecologici rivelino un'estrema sensibilità alle perturbazioni, la macroecologia dinamica sta ricevendo insufficiente attenzione e formalizzazione teorica.
In questo contesto, il principio di massima entropia (*MaxEnt*) può fornire un metodo d'inferenza efficace per studiare gli ecosistemi.
Dato che l'utilizzo del concetto di entropia, talvolta improprio al di fuori del suo contesto, conduce spesso ad incomprensioni, il capitolo d'apertura si occuperà di chiarire il significato di entropia seguendone l'evoluzione dalla termodinamica classica alla teoria dell'informazione.
Il secondo capitolo introduce allo studio degli ecosistemi dal punto di vista fisico. In particolare, la *MaxEnt Theory of Ecology* (*METE*) sarà il fulcro della presente trattazione. *METE*, imponendo restrizioni sulle variabili di stato, prevede le forme delle metriche macroecologiche in ecosistemi relativamente statici.
Le sue predizioni tendono tuttavia a fallire negli ecosistemi disturbati in quanto presentano variabili di stato che cambiano rapidamente nel tempo.
Nell'ultimo capitolo verrà dunque presentata *DynaMETE*, un'estensione dinamica della precedente teoria. Prevedendo le risposte ecologiche alle perturbazioni antropogeniche, *DynaMETE* può contribuire a comprendere la sorte degli ecosistemi disturbati e, di conseguenza, migliorare la gestione di *carbon sinks* come le foreste.
Delle strategie mirate nella gestione degli ecosistemi sono attualmente indispensabili per favorire l'interdipendenza tra il benessere umano e quello degli ecosistemi, evitando così di giungere a punti di non ritorno del cambiamento climatico.

Contents

Introduction **3**

1 What is Entropy? From Classical Thermodynamics to Information Theory and MaxEnt **5**
1.1 Entropy in Classical Thermodynamics 6
1.2 The Statistical Interpretation of Entropy 9
1.3 Shannon's Entropy and Information 12
1.4 The Principle of Maximum Entropy 15

2 Maximum Entropy and Ecology: A Theory of Abundance, Distribution and Energetics **18**
2.1 A Complex Systems Perspective on Ecological Systems 18
2.1.1 A Brief Introduction to Complex Systems 19
2.1.2 A Brief Introduction to Ecology 24
2.1.3 Ecosystems and Ecological Succession 26
2.1.4 Macroecology and Macroecological Patterns 28
2.1.5 Overview of Some Macroecological Models 39
2.2 The Maximum Entropy Theory of Ecology (METE) 43
2.2.1 Entities and Variables of State 43
2.2.2 The structure of METE 44
2.2.3 Summary of the Major Predictions of METE 51
2.2.4 Applications to Conservation Biology 53
2.3 Testing METE 54
2.3.1 A General Perspective on Theory Evaluation 54
2.3.2 Comparisons of the Predicted Distributions with Data 56
2.3.3 Patterns in The Failures of METE 58

3 DynaMETE: A Candidate Dynamic Theory of Macroecology in The Anthropocene **60**
3.1 The DynaMETE Theory's Predictions on Patterns Shifts in Perturbed Ecosystems 60
3.1.1 An Introduction and a Recall of METE 60
3.1.2 Architecture of DynaMETE 64
3.1.3 Summary of the Major Predictions of DynaMETE 69
3.1.4 Future Work 79
3.2 Ecological Feedbacks to Global Warming: The Potential Threat from Altered Vegetation Communities 81

3.2.1 The Current State of the Climate 81
3.2.2 Carbon Cycle Feedbacks in a Changing Climate 83
3.2.3 Management Strategies and Future Perspectives 86

Conclusions **89**

Appendix A **91**

Introduction

"From my youth on, my personal motto has been the old Latin tag, *Festina lente*, hurry slowly."

Italo Calvino, *Six Memos for the Next Millennium*

In Bologna, if you look up at the sky on a clear May day, you might notice tiny cotton balls floating in the air. Most likely, these are the seeds of the poplar striving to go as far away from their mother tree as possible, through a dispersion strategy refined by hundreds of millions of years of biological evolution. At the same time, you might notice that the temperature on that beautiful May day is well above the seasonal average. It may appear that the two phenomena are unrelated, yet this is not the case. Any ecology textbook will tell you that poplars typically disperse their seeds during the month of June, thus it is highly probable that the heatwave was responsible for this premature dissemination.
When examining historical graphs of the concentration of carbon dioxide in the atmosphere, an abrupt increase around the middle of the 19th century stands out instantly. Likewise, physics textbooks describe the development of classical thermodynamics as occurring during the same time period. Again, it may appear that these phenomena are utterly unrelated, yet this is not the case. The same engineers who founded thermodynamics were responsible for the technological advancements that led to the second industrial revolution and, consequently, the rise in CO2 concentrations.
The purpose of this discussion is to link the threads that connect these phenomena, thus creating a Calvinian "Ersilia" to better understand the modern world [1].
To accomplish this aim, I attempted to analyse damaged ecosystems from a thermodynamic perspective. In this context, the maximum entropy principle (MaxEnt) could provide a robust theoretical framework for studying ecosystems.
The first chapter of the dissertation will clarify the meaning of entropy by tracing its development from the thermodynamics of heat engines to information theory.
The second chapter introduces the study of ecosystems from the perspective of the physics of complex systems and the models derived from it.
The analysis will mainly focus on Professor J. Harte's "MaxEnt Theory of Ecology" (METE). By imposing limits on static state variables, METE predicts the forms of macroecological metrics in relatively static ecosystems across spatial scales, taxonomic groups, and habitats. Thus, the MaxEnt inference procedure can offer a new

approach to studying species abundance, distribution, and energetics.
However, its predictions tend to fail in disturbed ecosystems with state variables that vary rapidly over time. Therefore, in the final chapter, DynaMETE will be introduced as a dynamic expansion of METE. This dynamic macroecology theory combines explicit change mechanisms with an inference procedure that merges MaxEnt with explicit disturbance mechanisms.
DynaMETE can contribute to a better understanding of the fate of disturbed ecosystems by forecasting how macroecological patterns are expected to evolve in response to anthropogenic disturbances. This is in addition to a potential improvement in the conservation and management of carbon sinks such as forests.
As it will be explained in the last sub-chapter, these fundamental carbon sinks could regress as a result of persistent and rapid climate perturbations, thereby becoming carbon sources and triggering positive feedback that can significantly exacerbate global warming. Therefore, the implementation of targeted strategies in reforestation should be gradual but effective in the long term, thus following the natural succession of ecosystems.
Through this perspective, I wished to emphasise how the physicist's role should not be strictly limited to formal research. Since physics discoveries have the potential to reverberate through society, thus changing it, scientific research should always be followed by a strong sense of responsibility and engagement toward society.

Chapter 1

What is Entropy? From Classical Thermodynamics to Information Theory and MaxEnt

"[A law] is more impressive the greater the simplicity of its premises, the more different are the kinds of things it relates, and the more extended its range of applicability. Therefore, the deep impression that classical thermodynamics made on me. It is the only physical theory of universal content, which I am convinced, that within the framework of applicability of its basic concepts will never be overthrown."

A. Einstein, *quoted in M.J. Klein, (1967)*

Entropy is widespread in physics and plays a significant role in a wide variety of other fields, from logic and statistics to biology and economics.
However, a deeper examination reveals a more nuanced picture: entropy is defined differently in different settings, and even within the same area, many concepts of entropy are used. Certain of these are probabilistic, while others are not. The purpose of this chapter is to give an overview of the relationships between some of the most fundamental concepts of entropy.
Thermodynamics, in general, and entropy, in particular, can be approached and understood from many perspectives.
The first perspective we will cover reflects thermodynamics' origins which began with practical considerations on heat engines. Secondly, we'll discuss the concept of entropy as defined by Boltzmann and, lastly, how it can be generalized as Shannon's measure of information (SMI). This final concept is particularly relevant concerning the definition of entropy. Indeed, the ability to derive thermodynamic entropy from SMI provides a robust and well-established interpretation of entropy. Lastly, the principle of maximum entropy (MaxEnt), which is an offspring of information theory, will be illustrated.

1.1 Entropy in Classical Thermodynamics

Adam Smith published "Wealth of Nations" in 1776, seven years after James Watt (1736–1819) received a patent for his steam engine design (Fig. 1.1). Both were employed at the University of Glasgow. Nonetheless, Adam Smith's publication stated that coal's sole purpose was to provide heat for workers.

The eighteenth-century devices were propelled by wind, water, and animals. Although nearly 2000 years had passed since Hero of Alexandria used steam to spin a sphere, the capacity of fire to generate motion and power devices remained a mystery. Adam Smith (1723–1790) did not regard coal as a source of hidden wealth for nations.

The steam engine, on the other hand, opened new doors. Not only it was the invention that converted heat to mechanical motion, catalysing the Industrial Revolution, but it was also the invention that gave birth to thermodynamics as a science [2]. Unlike Newtonian mechanics, which began with ideas about the motion of celestial bodies, thermodynamics evolved from a more practical concern: the power of heat to generate motion.

With time, thermodynamics developed into a theory that quantifies macroscopic variables such as temperature, pressure, and volume, in order to describe processes such as heat transfer between two bodies or gas diffusion.

Thermodynamics is founded on two fundamental laws, the First Law of Thermodynamics and the Second Law of Thermodynamics, which deal with energy and entropy, respectively.

Traditionally, Sadi Carnot (1796-1832) is credited with discovering the Second Law. Although Carnot did not formulate the Second Law, his work laid the groundwork for its formulation by Clausius and Kelvin a few years later [3]. Carnot was an engineer who worked with heat engines, which are very loosely defined as engines that convert thermal energy to mechanical work. When we heat a volume of gas, its volume increases, and we can use this gas expansion to accomplish tasks such as lifting a weight placed on a piston from a lower level to a higher level. The weight can then be unloaded and the gas allowed to cool to its original temperature. It is possible to repeat the heating, expansion, cooling, and compression sequence. If we strictly adhere to the First Law of Thermodynamics (the Law of Energy Conservation), this principle of energy transition between different forms of energy would be unconstrained. This is unquestionably true for the conversion of work to heat: regardless of its temperature, a body can always be heated by friction, resulting in the same amount of energy in the form of heat as the work performed. On the other hand, electrical energy can always be converted to heat by passing an electric current through a resistance. However, the conversion of heat into work is severely constrained. If this were not the case, it would be possible to develop a machine capable of converting heat from its surroundings into work by cooling the surrounding bodies. Due to the virtually limitless supply of thermal energy contained in the soil, water, and atmosphere, this machine is nearly identical to a perpetuum mobile and is thus referred to as a perpetuum mobile of the second kind. The Second Law of Thermodynamics precludes the manufacture of a second-type perpetuum mobile.

To provide a more precise definition of the law stated previously, we will define

what a source of heat at a specified temperature is. A body that is constantly at temperature T and is sufficiently conditioned to exchange heat with its surroundings, without making work, is referred to as a source of heat at temperature T. This definition enables us to comprehend Lord Kelvin's following postulate:
"A transformation whose sole purpose is to convert heat extracted from a constant temperature source into work heat is impossible."
Lord Kelvin's postulate is critical in that the process must conclude with the conversion of heat to work. Indeed, converting into work heat taken from a source all at one temperature is not impossible, provided some other changes in the state of the system occur following the operation (for example, causing a volume change).
Clausius' formulation, which can be demonstrated to be identical to the preceding one [4], states as follows:
"A transformation whose sole purpose is to transfer heat from one body to another is impossible."
Clausius' formulation essentially states that no process exists that has the net effect of transferring heat from a cold to a hot body. In other words, it is extremely rare to observe the reverse process occurring spontaneously. Of course, this direction of heat flow can be achieved by performing work on the fluid (which is the way refrigerators work).
The Second Law of Thermodynamics, therefore, introduces a further element: the distinction between reversible and irreversible transformations. An irreversible transformation is a transformation that occurs spontaneously and it indicates the transition from a state of non-equilibrium to a state of thermodynamic equilibrium.
A reversible transformation, on the other hand, is an ideal limit in which the system is led from an initial state to a final state only through thermodynamic equilibrium states. In practice, a real transformation comes closer to reversibility the more it is subdivided into successive micro-transformations, each of which introduces a negligible (but inevitable, if the transformation takes place in a finite time) element of irreversibility.
A quasistatic transformation is defined as a thermodynamic transformation that occurs extremely slowly, in such a way that the system under examination, passing from an initial equilibrium state A to a final equilibrium state B, passes through a succession of infinite equilibrium states, separated from each other by infinitesimal transformations and infinitesimal variations of the system's properties.
The Second Law has numerous formulations or manifestations. For example, if a gas in a confined volume V is allowed to expand by removing the partition, the gas will always expand completely to fill the new volume, 2V, for example. It is never observed that this process reverses spontaneously. For example, a gas occupying volume 2V will never spontaneously converge to occupy a smaller volume, V. Similarly, two distinct gases will always mix when brought together. It is extremely rare to observe the spontaneous demixing of two gases occupying the same space.
All of these processes share one characteristic. They always proceed in one direction, never in the opposite direction spontaneously. However, it was clear that all of these processes are governed by a fundamental natural law. Clausius recognised the underlying principle that underpins all of these processes: that there is some quantity that determines the direction in which events unfold, a quantity that al-

ways changes in one direction during a spontaneous process. Clausius coined the term entropy as a result of this discovery, writing:
"I prefer going to the ancient languages for the names of important scientific quantities so that they mean the same thing in all living tongues. I propose, accordingly, to call S the entropy of a body, after the Greek word "transformation". I have designedly coined the word entropy to be similar to energy, for these two quantities are so analogous in their physical significance that an analogy of denominations seems to me helpful." [5]
With this definition, the Second Law can be stated as follows: "The entropy of any spontaneous process occurring in an isolated system never decreases". This comprehensive formulation sowed the seeds of the mystery surrounding the concept of entropy, a mystery involving a quantity that did not appear to be subject to a conservation law.
Leon Cooper adds the following after quoting Clausius previous passage:
"By doing that, rather than extracting a name from the body of the current language (say: lost heat), he succeeded in coining a word that meant the same thing to everybody: nothing."
Indeed, despite the Second Law's enormous generality, several authors extended its application beyond its applicability.
In modern thermodynamics, the Second Law is summarised by the statement that there exists a state function, denoted as S and referred to as entropy, that always increases during any spontaneous process occurring in an isolated system. When the thermodynamic state of the system is defined (for example, by specifying the temperature, pressure, and volume), the entropy of the system is also defined. Thermodynamics does not explicitly state that entropy is functionally dependent on the system's parameters. Nonetheless, it provides a general procedure for calculating the difference in entropy between two states of a system, A and B. Additionally, the Clausius definition specifies the change in entropy that occurs when a small amount of heat δQ is transferred to a system at a constant temperature T:

$$dS = \frac{\delta Q}{T} \tag{1.1}$$

The system is assumed to be at equilibrium at temperature T in this definition, and a very small amount of heat δQ is added to maintain the system's temperature constant. Qualitatively, an equilibrium state can be defined as one in which all the system's parameters that define its state remain constant over time.
To summarise, thermodynamics provides a method for determining the difference in entropy between any two equilibrium states (Eq. 1.1). It does not tell us the value of a system's entropy at equilibrium. Rather, it states that such a state function exists. When the variables E (energy), N (number of particles), and V (volume) define the state of the system, the entropy function must be a monotonically increasing function of each of these variables, and it must also have a negative curvature (or be concave downward) with respect to these variables.
More broadly, the Second Law states that any process that occurs spontaneously in an isolated system and involves the system transitioning from one equilibrium state to another must result in an increase in entropy.
In conclusion, thermodynamics does not explain what entropy is or why it changes

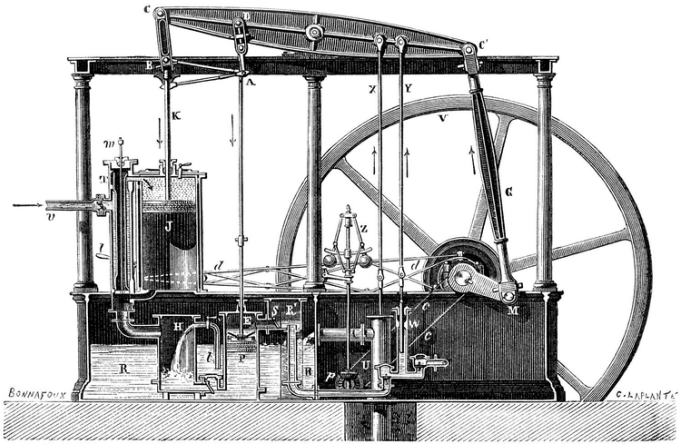

Fig. 59. — Machine à balancier de Watt.

e, Tuyau de prise de vapeur; T, tiroir; J, cylindre; H, condenseur; PE pompe d'épuisement; WY pompe alimentaire de la chaudière UX pompe d'alimentation de la bâche R; *p* Z régulateur; *dd* excentrique; ABCD parallélogramme; GM bielle et manivelle; V volant.

Figure 1.1: Watt's steam engine. (Amédée Guillemin. *La vapeur*, 1876.)

in only one direction [3]. Afterwards, it will be illustrated how the information theory derivation of entropy provides answers to both of these questions.

1.2 The Statistical Interpretation of Entropy

A considerable stride toward the understanding of entropy and the Second Law of Thermodynamics was made possible thanks to Boltzmann's statistical interpretation of entropy.
Ludwig Boltzmann (1844-1906), along with Maxwell and many others, developed what is known as the kinetic theory of gases or the kinetic theory of heat. This not only led to the identification of temperature, something which is very close to our perception, but also to the interpretation of entropy in terms of the number of states that are accessible to the system. A simple relationship between the entropy of a given state in a thermodynamical system and its probability was discovered. To understand this relationship, we will now assume, based on statistical considerations, that, in an isolated system, only those spontaneous transformations occur that lead to states with a higher probability and that the most stable state of such a system is the state with the highest probability consistent with the system's given total energy. This assumption generates a parallel between the probability W and entropy S as properties of the system, implying the presence of a functional link between them. This link is expressed by the following equation, which is also engraved on Ludwig Boltzmann's tombstone (Fig. 1.2):

$$S = k\, log(W) \tag{1.2}$$

Where k is a constant called the Boltzmann Constant and is equal to the ratio R/A of the gas constant R and the Avogadro's number A. The value of W was originally intended to be proportional to the "Wahrscheinlichkeit" (German for probability) of a macroscopic state for some probability distribution of possible microstates, the collection of (unobservable microscopic single particle) "ways" in which a system's

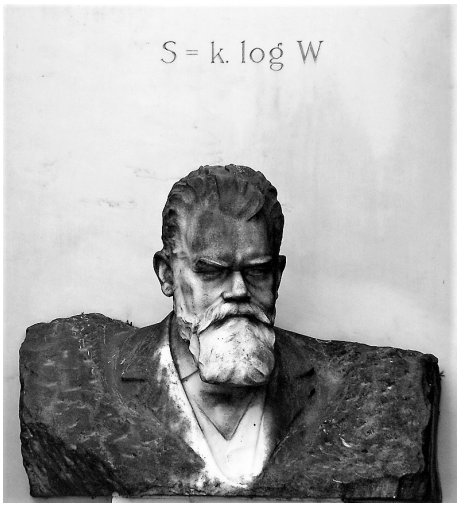

Figure 1.2: Boltzmann's tombstone in Vienna

(observable macroscopic) thermodynamic state can be obtained by assigning different positions and momenta to the respective molecules. Nonetheless, the term W is frequently misinterpreted as indicating the degree of disorder in a system. In fact, according to some popularisations of entropy, states with high entropy are perpetually "disordered," whereas those with low entropy are more organised [6]. While this is frequently true, it is not always accurate, and in any case, the concept of order is difficult to define objectively.
It is unquestionably true that when the barrier between two containers containing different gases is breached, the gases in one container expand into the other, the molecules mix, and the system becomes more disordered by any reasonable definition of order. However, the system's entropy changes as each gas expands into the doubled volume available to the molecules, not as a result of the mixing (disordering) process itself.
Furthermore, it should be noted that this relationship between entropy and state count holds only for isolated systems.
Statistical thermodynamics' first postulate remains valid only for isolated systems in which all mechanical states are equally probable.
Without going into the details [7], J. W. Gibbs (1839-1903) demonstrated the generalization of Eq. 1.2 that follows. Consider a system (often referred to as a thermodynamic system) composed of N gas molecules with a maximum energy of ϵ_i, $i = 1, ..M$. Assume that

$$p_i = \frac{n_i}{N}$$

is the percentage of molecules with energy ϵ_i. Then, using Eq. 1.2, the entropy of the system can be expressed as follows:

$$S_i = -k \sum_{i=1}^{M} p_i log(p_i) \tag{1.3}$$

The Boltzmann distribution of molecular energy levels in an ideal gas is obtained by maximising this entropy measure, subject to the constraints imposed by

$$\sum_i n_i = N \quad \text{and} \quad \sum_i n_i \epsilon_i = E$$

The underlying concept is that the probability of a system being found in a particular macrostate increases as the number of associated microstates increases. To summarise, the probabilistic formulation of the Second Law asserts that more probable macrostates are states of higher entropy because they are compatible with more microstates. Systems undergoing change are more likely to shift to more probable macrostates, not less probable ones, thereby increasing entropy [8]. Thus, thermodynamics' second law is a probabilistic proposition. This perspective was foreign to classical physics at the time, and as a result, many of Boltzmann's contemporaries criticised his formulation of the second law.

The reversibility objection's gist is that there appears to be a conflict between the so-called time reversal or time symmetry of Newtonian equations of motion and the time asymmetry of Boltzmann's entropy's behaviour.

This fundamental contradiction between the reversibility of molecular motion and the irreversibility implied by the Second Law could not be resolved at the time. It appeared impossible to derive a quantity that distinguishes between the past and the future from the equation of motion (i.e., a quantity which always increases with time). Boltzmann's response to the reversibility objection was that while the Second Law usually remains valid, in extremely rare cases, it can be reversed (i.e., entropy might decrease with time). It is extremely instructive to read what Boltzmann wrote in 1896 in response to this criticism:

"The reverse transition has a definite calculable (though inconceivably small) probability, which approaches zero only in the limiting case when the number of molecules is infinite. The fact that a closed system of a finite number of molecules, when it is initially in an ordered state and then goes over to a disordered state, finally after an inconceivably long time ($10^{10^{10}}$ years for example) must again return to the ordered state. [..] One may recognize that this is practically equivalent to never if one recalls that in this length of time, according to the laws of probability, there will have been many years in which every inhabitant of a large country committed suicide, purely by accident, on the same day, or every burned down at the same time, yet the insurance companies get along quite well by ignoring the possibility of such events. If a much smaller probability than this is not practically equivalent to impossibility, then no one can be sure that today will be followed by a night and then a day. In any case, we would rather consider the unique directionality of time given to us by experience as a mere illusion arising from our specially restricted viewpoint." [3]

Boltzmann recognised that the Second Law is not absolute and that even if it were, that would not imply that it defines the "arrow of time". This explanation was deemed unacceptable at the time, and like any other law of physics, the Second Law (nonatomic) of Thermodynamics was conceived and declared to be absolute, with no room for exceptions. Following that discovery, as a result of the Second Law's two irreconcilable interpretations, there appeared to be a state of stagnation. Regrettably, the atomic theory of matter did not gain widespread acceptance until after Boltzmann's suicide in 1906.

This paradigm shift was made possible by the discovery and development of a theory based on a phenomenon that appears to have no connection with the Second Law of Thermodynamics: the Brownian motion.
Robert Brown, an English botanist, was the first to observe the Brownian motion (1773-1858). The phenomenon is quite straightforward: when tiny particles, such as pollen particles, are suspended in water, they appear to move randomly. Initially, it was assumed that this ceaseless motion was caused by tiny living organisms propelling themselves into the liquid. Brown and colleagues demonstrated, however, that the same effect occurs when inanimate, inorganic particles are sprinkled into a liquid.
Einstein published a theory on this random motion as part of his doctoral dissertation in 1905. He asserted that if a large number of atoms or molecules jitter randomly in a liquid, fluctuations must also occur. When tiny particles are immersed in a liquid (tiny in comparison to their macroscopic size but large enough in comparison to the molecular dimensions of the liquid's molecules), they are randomly "bombarded" by the liquid's molecules. However, occasionally, there will be asymmetries in this bombardment of suspended particles, causing the tiny particles to move in a zigzag pattern.
Once experimentalists confirmed this theory, the acceptance of the atomistic view became inevitable.
Classical thermodynamics, which is entirely based on the continuous nature of matter, excludes fluctuations. Because these fluctuations are extremely small in a macroscopic piece of matter, we do not observe them. However, when small Brownian particles are used, the fluctuations are magnified and made visible.
The acceptance of matter's atomic composition coincided with the acceptance of Boltzmann's expression for entropy. It is worth noting that this definition of entropy was unaffected or modified by the two great revolutions in physics that occurred in the early twentieth century: quantum mechanics and relativity.
Boltzmann's heuristic relationship between entropy and the logarithm of the total number of states opened the way for understanding entropy's meaning.

1.3 Shannon's Entropy and Information

The third approach to the Second Law is based on Shannon's measure of information (SMI), and it may be loosely referred to as the "informational-theoretical" approach. Therefore, let's answer to what information is. Shannon devoted ten years (1939–1948), the majority of which was spent at Bell Laboratories during the wartime effort, to reflect on this notion. He did not publish a single article on the subject during this period, except a classified memorandum on cryptography in 1945. He referred to most of his work as "communication theory", not "information theory", and coined the term "uncertainty" for what became Shannon's "entropy" [9]. The term "information" or "mutual information" as a mathematical concept first appeared in Robert Fano's MIT seminars in the early 1950s. Shannon began by purposefully omitting semantic questions from the engineering task. At the start of his seminal 1948 paper (Fig. 1.3), he begins with a famous paragraph:
"The fundamental problem of communication is that of reproducing at one point

either exactly or approximately a message selected at another point. Frequently the messages have meaning; that is, they refer to or are correlated according to some system with certain physical or conceptual entities. These semantic aspects of communication are irrelevant to the engineering problem. The significant aspect is that the actual message is one selected from a set of possible messages. The system must be designed to operate for each possible selection, not just the one which will actually be chosen since this is unknown at the time of design." [10]
As a result, Shannon views the information source as a probabilistic device that chooses from a set of possible messages. Therefore, a message becomes a realisation of a stochastic process.
In brief, information is probabilistic, not semantic, according to Shannon.
Now, let's take a quantitative look. If we define a function $I(p)$ to represent the information gained from knowing something with a probability p of being "true" (remember that we are not dealing with actual augmentation of wisdom here, but rather with the conveyance of data), we obtain the following:

$$I(p) + I(p) = I(pp) \tag{1.4}$$

In other words, the product of the probabilities doubles the degree to which my uncertainty is reduced. So the solution to this equation is:

$$I(p) = klog(p) \tag{1.5}$$

Which is unique up to an overall constant k (which may be positive or negative) or, more precisely, up to an arbitrary logarithmic base.
More broadly, suppose a language contains L distinct letters and that, based on an examination of volumes of text written in that language, the letters occur at a frequency of p_i where $i = 1..L$. In a message of N letters, the ith letter of the alphabet should appear $n_i = p_i N$ times. Claude Shannon and Norbert Weiner independently demonstrated that the capacity of a language to inform, per symbol in a message, could be expressed as:

$$I_p = k \sum_{i=0}^{L} p_i log(p_i) \tag{1.6}$$

The notation I_p is used rather than $I(p)$ to reduce the amount of clutter in the following equations. Regarding Eq. 1.5, the latter equation makes sense: the information content of a collection of letters is equal to the expectation value of the information content of each letter, and the sum of p times log(p) equals that expectation value. k is chosen to be negative because we want the information to be a non-negative quantity and because $log(p) \leq 0$ if $0 \leq p \leq 1$.
Additionally, it is common practice to quantify information in terms of "bits" and consider the information content of a single binary choice to be one bit. Thus, taking $p = 1/2$, which corresponds to a binary choice such as a coin toss, you can get $klog(1/2) = 1$bit. As a consequence, it is customary to take $k = 1/log(1/2) \simeq -1.44$ in units of bits. When Eq. 1.6 is compared to the Boltzmann/Gibbs result, Eq. 1.3, and the connection between information theory and thermodynamics starts to

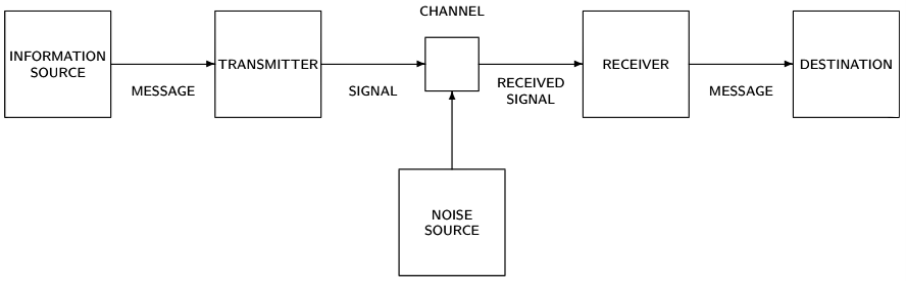

Figure 1.3: A reproduction of the schematic diagram of a general communication system, "the mother of models", from Shannon's 1948 paper. In this illustration, a source of information is transmitted over a noisy channel before being received by a recipient. For the first time the roles of source, channel and recipient, transmitter and receiver, signal and noise, were distinguished. (Source: O. Rioul, "This is IT", 2018)

become evident. The mathematics underlying the likelihood interpretation of thermodynamic entropy looks remarkably similar to the information content expression. Due to the positive value of the Boltzmann constant, thermodynamic entropy is not negative. A plausible non-negative measure of information entropy is then:

$$Information\ entropy \sim I_P \tag{1.7}$$

It is possible to become perplexed at this stage.

Previously, it was asserted that both information and information entropy are non-negative quantities. However, as discussed above, high-entropy states are those about which we know very little, states in which there are numerous microstates, and so our understanding (of which one the system is in) is relatively limited. We have very limited information regarding microstates in a high-entropy system. However, a proper definition of the term "information" resolves the issue. Equation 1.6 describes the information that a measurement can provide (i.e., knowing a person's name in a group). In a low-entropy system, such as a room with all the molecules concentrated on one side, the location of a single molecule contributes little to our prior information.

Thus, information entropy is a measure representing our uncertainty about the system's state. Notably, information entropy can be applied to any probability distribution, not only those expressing the frequency of letters in a language or the faces of a die.

Consider the likelihood that a species is randomly chosen from an ecosystem with N_0 individuals and S_0 species which have n individuals. In the following Chapter, this is referred to as the SAD $\Phi(n|S_0, N_0)$. According to Eq. 1.6, an information-theoretic measure of the distribution's information entropy is as follows:

$$I_\Phi = -\sum_{n=1}^{N_0} \Phi(n) log(\Phi(n)) \tag{1.8}$$

Because the constant preceding the summing in Eq. 1.6 is arbitrary, we can set it equal to one. The summation in Eq. 1.8 is over all possible individuals rather than over all species because by summing over n (the domain of the probability

distribution Φ), the product of (the probability of a species having n individuals) X (the information content in choosing a species with n individuals), we are effectively summing over the species.
This is analogous to how Boltzmann deduced energy distribution over molecules, in classical statistical mechanics, where an integral is calculated over all possible energy states of a molecule. To make an analogy, species are to molecules what abundances are to energy values.
In conclusion, the question of what entropy is has been answered.
In Thermodynamics, entropy is a special kind of measure of information (SMI) defined for a special set of distribution functions of macroscopic systems at equilibrium. However, we still have not answered to why this quantity increases.
The explanation is based on probability. Furthermore, it is the same answer to the question of why a system's state tends toward equilibrium: the probability of the equilibrium state is the highest.
Accepting the relative frequency interpretation, we can reach the conclusion that a system is more likely to be found in states with a higher probability. Specifically, it can be demonstrated for thermodynamic systems that the probability of equilibrium is close to one.
Thus, we can assert that a system will always evolve toward a state with a higher probability and will eventually reach the equilibrium state, whose probability is nearly one.
In other words, the tendency toward a state of a greater probability corresponds to the assertion that events that are envisaged to occur more frequently will occur more frequently. In this sense, the Second Law becomes a law of probability or common sense: a system will spend more time in states having a greater probability.
Moreover, regarding small "violations" of the Second Law, it is advisable to define the entropy function only for a system with a large number of particles at equilibrium (i.e. configurations which are near the one that maximises the SMI). In such systems, deviations from the state of equilibrium are negligible. Thus, the Second Law remains unviolated.

1.4 The Principle of Maximum Entropy

Considering some limiting examples, we can gain qualitative insight into the meaning of the "information entropy of a probability distribution" as defined in Eq. 1.8.
As a starting point, let us assume that the probability distribution Φ is uniform. As a result, any value of abundance is equally probable. Then $\Phi = 1/N_0$, and because the sum has N_0 terms, it follows:

$$I_\Phi = (N_0/N_0)log(N_0) = log(N_0)$$

Consider a situation in which Φ equals 0 or 1. In the latter case, all species have the same abundance, which is also the average abundance per species. Recalling that $xlog(x) \to 0$ as $x \to 0$, and that $log(1) = 0$, we see that $I_\Phi = 0$ when all abundances are equal. Therefore, the information entropy of a uniform probability distribution

is greater than that of a sharply peaked distribution.
Indeed, it is possible to demonstrate that information entropy is maximum when the distribution is uniform (Jaynes, 1982).
This interpretation of information entropy in Eq. 1.7 is coherent with what we previously stated. Entropy is a measure of our ignorance about the state of a system. When the probability distribution of a variable is most uniform, we know the least about it.
To avoid bias while inferring the shape of a probability distribution, we should make no assumptions about it.
This may imply that we should always assume the uniformity of unknown probability distributions:

$$P(x) = const \tag{1.9}$$

Consider the following qualitatively comparable operations for inferring the shape of an event's distribution:
(a) Maximizing our remaining uncertainty after accounting for our knowledge.
(b) Determining the most uniform distribution possible given our prior knowledge constraints.

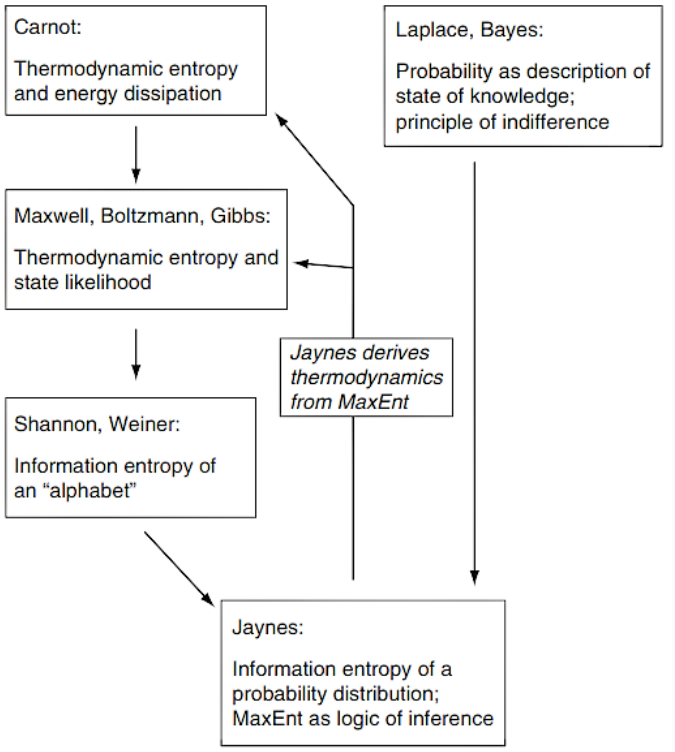

Figure 1.4: The historical context of MaxEnt

We will arrive at the least biased inference of our distribution using either of these operations. Statement (b) results in a specific mathematical procedure: maximizing information entropy subject to the constraints imposed by prior knowledge. That is what is meant by MaxEnt. The mathematical approach is referred to as the "Method of Lagrange Multipliers," described in Appendix A. It is a technique for

determining the unique functional form of probability distributions, such as $\Phi(n)$ in Eq. 1.8, that maximises $I(\Phi)$.

MaxEnt's approach, as described in Appendix A, implements the logical framework for inference to arrive at the least biassed conclusions possible in the face of uncertainty. The least biassed inference of the distribution's form is achieved by identifying the distribution with the highest information entropy that satisfies known criteria [8].

In an everyday sense, the chapter's lesson is that we may be most certain of our deductions if we embrace our ignorance completely, which includes not pretending to possess knowledge that we do not possess.

The intellectual forerunners of Jaynes' work date back to Laplace, well before Shannon and Gibbs (Fig 1.4). That physicist and mathematician, widely regarded as the greatest since Newton, grasped and utilised the concepts that underpin the MaxEnt approach to inference.

At present, thanks to its conceptual simplicity and broad applicability, the maximum entropy framework is being increasingly applied to construct descriptive and predictive models from economic to biological systems, as we shall see in the next chapter.

Chapter 2

Maximum Entropy and Ecology: A Theory of Abundance, Distribution and Energetics

2.1 A Complex Systems Perspective on Ecological Systems

"It is interesting to contemplate a tangled bank, clothed with many plants of many kinds, with birds singing on the bushes, with various insects flitting about, and with worms crawling through the damp earth, and to reflect that these elaborately constructed forms, so different from each other, and dependent upon each other in so complex a manner, have all been produced by laws acting around us. [...] And that, whilst this planet has gone circling on according to the fixed law of gravity, from so simple a beginning endless forms most beautiful and most wonderful have been and are being evolved."

C. Darwin, *The Origin of Species*

Wherever we gaze in nature, whether in a forest or a desert, we see specific patterns that reoccur. Throughout nature and culture, in fact, complex systems exhibit their emergent and repeated dynamics. Bird flocks moving in unison, the transmission of ideas, economic trends or the dynamics of an epidemic are all instances of complex macroscale events that result from fine-scale interactions at the individual level.
In many cases, even if we are interested in developing and fitting microscale dynamics models, measurements of the system are only possible at the macroscale level.
The Maximum Entropy Theory of Ecology (METE) implements the MaxEnt framework to infer probability distributions for species abundance, organism size, and spatial distributions from macroscale state variables.

2.1.1 A Brief Introduction to Complex Systems

"Clouds are not spheres, mountains are not cones, coastlines are not circles, and bark is not smooth, nor does lightning travel in a straight line. [...] Nature exhibits not simply a higher degree but an altogether different level of complexity."

Benoit B. Mandelbrot, *The Fractal Geometry of Nature*

Recently, physicists have developed a strong interest in the behaviour of complex systems. This endeavour resulted in a conceptual revolution, a paradigm shift with far-reaching implications for the foundations of physics. The study of complex systems is a relatively young discipline with interdisciplinary characteristics: consider the linkages to biology, computer science, systems theory, and ecology. Simultaneously, it is a very fashionable field, although it eludes those attempting to define it precisely.
In general, the purpose of a theory of complex systems is to discover laws governing the global behaviour of such systems, phenomenological principles that are not readily deducible from an analysis of the laws governing each of the individual constituents. Consider the following example: while the behaviour of individual neurons is presumably well understood, the reason why 10 billion neurons coupled via 100 trillion synapses form a thinking brain remains a mystery. [11]
Complex systems can be defined in a huge variety of ways. One possible definition is the following one. [12]
First, let's define the seemingly straightforward but frequently misunderstood concept of a system. A system is a collection of elements connected to one another or to the external environment via reciprocal relationships that behave as an organic, global, and organised entity.
As we shall see later, this hierarchy, architecture, and internal organisation combine to make the whole "greater than the sum of its parts", thus necessitating an analysis of the relationships between its components.
A complex system is essentially an open system composed of numerous elements that interact non-linearly and form a distinct organised, and dynamic entity capable of evolving and adapting to its environment. Let's consider the terms that have been highlighted:

- **Open**: an open system communicates with its environment via material, energy, or information flows. In computational terms, the system accepts inputs, processes them, and generates outputs. A complex system requires an ongoing supply of energy from its environment in order to grow, develop, and flourish in nature.

- **Non-linear**: Non-linear means that the output may behave irregularly when the input varies, not proportional to the input variation. When the time factor is included, the output loses not only its direct causal correlation with the input but also its temporal correlation, rendering the system unpredictable (i.e. even knowing precisely the inputs that a system receives, one cannot predict its future behaviour).

- **Organized**: The system has a hierarchical organisation, progressing in complexity.
- **Dynamic**: Dynamic implies that the structure and functions of the system are subject to temporal variation, evolving over time as a result of both internal and external changes.
- **Evolving and adapting to their environment**: Complex systems are capable of perceiving the conditions, changes, and stimuli in their environment and reacting consequentially, thus evolving.

With these premises in mind, let us attempt to dig deeper. Non-linearity in a system implies that the structure of the relationship between the elements is not a linear chain but rather a network of interconnections of processes.
A peculiarity of these networks is that through a phenomenon called “feedback", a process can influence the precedent in the sequence.
This phenomenon manifests itself in two fundamental and diametrically opposed forms: negative feedback and positive feedback.
The negative feedback contributes to a system's stability by compensating for changes in the external environment and thus assisting in the maintenance of homeostasis (i.e. the ability of an organism to regulate itself, to self-stabilise).
On the other hand, positive feedback facilitates change by increasing the possibility of divergence, growth, and the establishment of new levels of equilibrium. This occurs as a result of the cycle's ability to strengthen itself (i.e. by increasing the output). The input increases as well, which further increases the output, creating a vicious circle. Occasionally, however, positive feedback can create a cycle that is extremely difficult to break and ultimately results in the cycle's disintegration.
In contrast to complicated systems (such as large software, satellites, and laws), complex systems have the property of being resistant to these positive feedback loops. One reason underlying this mechanism is that these systems possess a property called "resilience".
In ecology, the latter term refers to an ecological system's ability to revert to its initial state after a perturbation that alters that state. This fundamental property of complex systems is augmented by another property referred to as "redundancy". This term refers to the presence of multiple elements operating concurrently in a network, which prevents a system from collapsing if a single element fails unexpectedly.
Additionally, to tolerate errors, life requires them in order to evolve. The term "error-friendliness" was coined to refer to the capacity of complex systems, particularly biological systems, to exploit errors creatively without having to minimise them.
Mutations occur as a result of errors in copying the genetic information contained in DNA, allowing a system to evolve, resulting in a great biological diversity from which natural selection can select the organisms best suited to survive and reproduce.
This adaptation is ensured by a phenomenon called "self-organisation". Despite its widespread presence in natural and artificial social systems, the mechanisms of the latter remain partially unknown. To better understand how it works, let us first

examine the organisational structure of complex systems. To begin, these have a hierarchical structure, in which the control of a system is composed of numerous elements that interact, thus allowing the formation of increasingly higher hierarchical levels. As one progresses through the levels, the combinatorial possibilities for element interaction increase exponentially. This brings us to a critical point: when does self-organisation occur in collective interactions? We can say that self-organisation occurs when a system crosses a critical complexity threshold and achieves a more complex structure through the cooperative action of several subsets. Thus, we have that the interaction of the individual elements determines the system's global and complex behaviour, which would be impossible to predict from the study of the individual components. This property, which elevates the organised whole above the sum of its constituent parts, is referred to as "emergent behaviour". The computer simulations of this kind of behaviour allow us to analyse the dynamics of complex systems such as an ecosystem, an economic market, or a brain in an effective manner.

Let's see what happens to the behaviour of complex systems when integrating the time variable as well.

A system tends to evolve spontaneously, according to the dynamics inherent in the system. This evolution tends to produce a state that is characterised by metastability or the presence of only a temporary equilibrium.

Indeed, in this state of precarious stability, referred to as the critical state, any external disturbance or natural fluctuation can have unpredictable effects on the system.

In most cases, the disturbance remains isolated and has only minor effects on the system before rapidly dissipating. However, in a few rare cases, small fluctuations cascade throughout the system, occasionally resulting in its destruction.

At this point, we shall attempt to structure this complex behaviour by describing it in terms of the "Chaos Theory", which astounded the scientific community in the 1960s. Jules Henri Poincaré (1854-1912) was the first to recognise the sensitivity of certain systems' behaviour to initial conditions, recognising that a small change could result in such a change in the subsequent evolution that long-term predictions were rendered useless. In his 1908 work, "Science and Method", he argued against all Lapalacian convictions that:

"We say that this effect is due to chance when a minor cause that escapes us determines a significant effect that we cannot ignore. If we knew the exact laws of nature and the state of the universe at the beginning, we could predict the state of the same universe at a later point in time. However, even if the laws of nature revealed no more secrets to us, we could only approximate the initial state. If this enables us to know the subsequent state with the same approximation, we will conclude that the phenomenon has been anticipated and that it is governed by laws. However, this is not always the case: small differences in the initial conditions can result in enormous differences in the final phenomena; a small error in the former can result in an enormous error in the latter. Prediction is rendered impossible; we are confronted by the phenomenon of chance" [13].

Despite this theoretical revolution, Poincaré's intuitions were too ahead for his time. As a consequence, the situation remained static for decades until, almost by chance,

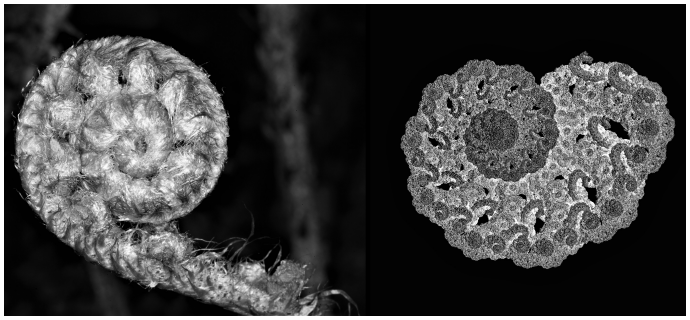

Figure 2.1: A fern frond is an example of a fractal object. It could be noted how individual branches resemble the larger fern as a whole. (Photo credits: G. Parker)

the issue resurfaced, thanks to the American meteorologist Edward Norton Lorentz (1917-2008). In 1961, Lorenz started simulating weather patterns with a rudimentary digital computer by modelling a few variables, such as temperature and wind speed. To his surprise, the machine's predictions of the weather were radically different from the prior estimate due to a rounded decimal number on the computer printout. Thus, Lorenz discovered that tiny alterations in initial conditions resulted in substantial long-term effects. The finding of Lorenz, which gave its name to Lorenz attractors, demonstrated that detailed atmospheric modelling could not, in general, produce precise long-term weather forecasts. In fact, there are no simple causal relationships that link the state of the atmosphere at one point in time to its state at another. The surprising aspect of these chaotic dynamics is that they can develop in deterministic equation-governed systems [14]. Tiny changes in the system's initial state will eventually result in large-scale consequences. This phenomenon is referred to as the "butterfly effect" after a lecture given by Lorentz in 1972 with the title "Does the flap of a butterfly's wings in Brazil set off a tornado in Texas?".

Positive feedback, which we discussed previously, enables a microscopic oscillation to become stronger, spread, and disrupt the system. Thus, chaos arises when multiple perturbations are amplified simultaneously and rendered completely unpredictable, even though they are frequently governed by deterministic rules. In fact, if you plot the trend of a chaotic variable, you will notice an odd internal consistency. If you zoom in closely on the curve, you'll get a similar image to the original. By repeatedly performing the operation, we will always obtain the same shape, demonstrating how each component contains the same level of regularity as the entire figure. A fractal is a shape of this type. Fractal geometry, which emerged independently of chaos theory in the 1960s and 1970s, provides a mathematical framework for describing the structure of chaotic attractors (i.e., the region towards which a dynamical system tends to evolve).

Benoit Mandelbrot (1924-2010), the founder of this geometry, defines it as "a language for communicating with clouds", capable of analysing and describing the complexity of the shapes found in the natural world (see Fig. 2.1).

The surprising property of fractal shapes is that the structures that define them continually repeat on decreasing orders of magnitude, such that the parts have a shape that is similar to the whole in all dimensions.

Every system experiences fluctuations as a result of external perturbations or natural events occurring within the system. As previously stated, homeostasis enables a complex system to absorb perturbations without sustaining damage or significant changes. However, as the system evolves, it reaches and exceeds a critical point at which homeostasis is no longer effective, and self-stabilizing negative feedback loops become dysfunctional. This critical point or critical level may be exceeded for one of the following reasons: a system that evolves spontaneously or an excessive external perturbation.
In the first case, the organisation and interactions of the system change in such a way that the system becomes destabilised. As a result, the system becomes extremely sensitive to the slightest perturbation, which can cause it to collapse.
In the second case, an excessive external perturbation takes place that exceeds the system's natural homeostatic capacity. In both cases, the system reaches a point of critical instability, where fluctuations no longer act as a constraint and thus enters a phase known as "catastrophic bifurcation". During this time period, every point in the system is unstable, and even the smallest perturbation is amplified by positive feedback loops, resulting in unpredictable future behaviour.
However, at some point, one of the violent fluctuations catapults the system into a new attractor, a new stable state, allowing the system to "crystallise into a functional island" and reclaim its internal organisation.
As a result of the bifurcation, the system may find itself in a better management state for at least one of the three primary factors that enable it to exist: information processing, energy management, and material management.

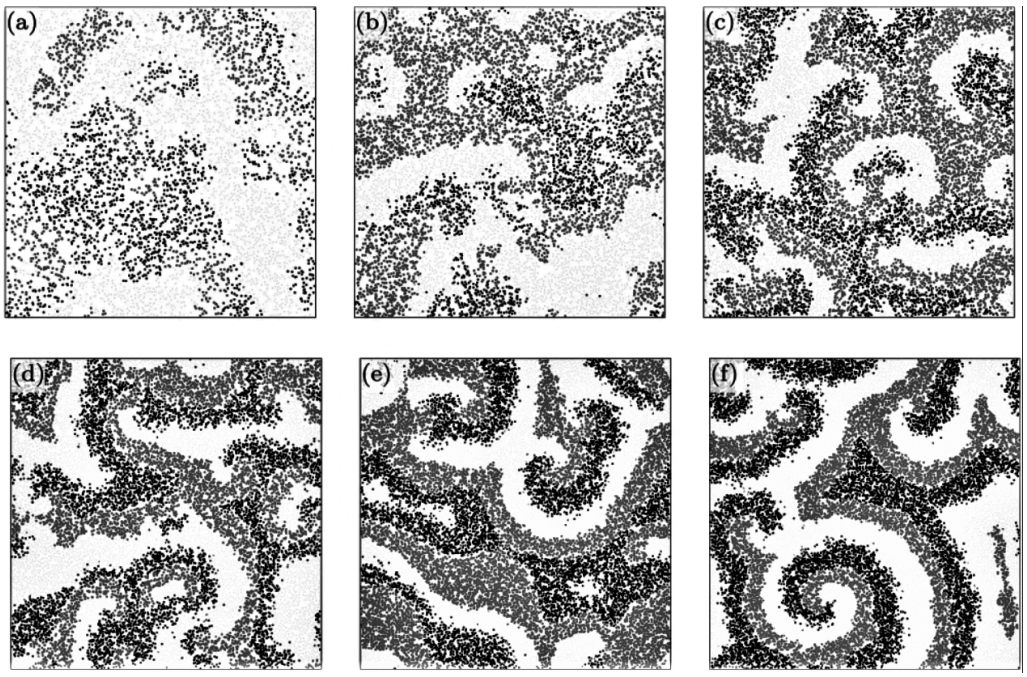

Figure 2.2: A modelisation of the characteristic spatial distributions of species for different values of the local carrying capacity M. The different shades of grey represent the three competing species, while the empty space is marked by white. The comparison highlights clearly that the rotating spiral pattern becomes more evident as M is increased. (Source: D. Bazeia et al., Nature, 2021.)

The characteristics of complex systems that we have highlighted are crucial to the comprehension and modelling of phenomena ranging from the movement of markets to the migration of birds. Vito Volterra (1860-1940) and Alfred J. Lotka were among the first scientists to embrace the hybridisation of mathematics and ecology. Volterra investigated the use of probability calculus in biology between 1900 and 1906 and published three brief papers on applying mathematics to this discipline. Volterra's curiosity was sparked by a real issue involving fishing statistics in the ports of the northern Adriatic. Volterra developed a model that classified the marine population into two broad groups: prey and predators. That marked the very beginning of a paradigm change in math and physics. The mathematician's aim expanded beyond theoretical speculation to encompass real-world problems and the depiction of the natural world. Also, thanks to the work of Volterra, we have developed extremely detailed theories to describe the natural world, such as the research on cyclic dominance of competing species [15] represented in Fig.2.2 and Giorgio Parisi's research on bird flocks [16].
Now that we have seen what complex systems are, we can focus on a particular kind of them: ecosystems.

2.1.2 A Brief Introduction to Ecology

Ecology is a branch of biology that studies the distribution, abundance, and productivity of living organisms, as well as their interactions with one another and with their physical environment [17]. As a scientific discipline, it is still in its infancy and lacks the body of generally accepted principles and theories that older disciplines such as Physics and Chemistry possess.
The term "Ecology" was coined by Ernest Haeckel in his work published in 1866, entitled "General Morphology of Organisms" (Fig. 2.3). The word is derived from the Greek "oikos", which means "house, family, family property". Ecology could therefore be regarded as the study of the "domestic life" of the living beings. Later on, it has been defined in a variety of ways, including scientific natural history (Elton, 1927), the study of nature's structure and function (Odum, 1971), and the scientific study of the interactions that determine organisms' distribution and abundance (Krebs, 1978). The definition chosen for ecology is irrelevant as long as the focus is on the interactions between living organisms and their biotic (living) and abiotic (nonliving) environments. There is frequently some confusion over just what ecology covers and is not already covered by other more traditional disciplines such as Botany, Zoology, Soil Science, Meteorology, and Microbiology. To appreciate Ecology's singular contribution, it is necessary to understand the concept of levels of biological organisation and the related concepts of levels of biological integration. Almost all of biology's traditional subdivisions are concerned with organisational levels at or below the level of the individual organism. Ecology, on the other hand, is concerned with:

- The relationship of individual organisms to other organisms and the nonliving environment.
- Congregations of organisms belonging to the same species (populations)

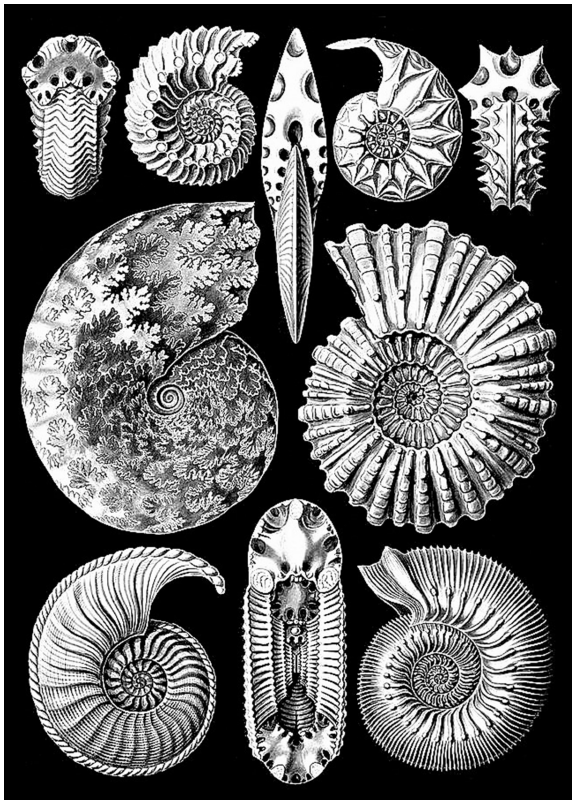

Figure 2.3: A collection of ammonites, the 44th plate from Ernst Haeckel's "Kunstformen der Natur" ("Art Forms In Nature") of 1904.

- Natural assemblages of populations of different species (communities)
- Entire natural systems are made up of communities and their physical environment (ecosystems).

In other words, Ecology is concerned with levels of organisation from the organism upward. In common with other biological disciplines, ecology knows no taxonomic boundaries. Ecology is a science divided into several subdivisions, each of which corresponds to a different level of biological organisation.

- **Autecology**: Autecology is frequently used to refer to the study of an individual species' life history and response to its environment, for example, the life history of an eagle, the food requirement of a deer, or the thermal tolerance of Douglas fir seedlings.

- **Population Ecology**: Population Ecology is the study of the abundance, distribution, productivity, and dynamics of a group of organisms of the same type (a single species population). For example, an investigation of competition for light and nutrients in a pine plantation, the role of disease in regulating the number of insects on a tree, or the rate of growth and mortality of individuals in a salmon population would be classified as Population Ecology.

- **Community Ecology**: Community Ecology refers to studies that involve the description and quantification of some aspect of a natural assemblage of species or organisms, such as the study, classification, and mapping of forest plant associations or forest types; the description of an animal community in a small lake; or the study of plant and animal communities over time in an area. Synecology is a term that is sometimes used to refer to both Population Ecology and Community Ecology.

- **Ecosystem Ecology**: Ecosystem Ecology is a field of study that encompasses both the biotic community and its abiotic environment. Such studies may be primarily descriptive, as in the classification and mapping of different types of ecosystems. However, they can also be functional, such as the study of the interactions between the plant community and the soil or the distribution and movement of energy and nutrients within and across an ecosystem.

- **Macroecology**: Macroecology is another subfield of Ecology, which will be discussed in detail later on.

2.1.3 Ecosystems and Ecological Succession

The word ecosystem was suggested by an English ecologist, Sir Arthur Tansley. He defined it as including not only the organism complex but the whole concept of physical factors forming what we call the environment (Tansley, 1935). Whittaker suggested that an ecosystem is a functional system that includes the assemblage of interacting organisms (plants, animals, and saprobes) and their environment, which acts on them and on which they act (Whittaker, 1975).
Ecosystems are not static, unchanging systems. Along with the continuous exchanges of matter and energy, the ecosystems' entire structures and functions change over time. [18]
Ecological succession is a process of ecosystem development that occurs in virtually every type of environment on the planet, though the details vary by ecosystem type. For example, a landslide-exposed fresh rock surface, a layer of sediment deposited by a retreating glacier, a new lake formed as a result of dam construction, or a volcanic island formed as a result of a volcanic eruption are all examples of primary succession. Secondary succession occurs when a succession begins in an environment that living organisms have already modified. Secondary successional ecosystems include clearcut forests and abandoned agricultural fields. The reasons underlying succession are not always consistent. Often, the replacement of one community with another occurs as a result of changes in the physical, chemical, and biotic environment caused by resident organisms. These changes frequently degrade the site's suitability for the organisms that caused the change and enhance it for the organisms that replace them. This is referred to as autogenic succession, as opposed to allogenic succession, which occurs when physical processes that are more or less independent of the biotic community and external to it cause changes in the physical environment. While changes in the composition of the biota over time are a fundamental characteristic of all ecosystems, the rates of change vary significantly between several stages. Change does not occur indefinitely in many areas.

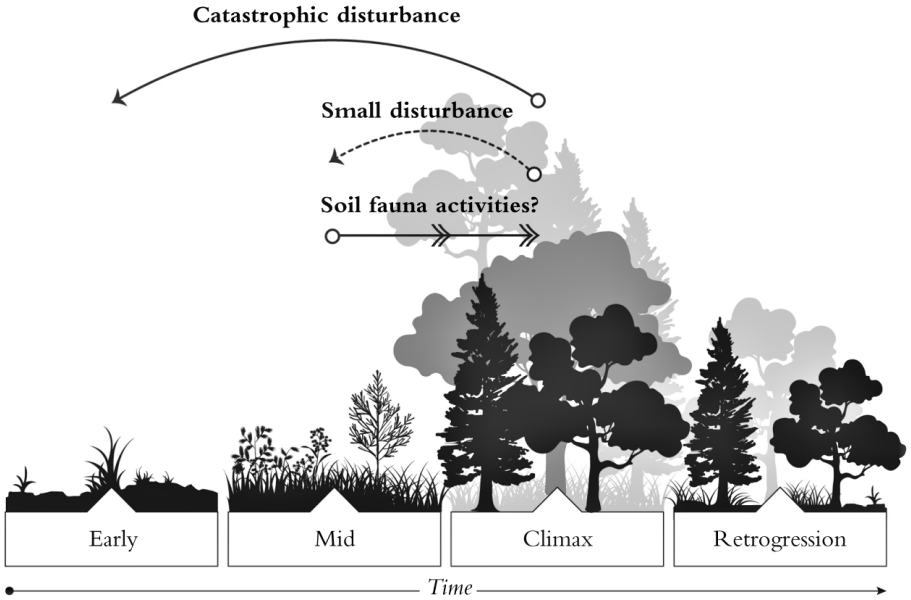

Figure 2.4: A schematic illustration of ecological succession. (Source: U. N. Nielsen, "Soil Fauna Assemblages", 2019)

Communities form when change occurs at an extremely slow rate or when the biota composition remains relatively constant over time. The term climax communities, or simply climax, refers to such relatively stable communities that represent the final or a prolonged intermediate stage.
Numerous contradictory theories exist that address the concepts of ecological succession and climax. Clements (1916) conceived of each biotic stage's community of species and individuals as a superindividual. After the climax community is removed, as when an old organism dies, a new succession, as when a new organism is born, is initiated. A corollary to this theory is that the superorganism does not fail to reach its final stage in the same way that an organism does. Climate controls this process, ensuring that the climatic climax occurs. Later, Sir Arthur Tansley developed the polyclimax theory, in which he demonstrated that, in addition to the climate modulating the succession toward the final steady-state stage, other variables, such as the soil, the fire cycle, and the animals could determine the ecological succession to the climax stages not determined by the climate. The monoclimax and polyclimax both presuppose the presence of distinct plant communities that are mutually exclusive of a particular succession stage. Rather than that, the climax pattern hypothesis implies that the species are autonomous and can be combined in a variety of ways, thus defining the climax pattern hypothesis. The earlier theories were broad generalisations based on the observations that: natural vegetation within a climatic region tends to follow a characteristic pattern of change after disturbance, and these changes often involve a succession of communities dominated by species with increasingly maximum size, age and shade tolerance and progressively lower growth rates and dispersal abilities (Fig. 2.4). Different explanations exist for the observed sequence of several stages. Tilman (1982) suggested that what can outperform competitors at a given level of resource availability will become competitively dominant. Tilman describes his theory as the resource ratio hypothesis. Apart from

the mechanisms for the occurrence of ecological succession, current conditions of rapid climate change are challenging the conditions of existence of a final condition where the tendency for the equilibrium of ecosystem resources and exchange is reached. Model data-fusion studies (e.g., Carvalhais 2008) already find a better performance of biogeochemical models when the model parameters related to the final stability are relaxed.
It is, therefore, necessary to develop new models and theories where dynamic climatic conditions are an integral part of the model, being the current ecosystems departing from stability. Increased temperature, carbon dioxide concentration, and atmospheric reactive nitrogen in the atmosphere are currently forcing the world's terrestrial biomes from any prescribed final stability conditions.

2.1.4 Macroecology and Macroecological Patterns

While Ecology tries to understand the structure and origins of patterns in the abundance, energetics, and geographic distributions of taxa across spatial scales and between habitat types, Macroecology is the study of such patterns. The term Macroecology was coined in a small monograph published in 1971 by Guillermo Sarmiento and Maximina Monasterio, two Venezuelan researchers working in tropical savanna ecosystems.
In specific, Macroecology is a subfield of Ecology concerned with the study of interactions between organisms and their environment on broad spatial dimensions to characterise and explain statistical patterns of abundance, distribution, and diversity. Macroecology develops the capability to estimate species diversity from limited data, forecast extinction rates in the face of habitat loss, and interpret the processes that drive ecosystem structure and function [8].
In Macroecology, the term "metrics" refers to the functions that express correlations between various forms of data. For instance, if a field book contains two columns of data, one representing the area, A, of censused plots and the other representing the number of species, S, seen in each of those plots, the function S(A) represents a measure known as the species-area relationship. Likewise, suppose your field book provides data on the abundance of each species in a collection of species. In that case, ranking the species from most to least abundant creates a rank–abundance distribution statistic.
While species are frequently the taxonomic unit of interest in macroecology, the research of macroecological trends is not limited to them. For instance, it would be possible to discover that a relationship between genera or families is more interesting than a link between species or that it could be interesting to know the distribution of abundances over populations rather than species.
Even after selecting species and individuals as the macroecological analysis units, it would be still necessary to decide which species to include in your study.
There are several options, and the selection should be driven by the scientific questions you are attempting to address. Regardless of the system under examination, a complete macroecological theory should apply. What is critical is that the objective is to provide an unambiguous criterion for determining what to count.
Macroecological measures are classified into species-level and community-level. Met-

rics at the species level explain numerous features of a single species within an ecosystem, whereas metrics at the community level represent the attributes of a group of species co-inhabiting the same environment. The term "ecosystem" here refers to anything from a tiny patch of land to an extensive biome. The metrics take the form $f(X|Y)$, where X and Y may refer to a single or many variables. The notation is interpreted as "f of X given Y". The notation is conventional for a conditional function. It indicates that the function f's dependency on the variable X is conditional on the values of the conditionality variable Y. The conditionality variables have been chosen to be reasonable but are not established at this point in the exposition. Later on, what METE truly forecasts will be examined. The values A_0, S_0, N_0, and E_0 that occur as conditionality variables in several of the metrics are what are referred to as state variables. Using this notation does not imply that Y has been measured and the distribution of X is projected in all applications. Indeed, it will be shown how the metric may be used to deduce the value of Y from the measurement of X in some cases. Certain symbols have a line above them, for example, S. Throughout the dissertation, this notation will be used to express the average of a quantity. There is a critical difference to point out. A closer examination reveals that some of the metrics reflect probability distributions or probability density functions, while others show dependent connections. Normalised to 1, a probability distribution tells us of the relative likelihood of various values of its argument. By contrast, a dependency connection informs us about the link between two ecological variables, such as the relationship between the average metabolic rate of individuals within a species and the species' abundance. Except for one case (the metabolic rate), the Greek letters are used to designate macroecological metrics that are probability functions and Latin letters to denote the dependent and independent ecological variables in dependency relationships. Finally, Latin letters are often used when referring to generic probability distributions. For instance, if the discrete probability distribution $p(z|x)$ is known, the dependency on x of the mean of z (designated by 1) on the distribution $p(z|x)$ is as follows:

$$\bar{z} = \sum_z zp(z|x) \tag{2.1}$$

$\bar{z}$ will be a function of x, implying that the connection is dependent on x. If p is a continuous distribution, the summation in Eq. 2.1 is replaced by integration. As a result of these links between probability distributions and dependence relationships, not all of the macroecological metrics are independent. Finally, probability distributions are classified into two types based on the independent variable's discrete or continuous nature. A probability distribution, $p(n)$, where n is a discrete variable, such as species abundance, and the sample space is a collection of species, means that for each value of n, $p(n)$ is the likelihood that a random draw from the pool of species results in a species with abundance n. In this scenario, $p(n)$ may be experimentally calculated as the proportion of the sample space that contains that discrete n-value. P is defined as follows for a probability distribution specified over a continuous variable, $p(\epsilon)$, where ϵ is, for example, metabolic energy: The chance that a random draw from the sample space has an energy value between and d is denoted by $p(\epsilon)d\epsilon$. A probability density function is a distribution over a continuous variable, such as p, which is commonly abbreviated as a "pdf".

A glossary is added below together with a table describing some macroecological metrics in order to clarify their meanings in the text.

Symbol and Name of Metric		Description of Metric
$\Pi(n\|A, n_0, A_0)$	intra-specific spatial-abundance distribution	Probability that n individuals of a species are found in a cell of area A if it has n_0 individuals in A_0.
$B(A\|n_0, A_0)$	box-counting range-area relationship	Dependence on cell size of a box-counting measure of range for a species with n_0 individuals in A_0.
$C(A,D\|n_0, A_0)$	intra-specific commonality	Dependence on A and D of the fraction of pairs of cells of area A, separated by a distance D, that both contain a species with n_0 individuals in A_0.
$\Omega(D\|n_0, A_0)$	O-ring measure of aggregation	Average over each occurrence of an individual, of the density of individuals within a narrow ring at a radius D, divided by the density in the ring expected in a random distribution.
$\Theta(\epsilon\|n_0, S_0\, N_0\, E_0)$	intra-specific energy distribution	Probability density function for an individual from a species with n_0 individuals to have a metabolic energy rate between ϵ and $\epsilon + \mathrm{d}\epsilon$.
$\Delta(D\|n_0, A_0)$	intra-specific dispersal distribution	Probability density function for an individual in a species with n_0 individuals in A_0 to have a dispersal distance between D and $D + \mathrm{d}D$
$\Phi(n\|S_0, N_0, A_0)$	species-abundance distribution (SAD)	Probability that in a community with S_0 species and N_0 individuals, a species has abundance n.
$\bar{S}(A\|S_0, N_0, A_0)$	species–area relationship (SAR)	Average number of species in a cell of area A if S_0 species in A_0
$\bar{S}(N\|S_0, N_0)$	collector's curve	Average number of species found in a random sample of N individuals.
$\bar{E}(A\|S_0, N_0, A_0)$	endemics-area relationship (EAR)	Average number of species unique to cell of area A if S_0 species in A_0.
$\bar{X}(A,D\|S_0, N_0, A_0)$	community-level commonality	Average fraction of the species in cells of area A that are found in common to two cells of area A a distance D apart, if S_0 species in A_0.
$\Psi(\epsilon\|\ S_0, N_0, E_0)$	community energy distribution	Probability density function for an individual in a community with $S0$ species, $N0$ individuals, and total metabolic rate, $E0$, to have metabolic rate between ϵ and $\epsilon + \mathrm{d}\epsilon$.
$\bar{\epsilon}(n\|\ S_0, N_0, E_0)$	community energy-abundance relationship	Dependence of average metabolic rate of the individuals within a species on that species' abundance, n.
$\Lambda(l\|S_0, L_0)$	link distribution in a species network	probability that a species in a network with S_0 species and L_0 links is connected by l links to all other species

Table 2.1: Macroecological metrics. In the upper part species level metrics are presented, while in the lower part the are community level metrics. Notice that not every metrics is presented in the text. The variables upon which the distributions are dependent will be presented in the text and in the glossary in Tab. 2.2 [8].

A_0:	the area of an ecosystem in which we have prior knowledge
A:	the area in which we seek to infer information
N_0:	the total abundance of all species under consideration in an A_0
S_0:	the total number of species under consideration in an A_0
E_0:	the total rate of metabolic energy consumption by the N_0 individuals in an A_0
n_0:	the abundance of a selected species in an A_0
n:	a variable describing the abundance of a species
$n_{\max}$	the abundance of the most abundant species in a community
r	rank, as in a rank-ordered list of abundances
D:	a geographic distance
L_0:	the total number of links in a network
l:	a variable describing the number of links connected to a node (usually a species) in a network
x	$e^{-\lambda_n}$
ε:	a variable describing the metabolic rate of an individual
$\bar{\varepsilon}$:	average metabolic rate of the individuals in a species
λ_1:	Lagrange multiplier corresponding to the constraint on $R(n, \varepsilon)$ imposed by average abundance per species
λ_2:	Lagrange multiplier corresponding to the constraint on $R(n, \varepsilon)$ imposed by average metabolic rate per species
λ_Π	Lagrange multiplier corresponding to the constraint on $\Pi(n)$ imposed by average number of individuals per cell.
β:	$\lambda_1 + \lambda_2$
σ:	$\lambda_1 + E_0 \cdot \lambda_2$
γ:	$\lambda_1 + \varepsilon \cdot \lambda_2$
σ_{SB}	Stefan–Boltzmann constant (5.67×10^{-8} watts per m^2 per (degree K)^4

Table 2.2: Glossary of symbols [8]

Species-level spatial abundance distribution

While walking through a forest, one cannot help but notice how certain trees grow close to others while others are more secluded. Generally, ecosystems show this propensity towards inhomogeneity on a broad scale. With the knowledge of the various species, it can be seen that each species has areas with numerous individuals and patches with few or no individuals. This might imply that individuals are randomly located and that unpopulated regions occur by coincidence, or it could

show non-randomness.
The first species-level metric, $\Pi(n)$, informs us of the discrete distribution of the numbers of individuals across cells of area A for each species and allows us to answer, for example, if a pattern is random. When the geographical distribution of individuals within a species is expressed using the metric $P(n|A, n_0, A_0)$, a strong statement is implicitly made. For instance, consider all the variables that might affect the chance that A contains n individuals. If it is a plant, the colour of its bloom, the type of its pollinator, the mechanism by which it disperses, or the qualities of the other species with whom it shares space may all affect that chance. According to that hypothesis, only cell areas A and A_0, as well as the species' abundance in A_0, affect the likelihood indicated by the metric. That is a significant simplification, and of course, a test of the hypothesis is needed in order to see whether it is an unreasonable oversimplification.

Range-area relationship

The challenge of defining a species' range, or rather indicating the location of the species, is ambiguous in the same way as defining the length of the shoreline is ambiguous. To investigate the ramifications of this, it is possible to turn to fractals, not because the geographical distributions of individuals within species are fractals, but because the mathematics used to research fractals is extremely strong and pertinent to our situation. The shape of such graphs can indicate whether or not the shoreline is fractal in shape (Mandelbrot, 1982). This description of a coastline's length may be generalised to two dimensions to provide a helpful representation of a species' range as determined by occupancy statistics. Assume that a largeleaf linden species exists in patches over the continent. If the continent is covered by cells of area A, the species will be found in a fraction of those cells. Therefore, instead of length l, consider cell area A, and instead of N being the number of times the stick may be laid down, consider the number of cells in area A inhabited by the species. We may define a species' "area of occupancy," B(A), by multiplying N by A: B(A) 1/4 N(A) A. The shape of a log(B) vs log(A) graph indicates the fractal nature of the occupancy pattern. This area of occupancy metric, B, is occasionally referred to as a "box-counting" measure. The explanation for this is that if we consider each cell in area A to be a box, then N(A) is just a count of the occupied boxes. Thus, the metric B, reflects the relationship between this range measure and the size of the cells utilised to calculate it (Kunin, 1998; Harte et al., 2001). $B(A|n_0, A_0)$ may be calculated using the metric $P(n|A, n_0, A_0)$ for species-level abundance distributions: $\Theta(n)$ On the right, the first term represents the proportion of area A cells that are occupied, and the second is the total number of area A cells inside A_0. Their product is the number of occupied cells, denoted as N(A). The third word is the area of the cells in question.

Species-level commonality

Another interest of Macroecology are individual co-occurrences. If you choose a species with n_0 individuals in A_0 and two cells in area A that are separated by a

distance D. $C(A, D|n_0, A_0)$ is the proportion of such pairings of cells in which both cells contain at least one person from that species. This measure is used to define a relationship between two variables that is dependent on both of them. The notation implies that the value of this measure is conditional on the variables n_0 and A_0 for any defined value of A and D. When C(A,D) is considered as a function of D, with cell area A remaining constant, the metric is sometimes referred to as a "distance-decay" metric. This naming is suitable since the function is frequently a decreasing function of inter-cell distance, indicating the tendency of individuals within a species to live in close proximity to one another rather than far apart.
There is a critical contrast between measures such as commonality, C, and metrics such as the spatial abundance distribution of species, P. The latter is a function that represents information on a single cell, whereas the former describes the simultaneous activity of two cells. The former provides spatial correlation information, whereas the latter does not.

Intra-specific energy distribution

It's possible to look at a group of individuals and wonder who consumes the most energy in their everyday life and who consumes the least. You might continue by inquiring about the distribution of energy consumption rates within the group.
Individuals within any species in an environment may be studied to answer the same question. The response is $\Theta(\epsilon)$, a probability density function. It is a term that refers to the distribution of metabolic energy rates across members of a species in an ecosystem. As with the other species-level measures, the species is assumed to have an abundance of n_0 in A_0. Because it is an energy distribution over individuals rather than an abundance distribution over space, you might expect it to be independent of A_0, but it may be dependent on the total amount of energy consumed by the species in question, as well as the total number of species and individuals in the system. This measure is conditional on the total number of species, S_0, the total abundance, N_0, and the total metabolic rate, E_0; as demonstrated in the next chapter, METE predicts that this is actually the case.

Dispersal distributions

In plant and animal ecology, the idea of dispersion distribution is frequently utilised slightly differently. It is often used in plant ecology to refer to the distribution of distances travelled by seeds from the parent plant to their final destination. However, most seeds never germinate and grow into viable plants. In animal ecology, the dispersion distribution of a species, such as a bird, is sometimes defined as the range of distances between the nest site where the bird is born and the place where the progeny eventually nests. Because this term has a variety of advantages in spatial macroecology, it will be applied to both plants and animals. Thus, the dispersion distribution of a plant species is the distribution of distances between the locations of seed production and the locations of germinating seeds that develop to maturity. The two forms of dispersion distributions can take on quite distinct patterns, as would be the case if seeds that fall extremely far from their parent are less likely

to germinate and survive than seeds that fall closer. According to the way that the dispersion measure, $\Delta(D|n_0, A_0)$, is expressed, the distribution of dispersal distances appears to be governed by the species' abundance, n_0, in A_0. Indeed, an opposite interpretation makes more sense. The eventual density of the species is likely to be governed by the dispersion distance distribution. It is critical to remember that the structure of the metrics' conditionalities (i.e. which variables are to the left of the conditionality symbol "|" and which are to the right of it) should not be taken as indicating the direction of impacts.

The species abundance distribution (SAD)

Ecosystems are intriguing to analyse in part since certain species are quite common while others are highly uncommon. Between frequent and uncommon lies a probability distribution which is one of the most extensively researched metrics in ecology. The SAD is a probability distribution in the conventional meaning of the term used in probability theory. As a parallelism, you can consider a box filled with balls of various colours, each representing a distinct species. There may be just a few yellow balls, but there are numerous red ones. If you reach into the box and extract a ball, the likelihood is that it will be of a hue that is well-represented in the box. By sampling the box frequently, replacing the ball after each sample, and documenting the colour of the ball, you can generate a probability distribution for the abundances. The data obtained from a thorough and well-designed census is equivalent to pouring the contents of the box on the ground and counting each ball.

Species area relationship (SAR)

As with the SAD, SAR is a frequently researched metric in macroecology. Although the idea that species richness grows with sample size probably dates back millennia, Olaf Arhennius was the first to publish the measurement of a SAR, along with a clear suggestion for its mathematical form. The SAR concept is straightforward. It is almost obvious to find more species when you examine larger and greater regions of habitat, each larger area incorporating the smaller areas. When a census is conducted in this manner, the resulting SAR is referred to as a nested census since tiny plots are nested inside larger plots. The fact that species richness grows with area for a nested census does not seem significant because unless all individuals in each species were discovered throughout the biggest region surveyed, which is highly improbable, larger areas would naturally include more species. However, the SAR is more than that. To begin, several explanations for the rise in species richness with census area were postulated. Larger regions often have a greater variety of environmental variables, such as soil moisture content, slope, and aspect, and this increased diversity of abiotic niches may sustain a greater number of species. Additionally, more migrants and dispersers from other areas are more likely to arrive in a greater region, and so there may be more species in a wider area just by chance. Because a greater territory may support more individuals of a particular species and because local extinction is more likely when the population number falls below a critical level, extinction rates may also be lower in a wider area.

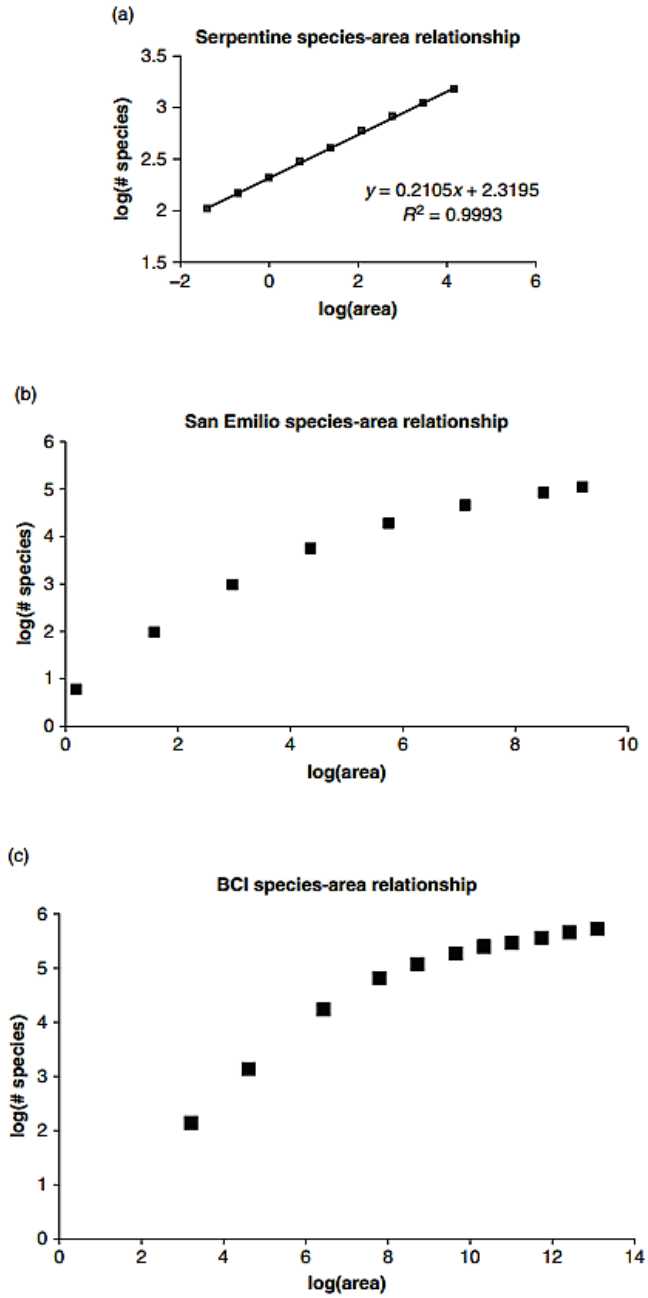

Figure 2.5: Observed species–area relationships for: (a) the serpentine grassland plot (1998 data); (b) San Emilio 10-ha dry tropical forest plot (Enquist et al., 1999); (c) the Barro Colorado Island (BCI) 50-ha plot (Condit, 1998; Hubbell et al., 1999, 2005).

Finally, there may be an intrinsic function for the area that results in more species being able to coexist within a bigger region even when the environment is uniform and the other processes outlined above are not active. Secondly, the actual shape of the rising SAR may provide information about a variety of ecological phenomena, including inter-and intraspecific competition, the distances over which seeds of

different plant species are dispersed, or animals migrate, the nature of soil types, land-surface topography, and other abiotic landscape features, and, more broadly, the forces that shape the partitioning of resources among species. Thirdly, the SAR's actual form has huge consequences for conservation biology, which will be described in further detail later. The likelihood that a species with n_0 individuals in the broader plot will be found in the cell is one minus the probability that it will be missing, $1-\Pi(0|A, n_0, A_0)$. Assuming that the spatial abundance distribution at the species level are independent of one across species one may write:

$$\bar{S}(A|N_0, S_0, A_0) = \sum_{Species} (1 - \Pi(0|A, n_0, A_0)) \tag{2.2}$$

The previous equation is just the summation of the odds of each species occurring to determine the expected number of species' abundances. This is the formula you would use to obtain the distribution if the real value of species abundances is known. However, if the real value of species abundances is not known, but one could understand the abundance distribution, equation 2.2 becomes:

$$\bar{S}(A|N_0, S_0, A_0) = \sum_{n_0=1}^{N_0} [1 - \Pi(0|A, n_0, A_0)]\Phi(n_0|N_0, S_0, A_0) \tag{2.3}$$

Therefore the predicted number of species in A is given by the sum over n_0 of the product: [chance that a species with n_0 individuals in A_0 is present in A]X[proportion of species in A_0 with an abundance of n_0]. S(A) is the estimated number of species in A when the proportion above is multiplied by the total number of species in A_0.

The endemics-area relationship (EAR)

If a species is found exclusively in a certain place, it is considered to be endemic to that region. Similarly to Eq.2.3, it is possible to develop an equation for $\bar{E}(A)$ in terms of the spatial abundance distributions at the species level and the species abundance distribution.

$$\bar{E}(A|N_0, S_0, A_0) = S_0 \sum_{n_0=1}^{N_0} [\Pi(n_0|A, n_0, A_0)]\Phi(n_0|N_0, S_0, A_0) \tag{2.4}$$

This formula follows the same logic as Eq. 2.3, except that the species-level spatial abundance distribution is now assessed at $n = n_0$. To see why consider that a species with n_0 individuals in A_0 is endemic to a cell of area A if all n_0 of its individuals are located there. The likelihood of that occurrence is exactly $\Pi(n|A, n_0, A_0)$.

Community commonality

This statistic quantifies species co-occurrence. Consider all feasible pairings of cells with an area A that are separated by a distance D. Calculate the number of species shared by any such pair and then average that number across all pairings. The metric $\bar{\chi}(A, D|S_0, A_0, N_0)$ is calculated by dividing the average by the average number of

species detected in a cell of area A. Eqs. 2.3 and 2.4 can be related to the sum of the species-level commonality metric's abundances:

$$\bar{\chi}(A, D|S_0, A_0, ..) = \frac{S_0 \sum_{n_0=1}^{N_0} C(A, D|n_0, A_0, ..)\Phi(n_0|N_0, S_0, A_0, ..)}{S_0 \sum_{n_0=1}^{N_0}(1 - \Pi(0|A, n_0, A_0, ..)\Phi(n_0|N_0, S_0, A_0, ..))} \tag{2.5}$$

As it refers to Eq. 2.3, the denominator on the right-hand side of Eq. 2.5 represents the average number of species detected in a cell of area A. Using the same logic as in Eq. 2.3 and recalling the concept of species-level commonality, C(A,D), we find that the numerator is equal to the number of species present in both cells of region A. The Sorensen index is the name given to measure $\bar{\chi}$.
The idea of beta diversity, which is designed to characterise species turnover, is related to our statistic of community-level species commonality. A metric $\bar{T} = 1 - \bar{\chi}$ is one approach to quantify turnover. As with $\bar{\chi}$, $\bar{T}$, the value can vary from 0 to 1, with 1 indicating that two patches share no species, indicating that turnover is complete. Beta diversity is frequently used in contrast to alpha and gamma diversity. Alpha diversity is concerned with local diversity, or the average species richness within a limited area. Gamma diversity is concerned with the variety of species present throughout many environments and hence is seen as a large-scale metric. Beta diversity, in this sense, refers to variety within a habitat type but over a greater distance. Due to the difficulty of quantifying habitat types and the possibility that different species perceive habitat transitions differently, it is difficult to determine whether a change in slope or aspect, for example, within a large forest warrants referring to the diversity across that change as beta or gamma diversity. It could be preferable to stick with the mentioned metric $(1-\bar{\chi})$ as a scale-independent measure of evolving variety throughout space.

Community energy distribution

$\Phi(\epsilon|S_0, N_0, E_0)$ is a generalisation of the species-level energy distribution $\Theta(\epsilon)$ at the community level. Φ is the probability density function for the distribution of metabolic energy rates among all community members. As with $\bar{\epsilon}$, evaluating a predicted form for Φ involves either challenging measurements of real metabolic rates or simple measurements of body mass paired with theory relating body mass and metabolism.

Energy and mass abundance relationships

Picture yourself going through a forest, counting the number of trees of various sizes. To begin, imagine that you choose a species that is easily identifiable, even as a seedling. You're likely to discover several little seedlings of that species, fewer saplings, even fewer medium-sized trees, and an even smaller number of fully grown trees towards the end of their existence scattered among all these plants. Although that would be expected, death can occur at any age, and so, if the forest is in demographic equilibrium, the numbers must drop with age and hence, on average, with size. If individuals are binned into equal size intervals, a bar graph of their numbers versus size will show a rapid decline in bar height with increasing size.

If the logarithmic size intervals are used, the decline will be much slower, and the graph may appear flat or even show bar height increasing with size. There is a second technique to evaluate the distribution of tree sizes: do the same survey but without making any distinctions between species. As a third option, you may investigate the link between the number of trees in each species and their average mass. There is no reason to believe that connection would be similar to either the first or second relationship described above. Each of these relationships is a mass–abundance relationship (MAR), and they are all significant. Of course, the same studies might be performed on animal data or any other wide category of life. It is not expected to find the same patterns as you see with trees in such circumstances for two reasons: trees grow until they die, but animals normally do not, and the ratio of mature giant trees to seedlings is far larger than the ratio of mature mammals or birds to their young. This metrics enable us to conduct a more quantitative and systematic examination of these numerous interactions. The metric $\bar{\epsilon}(n_0|..)$ represents the connection between these variables. This statistic may be calculated by examining the intra-specific energy distribution, $\Theta(\epsilon|n_0)$. In fact,

$$\bar{\epsilon}(n) = \int d\epsilon \epsilon \Theta(\epsilon|n) \tag{2.6}$$

To translate $\Theta(\epsilon)$ to a connection between the average mass of individuals within a species, and the species' abundance:

$$\bar{m}(n) = \int dm m \rho(m|n) \tag{2.7}$$

where $\rho(m|n)$ is the mass distribution.
Probability distributions for energy and mass, defined across the sample space of species, may be generated from these energy–abundance and mass–abundance connections. The relationship between density and mass is the inverse 3/4-power and it is called the Damuth rule (Damuth, 1981). This assuming general scaling relation between mass and metabolism of the form $\epsilon(m) = Cm^b$. For instance, beginning with species abundance, $\Phi(n)$, the distribution of the average metabolic rates of individuals within species (which we designate by $\nu(\bar{\epsilon})$) is given by:

$$\nu(\bar{\epsilon}) = \Phi(n(\bar{\epsilon})(\frac{dn}{d\bar{\epsilon}}) \tag{2.8}$$

The term $(\frac{dn}{d\bar{\epsilon}})$ in this formula is generated by inverting and differentiating the function $\bar{\epsilon}(n)$ in Eq.2.6. This inversion method can be carried out analytically in certain circumstances but must be carried out numerically in others. It is possible to create an equation for the distribution of the average mass of individuals in a species over the species, $\mu(\bar{m})$:

$$\mu(\bar{m}) = \Phi(n(\bar{m}))(dn/d\bar{m}) \tag{2.9}$$

Where $n(\bar{m})$ is produced by inverting the function $\bar{m}(n)$ in Eq. 2.7 . Because organisms' sizes or masses are more easily quantifiable than their metabolic rates, we will focus our attention on mass–abundance correlations. Eq. 2.7 illustrates one such relationship, with m(n) denoting the link between a species' abundance and its average mass of individuals. However, there are several sorts of size–or mass–abundance

connections (MAR).
The empirical patterns discussed thus far appear to be ubiquitous over a wide variety of geographical dimensions, taxonomic groupings, and environments. This demonstrates that what Darwin referred to as nature's "exquisitely built forms" were really "created by laws working around us." And this alone is enough to be concerned about macroecological patterns, as they provide insight into the nature of these laws.
However, there are further practical reasons to attempt to comprehend the patterns or shapes that these measures adopt, not just visually from graphs but also analytically if feasible. It derives information more confidently from analytical equations, which are functions of independent variables, than we can from visuals. In addition, increasing our capacity to extrapolate information advances us significantly in our efforts to employ ecological theory more effectively in conservation biology. Estimates of the number of species of plants, birds, mammals, and other vertebrates on a continental scale are reasonably accurate but are likely wrong by no more than a few per cent. However, understanding the species richness of insects, other invertebrates, and microbes is significantly less complete. It is a major interest in Ecology to estimate the number of such species because it is necessary to know what the Earth is losing due to habitat loss. Finally, it is intrinsically exciting to learn what evolution is capable of also generating because this information has the potential to help us in different ways.

2.1.5 Overview of Some Macroecological Models

In this section, I will discuss several models and theories that have been suggested to explain the observed behaviour of macroecological metrics. The objective is to make an introduction to the fundamental ideas and some of the mathematical tools necessary for comprehending a range of theoretical frameworks in Macroecology. These frameworks illustrate several strategies for making sense of the numerous patterns mentioned in the preceding sub-chapter. A statistical model comprises randomly selecting individuals from a predicted distribution and utilising the outcome of that selection to answer a question. A growing field of ecology theory development is predicated on the premise that distinctions between biological objects of study can be ignored. One such assumption is that species-level differences in features can be ignored. Another form of neutrality is the assumption that while variations between species will not be ignored, differences between individuals within species will be. Clearly, if one is investigating natural selection in a species, and genetic distinctions between individuals are required to explain the observed occurrence, one cannot use the assumption that individuals within a species are indistinguishable.
To advance, it is necessary to revisit concepts pioneered by the mathematical scientist Pierre Simon Laplace. In probability analysis, he posed the following problem. Imagine that you have the standard urn with two types of balls, red and blue, but you have no way of knowing how many of each type there are. Assume you reach inside and remove a red one without replacing it. The question is: "What is the best inference you can make regarding the probability that the second ball you remove will be red as well?". Laplace demonstrated that the correct solution is 2/3 with

two balls. In general, if there are two possible outcomes, R and B, and your prior knowledge consists solely of the knowledge that one of the extracted balls was red and the other two were blue, the best estimate of the chance that the next ball extracted will be red is:

$$P(n_R + 1|n_R, n_B) = \frac{(n_R + 1)}{(n_R + n_B + 2)} \tag{2.10}$$

This is referred to as Laplace's "successive rule". This rule can be applied to the assembly of individuals from a species onto a landscape.
It is possible to begin by populating the plot's two sections. Using red for the left side and blue for the right, the first individual to join the plot will have a 50–50 chance of entering on the left half. However, as additional individuals are added, the chance of the next member in the sequence being assigned to the left side is provided by:

$$P(next\ individual\ to\ left\ half|n_L, n_R) = \frac{(n_L + 1)}{(n_L + n_R + 2)} \tag{2.11}$$

Where n_L is the leftmost number and n_R is the rightmost number shortly before the following individual is added. This rule can be used to construct a uniform distribution as follows:

$$\Pi(n|\frac{A_0}{2}, n_0, A_0) = \frac{1}{n_0 + 1} \tag{2.12}$$

This concept of equal probability for all conceivable outcomes is also referred to as the principle of indifference: when there is no a priori justification to assign different probabilities to two events, their probabilities must be assumed to be the same. Laplace articulated the notion of indifference for the first time, and it serves as the foundation for his rule of succession.
Consider a coin-toss strategy to assign molecules between two halves of a room. This is an illustration of a Bernoulli process used to generate a binomial distribution. Each toss has a 50–50 chance of landing in one of the parts say the left, and with a large number of molecules, the result will be a virtually equal distribution of molecules between the two halves. It is irrelevant whether the molecules are regarded as distinct or indistinguishable—what matters is that the outcome of each toss is independent of the previous results. Consider a bag of coins, each from a different country and bearing a heads-up or tails-up design. Each one is flipped and placed on the left or right side of the room according to whether it landed on heads or tails. Even though each coin was unique, the outcome will be the binomial distribution.
It could be noticed that the assembly rule is a "the wealthy get richer" rule, in which the chance of the next individual moving to that half increases as more individuals accumulate on one half, either left or right. By comparison, the result of the binomial distribution is egalitarian.
Let's take a closer look at the example of classical statistics for distinct objects. The gas molecules in your room are nearly evenly distributed between the left and right sides. The binomial distribution accurately predicts that the likelihood of a difference in the number of molecules in the two halves of even 1/100 or larger is

insignificant. The binomial distribution's narrow peak at 50 per cent allocation is due to a large number of air molecules in a room, but even with only 100 molecules, the probability of there being an exact 50 per cent split is significantly greater than the probability of there being, say, five on the left and 95 on the right. With indistinguishable molecules, it is predicted that you would likely suffocate if you sat at one end of a room for an extended period of time. However, this is most likely not the case. If the distribution of air molecules became detectably unequal, a pressure gradient would form, rapidly readjusting the distribution to near equality in numbers. The fact that you are not suffocating right now is due to equalising pressure forces, not to the binomial distribution.
Later on, we will demonstrate that METE accurately predicts Eq.2.12. Then, we shall also prove that Eq.2.12 adequately represents the distributions of individuals within a considerable fraction of, but not all, species at plot scales. To the degree that Eq. 2.12 more accurately characterises the spatial distributions of some species than the binomial distribution does, we can deduce that pressure forces (for example, those resulting from intra-specific competition) are relatively mild for those species.

The Coleman model

Coleman detailed the ramifications of presuming random placement of individual species in an ecosystem in a seminal paper. The random placement model (RPM) predicts the spatial abundance distributions of species at the species level, P(n), the box-counting area-of-occupancy relationship at the species level, $\Pi(n)$ and species-level commonality, C(A,D). It does not predict the SAD, $\Phi(n)$, but in order to infer a species-area connection in this model, an abundance distribution must be postulated or observed. Coleman conducted the former, predicting SAR forms based on a variety of different assumptions about $\Phi(n)$. Additionally, the RPM does not forecast the shape of our energy or mass distributions or connections. The binomial distribution describes the likelihood that a species will have n individuals in a cell of area A if the species has n0 individuals in a wider region, A_0, that encompasses A.

$$\Pi(n|A, n_0, A_0) = \frac{n_0!}{n!(n_0 - n)!} p^n (1 - p)^{n_0 - n} \tag{2.13}$$

The probability, p, is simply the likelihood that an individual will settle in cell A following a single random placement on the plot A_0. This likelihood is proportional to the cell's entire area, which means:

$$p = \frac{A}{A_0} \tag{2.14}$$

The number $(n_0 - n)$ denotes the likelihood that n individuals are allocated to a cell and $(n_0 - n)$ individuals exit the cell into an area $(A_0 - A)$ space. Notably, this implies that the chance of any given individual being discovered in a particular cell of area A is independent of the number of individuals already found there or elsewhere. The factorials in the equation emerge as a result of the fact that the n persons discovered in cell A can be any n from the total number,n_0. By assuming the

combinatorics outlined above, it is assumed that individuals within a species may be viewed as distinct elements and that the sequence in which they are disposed is irrelevant. However, if the order was relevant, it would be necessary to make distinctions between individuals and deal with a different probability distribution.
If the mean value of occupancies in the cells of area A is more than one:$n_0 A/A_0$, the binomial distribution is steeply peaked around its mean. Indeed, it is possible to demonstrate that the distribution approaches Gaussian in the region of the mean value of n. When the value is $n_0 A/A_0 < 1$, on the other hand, the distribution is monotonically declining. When $p = A/A_0 << 1$ is used, it can be demonstrated that the Poisson distribution closely approximates the binomial distribution.
Given the widespread lack of consistency between known geographical abundance distributions and RPM projections, one could anticipate the RPM to perform poorly in predicting SARs. To use the RPM to forecast the SAR, the total number of species in the plot and their abundance distribution n_0 must be derived either theoretically or empirically. Coleman (1981) demonstrated that only a small proportion of empirical SARs are well characterised by the model.
The RPM's demise is outlined as follows: for most species at most geographic scales, but notably for A_0, the observed values for $\Pi(0)$, the likelihood that a species is absent from a cell surpasses the RPM prediction. This lower-than-expected probability of absence shows that the RPM spreads individuals too uniformly throughout the plot, resulting in less aggregation.

Generalized Laplace Model

Previously, the distribution of individuals across the two halves of a plot was analysed, assuming individuals are indistinguishable. Then, the question becomes what patterns might be predicted at finer spatial scales under the same premise. As a result, we are left with two options: a generalised Laplace model or the HEAP model (see next section).
Consider assigning individuals to the four quadrants of A_0, each of which has an area of $A = \frac{A_0}{4}$. Now a number of options are possible. One alternative is to generalise the model of indistinguishable individuals. In particular, if one considers an indistinguishable particle in a box and divide it into the left and right side. Then, when a particle is added to the box, the probability of that particle being in a determined half (one can take the left half without loss of generality) is given by:

$$Probability(next\ individual\ to\ left\ half) = \frac{(n_L + 1)}{n_L + n_R + 2} \tag{2.15}$$

With n_L and n_R respectively number on the left and on the right. The generalisation of the previous equation would give:

$$P(next\ individual\ to\ upper\ left\ quadrant | n_{UL}, n_{LL}, n_{UR}, n_{LR}) = \frac{n_{UL} + 1}{n_{UL} + n_{LL} + n_{UR} + n_{LR} + 4} \tag{2.16}$$

where, for example, n_{LR} is the number of individuals discovered in the lower-right quadrant prior to the introduction of the following individual.

HEAP

The extended Laplace model discussed above is one method for modelling the spatial distribution of indistinguishable individuals. Another possibility is to iteratively solve Eq. 2.15 at ever finer scales. This results in a model dubbed HEAP (Harte et al., 2005), where HEAP stands for Hypothesis of Equal Allocation Probabilities. At the first bisection, $A = \frac{A_0}{2}$, HEAP predicts a spatial abundance distribution that accords with Eq. 2.15, but at finer scales, it deviates from Eq. 2.16 and the generalisation of Eq. 2.16 to finer scales provided by the following equation:

$$\Pi(n|A, n_0, A_0) = \frac{g(n_0 - n, M_0 - 1)}{g(n_0, M_0)} \tag{2.17}$$

2.2 The Maximum Entropy Theory of Ecology (METE)

This chapter will present METE, a complete and testable theory of species distribution, abundance, and energetics across spatial scales. This chapter will develop the theory's structure and predictions, with the theory's evaluation occurring in Sub-chapter 2.3.

2.2.1 Entities and Variables of State

The MaxEnt concept can be applied to any complex system that involves a determination of the fundamental entities (in the standard thermodynamic example, molecules) and the specification of a collection of state variables. METE predicts probability distributions for two types of entities, "individuals" and "species". We define "species" as any well-defined collection of "individuals." The groups could be taxonomic species (as presumed here), genera, or even trait groups. Furthermore, the term "individuals" shall be defined in the conventional sense of individual organisms. The only criterion for selecting entities in a MaxEnt application is that they are explicitly defined in a way that allows specification of the numerical values of the state variables and, consequently, of the quantitative constraints on the probability distributions, as we shall see. Here the macroecology's state variables will be defined, as the system's area, A_0, the number of species,S_0, in any specified taxonomic category, such as plants or birds, in that area, and the total number of individuals, N_0, in all those species, and the total rate of metabolic energy consumption, E_0, by all those individuals.
There is no way to justify this or any other choice of state variables a priori. Similarly to thermodynamics, only the empirical success of theory can explain the choice of fundamental entities (for example, molecules or individual organisms) and state variables (for example, pressure, volume, number of moles, or A_0, S_0, N_0, E_0) upon which theory is built.

2.2.2 The structure of METE

The theory is founded on two MaxEnt calculations: the first generates all the metrics used to describe abundance and energy distributions, while the second specifies the spatial scaling features of species distributions.

Abundance and energy distribution

METE's fundamental theoretical concept is a joint, conditional probability distribution $R(n, \epsilon|A_0, S_0, N_0, E_0)$. Because this distribution is of critical importance to METE, it will be referred to as the ecosystem structure-function. It is defined in A_0 over species and individuals (within any given taxonomic group), and it describes the distribution of individuals across species and the distribution of metabolism across individuals. R is a continuous distribution in terms of metabolic energy rate and a discrete distribution in terms of abundance, n.
$Rd\epsilon$ is the chance that if a species is randomly chosen from its pool, it will have an abundance of n, and that if an individual from that species is randomly chosen, its metabolic energy need will be in the interval $(\epsilon, \epsilon + d\epsilon)$. It is important to underline that it is a rate of energy consumption, not an amount of energy, and hence is a measure of power, not energy. It is supposed that there is a minimal metabolic rate, ϵ_{min}, below which no individual, regardless of how tiny the pool of No individuals is chosen to be, may exist. By virtue of our choice of energy units, ϵ_{min} is set to 1. This choice of units implies that if we assume a power-law connection between an individual's metabolic rate and body mass of the form $\epsilon = cm^b$, we may set the constant c equal to 1. The following is the normalisation requirement for R:

$$\sum_{n=1}^{N_0} \int_{\epsilon=1}^{E_0} d\epsilon R(n, \epsilon|A_0, S_0, N_0, E_0) \tag{2.18}$$

The three state variables S_0, N_0, and E_0 place two more constraints on the ecosystem structure-function. These state variables define two unique ratios: $\frac{N_0}{S_0}$ denotes the species' average abundance, whereas $\frac{E_0}{S_0}$ denotes the species' average metabolic rate. As a consequence, the following constraint equations for R are obtained:

$$\sum_{n=1}^{N_0} \int_{\epsilon=1}^{E_0} d\epsilon n R(n, \epsilon|A_0, S_0, N_0, E_0) = \frac{N_0}{S_0} \tag{2.19}$$

and

$$\sum_{n=1}^{N_0} \int_{\epsilon=1}^{E_0} d\epsilon n \epsilon R(n, \epsilon|A_0, S_0, N_0, E_0) = \frac{E_0}{S_0} \tag{2.20}$$

The distribution $R(n, \epsilon)$ may be obtained by optimising the distribution's information entropy:

$$I_R = -\sum_{n=1}^{N_0} \int_{\epsilon=1}^{E_0} d\epsilon R(n, \epsilon) log(R(n, \epsilon)) \tag{2.21}$$

Subject to the constraints of Eqs 2.18-2.20. By setting the units of the continuous variable such that the lower limit of integration equals the lowest attainable

metabolic rate, it is avoided the requirement for a prior distribution to verify that the MaxEnt solution for $R(n, \epsilon)$ is unit independent Numerous metrics can be deduced from the distribution R. For instance, the species–abundance distribution is obtained by subtracting the energy variable from the equation:

$$\Phi(n|S_0, N_0) = \int_{\epsilon=1}^{E_0} \epsilon R(n, \epsilon|S_0, N_0, E_0) \tag{2.22}$$

Likewise, the community energy distribution is determined by:

$$\Psi(\epsilon|S_0, N_0) = \frac{S_0}{N_0} \sum_{n=1}^{N_0} nR(n, \epsilon|S_0, N_0, E_0) \tag{2.23}$$

The intra-specific metabolic rate distribution $\theta(\epsilon|n)$ can be easily deduced from the definition of the ecosystem structure function $R(n, \epsilon)$. $\theta(\epsilon|n)$ is the probability that an individual has a metabolic rate in the interval $(\epsilon, \epsilon + d\epsilon)$ if the species has abundance n, and $\Phi(n)$ is the probability that a species has abundance n. As a result of fundamental rule $P(A|B)P(B) = P(A, B)$, we can write:

$$\theta(\epsilon|n) = \frac{R(n, \epsilon)}{\Phi(n)} \tag{2.24}$$

Species-level spatial distributions across multiple scales

The measure P is highlighted in this section $\Pi(n|A, n_0, A_0)$. It will be seen that there are two equally reasonable a priori strategies to generate this metric at various spatial scales using MaxEnt. Only the comparison with data will reveal which one is correct. The MaxEnt concept can be applied to any complex system, which involves a determination of the fundamental entities (in the standard thermodynamic example, molecules) and the specification of a collection of state variables. METE predicts probability distributions for two types of entities, "individuals" and "species". The term "species" is defined as any well-defined collection of "individuals". The groups could be taxonomic species (as presumed here), genera, or even trait groups. Furthermore, the term "individuals" shall be defined in the conventional sense of individual organisms. The only criterion for selecting entities in a MaxEnt application is that they are explicitly defined in a way that allows specification of the numerical values of the state variables and, consequently, of the quantitative constraints on the probability distributions, as we shall see. However, this does not mean that if MaxEnt produces good predictions for one set of fundamental units, it will inevitably produce accurate forecasts for others. We define macroecology's state variables as the system's area, A_0, the number of species,S_0, in any specified taxonomic category, such as plants or birds, in that area, and the total number of individuals, N_0, in all those species, and the total rate of metabolic energy consumption, E_0, by all those individuals. There is no way to justify this or any other choice of state variables a priori. Similarly to thermodynamics, only the empirical success of the theory can justify the choice of fundamental entities (for example, molecules or individual organisms) and state variables (for example, pressure, volume, number

of moles, orA_0, S_0, N_0, E_0) upon which theory is built. We have the normalisation

$$\sum_{n=0}^{n_0} \Pi(n|A, n_0, A_0) = 1 \tag{2.25}$$

At any scale, A. Because the mean value of n is given by:

$$\bar{n} = \frac{n_0 A}{A_0} \tag{2.26}$$

over cells in area A, we also have the constraint equation:

$$\sum_{n=0}^{n_0} n\Pi(n|A, n_0, A_0) = \frac{n_0 A}{A_0} \tag{2.27}$$

Then, subject to the limits imposed by Eqs 2.25 and 2.27 , the information entropy is maximized: $-\sum_n \Pi(n) log(\Pi(n))$.

Solutions: $R(n, \epsilon)$ and the metrics derived from it

Utilising the methods outlined in Appendix A, the maximum of information entropy I_R in Eq. 2.21 results in the following:

$$R(n, \epsilon) = \frac{1}{Z} e^{-(\lambda_1 n)-(\lambda_2 n\epsilon)} \tag{2.28}$$

Z is the partition function, and the two Lagrange multipliers, λ_1 and λ_2 are obtained by applying.

$$\frac{\delta log(Z)}{\delta \lambda_k} = - < f_k > \tag{2.29}$$

to $< f_1 >= \frac{N_0}{S_0}$ and $< f_2 >= \frac{E_0}{S_0}$. To facilitate future reference, we now define:

$$\beta = \lambda_1 + \lambda_2 \tag{2.30}$$

$$\sigma = \lambda_1 + E_0 \lambda_2 \tag{2.31}$$

$$\gamma = \lambda_1 + \epsilon \lambda_2 \tag{2.32}$$

Making some approximations and assuming $e^{-S_0} << 1$, result in the approximate forms for the distributions $\Phi(n)$, $\Psi(\epsilon)$, and $\theta(\epsilon|n)$. It is possible to write these distributions explicitly with the conditional variables:

$$\Phi(n|S_0, N_0) \approx \frac{1}{log(\beta^{-1})} e^{\frac{-\beta n}{n}} \tag{2.33}$$

$$\Psi(\epsilon|S_0, N_0, E_0) \approx \lambda_2 \beta \frac{e^{-\gamma n}}{(1 - e^{-\gamma})} \tag{2.34}$$

$$\Theta(\epsilon|n, S_0, N_0, E_0) \approx \lambda_2 n e^{-\lambda_2 n(\epsilon-1)} \tag{2.35}$$

Comparing these metrics to empirical data is most effectively achieved using cumulative distribution functions or their related rank–abundance and rank–metabolism

functions. We obtain closed-form equations for the rank–energy functions from Eqs 2.34 and 2.35 and analyse the rank–abundance relationship deduced from Eq. 2.33 in the following subsection. Although no closed-form rank–abundance connection can be established from Eq. 2.33, a useful and simple formula for the expected number of rare species can be constructed, as will be demonstrated later. Consider first the distribution of metabolic rates among all community members. For this we turn to $\Psi(\epsilon)$ given in Eq.2.34. Referring to $\Phi(n) = -(1/S_0)/(dn/dn)$, which shows how to relate rank–variable relationships to probability distributions, we can derive the rank–metabolism relationship corresponding to $\Psi(\epsilon)$ (for the complete derivation see [8]).
We can construct the rank–metabolism connection for $S_0 > 4$ by relating rank–variable relationships to probability distributions. We will associate the individual with the highest metabolic rate with rank and the individual with the lowest metabolic rate with rank $r = N_0$ value. Keeping in mind that metabolic rate units are chosen in such a way that the lowest feasible rate is one, it is obtained:

$$\int_1^{\epsilon\Psi(r)} d\epsilon\Psi(\epsilon) = \frac{1}{N_0}\int_{r-\frac{1}{2}}^{N_0} dr = 1 - \frac{r-\frac{1}{2}}{N_0} \tag{2.36}$$

This expression's factor of $\frac{1}{2}$ requires some more explanation. The factor of two is included in this expression because, on a graph with metabolic rate as the horizontal axis and each individual receiving an equal share, $\frac{1}{N_0}$, of probability, the most energetic individual should have a metabolic rate that is intermediate between the maximum possible rate (E_0) and the rate that is roughly halfway between its actual rate and that of the second-highest individual. As a result, about half of its probability share ($\frac{1}{N_0}$) should correspond to values of $\epsilon > \epsilon_{max}$. Fortunately, the rank distribution is only a little affected by the factor $\frac{1}{2}$ in the expression $\frac{1}{2}N_0$. Using Eq. 2.34, the remaining integral in Eq. 2.36 can be solved by substituting $x = e^{-\gamma}$ for $\gamma = \lambda_1 + \lambda_2\epsilon$. By excluding terms from order β^2, the following results:

$$\int_1^{\epsilon\Psi(r)} d\epsilon\Psi(\epsilon) \approx -\frac{\beta}{1 - e^{-(\lambda_1+\lambda_2\epsilon\Psi(r))}} \tag{2.37}$$

By substituting this expression for the right-hand side of Eq. 2.36, we can write:

$$\epsilon_\Psi(r) = \frac{1}{\lambda_2} log(\frac{\beta N_0 + r - \frac{1}{2}}{r - \frac{1}{2}}) - \frac{\lambda_1}{\lambda_2} \tag{2.38}$$

A similar approach can be used to determine the rank–metabolism rate of individuals within a species. This is accomplished by referring to the distribution $\Theta(\epsilon|n)$ in Eq. 2.35. Due to the fact that it is defined across all individuals within a species of abundance n, the rank values will range from 1 (the most energetic individual) through n (the least energetic individual). As a result,

$$\epsilon_\Theta(r, n) = 1 + \frac{1}{\lambda_2 n} log(\frac{n}{r - \frac{1}{2}}) \tag{2.39}$$

Predicted forms of other energy and mass metrics

From Eq. 2.35, we can now extract the predicted form of the energy metric $\bar{\epsilon}(n|..)$ which describes the average metabolic rate of individuals in a species as a function of their abundance:

$$\bar{\epsilon}(n|S_0, N_0, E_0) = \int d\epsilon \epsilon \Theta(\epsilon|n) \approx 1 + \frac{1}{n\lambda_2} \tag{2.40}$$

Now we can identify the conditional factors on which $\bar{\epsilon}(n|..)$ is dependent: the state variables S_0, N_0 and E_0 that determine λ_2.
We can deduce the form of $\nu(\bar{\epsilon}|..)$ from Eq. 2.40 which represents the distribution of average metabolic rates across all species. To begin, we note from Eq. 2.40:

$$\frac{d\bar{\epsilon}}{dn} \approx \frac{-1}{n^2\lambda_2} \tag{2.41}$$

As a result, using Eq. 2.33:

$$\nu(\bar{\epsilon}|S_0, N_0, E_0) = \Phi(n(\bar{\epsilon}))|(\frac{d\bar{\epsilon}}{dn})^{-1}| \approx \frac{1}{log(\beta^{-1}}\lambda_2 n(\bar{\epsilon}) e^{-\beta n(\bar{\epsilon})} \tag{2.42}$$

As we can see, the conditional variables that influence the distribution of average metabolic rates among species are identical to the state variables that determine λ_2 and β. To illustrate the structure of this energy distribution more precisely, we utilise Eq. 2.40 to write:

$$n(\bar{\epsilon}) \approx \frac{1}{\lambda_2(\bar{\epsilon} - 1)} \tag{2.43}$$

Substituting this into Eq. 2.42 results in the following:

$$\nu(\bar{\epsilon}|S_0, N_0, E_0) \approx \frac{1}{log(\beta^{-1})} \frac{e^{\frac{\beta}{\lambda_2(\bar{\epsilon}-1)}}}{(\bar{\epsilon} - 1)} \tag{2.44}$$

If $S_0 << N_0 << E_0$, as is frequently the case, the term $\frac{\beta}{\lambda_2}$ in the exponent will be $>> 1$. Equation 2.44 predicts a unimodal distribution, increasing fast at minuscule $\epsilon - 1$ to a value peaking at $\epsilon = \frac{\beta}{\lambda_2}$, and then gradually decreasing to $\frac{1}{(\epsilon-1)}$ for $\epsilon >> \frac{\beta}{\lambda_2}$. This behaviour is illustrated by plotting the distributions versus $\bar{\epsilon}$ for a variety of state variable selections. Regardless of the state variables' values, and therefore of $\frac{\beta}{\lambda_2}$, the distributions plotted against $log(\bar{\epsilon})$ have an extended tail to the right of the mode. Despite appearances, the distributions are all normalised to one when plotted against the logarithm of $\bar{\epsilon}$.

Solutions: $\Pi(n)$ and the metrics derived from it

Along with the normalisation requirement, a single additional limitation on the species-level spatial abundance distribution can be placed $\Pi(n|A, n_0, A_0)$. This constraint, denoted by Eq. 2.27, can be conceived of in two ways. Either the abundance, n_0, is predetermined since it is measured, or it is chosen from the species–abundance distribution, $\Phi(n)$, which is known or estimated for the state variables S_0, N_0. It is advisable to focus on circumstances when n0 is actually measured on draws from

the species–abundance distribution when evaluating the prediction for $\Pi(n)$. Under the restrictions of Eqs 2.25 and 2.27:

$$I_\Pi = -\sum_{n=0}^{n_0} \Pi(n) log(\Pi(n)) \tag{2.45}$$

provides the distribution:

$$\Pi(n) = \frac{e^{-\lambda_\Pi n}}{Z_\Pi} \tag{2.46}$$

The summation of the normalising functions can be performed precisely, providing the partition function:

$$Z_\Pi = \sum_{n=0}^{n_0} = 1 - e^{\frac{-\lambda_\Pi (n_0+1)}{1-e^{-\lambda_\Pi}}} \tag{2.47}$$

The Lagrange multiplier is then obtained by solving Eq. 2.27. To simplify the notation, we define $= e^{-\lambda_\Pi}$, which results in:

$$\bar{n} = \frac{n_0 A}{A_0} = \frac{\sum_{n=0}^{n_0} n x^n}{\sum_{n=0}^{n_0} x^n} \tag{2.48}$$

Consider the implications of Eqs 2.46, 2.47, and 2.48 for the situation already discussed. It was analysed how individuals are assigned to the two halves of a bisected plot: $A = A_0/2$. For any n_0, the solution to Eq. 2.48 is $\lambda_\Pi = 0 (x = 1)$, and Z is now equal to $n_0 + 1$. Thus:

$$\Pi(n|\frac{A_0}{2}, n_0, A_0) = \frac{1}{1 + n_0} \tag{2.49}$$

In other words, the MaxEnt result establishes that the probability distribution defining the division of individuals between the two sides of a plot is uniform.

The predicted species-area relationship

Assume you want to know the number of species of plants, or other taxonomic groups, that inhabit a given region. This area may be an entire biome, or it could be as little as a square kilometre of a particular habitat. The prior information may include the species and individuals present in a sample of smaller plots within the broader region. This is the difficulty of increasing the species' richness on a larger scale. The same principle that could be used to up-scale may also be used to down-scale: to forecast the average number of species found in tiny plots based on information on the species richness in the wider region encompassing those small plots.

We can begin by using Eq.2.3 which establishes a relationship between the number of species per unit area and the number of species per unit area.

A equals the value in area A_0. Regardless of whether we are up or down-scaling, the notation $A < A_0$ will always be utilised. To begin downscaling, empirical information of S_0 and N_0 in A_0 are used to forecast 0 for $A < A_0$ using Eq. 2.3. $\bar{S}(A)$ denotes the average species richness across a specified number of cells in area A.

$\bar{S}(A)$ would be the anticipated average across all cells in region A upon downscaling. $\bar{S}(A)$ is most often a weighted average across a selection of cells in area A for which empirical values of species richness are available, and we use Eq. 2.3 to infer $S_0 = S_0(A)$ for values of $A_0 > A$.
We can down- or up-scale by doubling or halving the area at each step and readjusting the species–abundance distribution to account for the new knowledge about S and N. In such a scenario, knowledge of $\Pi(n|A, n_0, A_0)$ is sufficient for values of $A_0/2$. An alternative strategy is to assume the METE form for the spatial abundance distributions at the species level $\Pi(n|A, n_0, A_0)$ at each scale ratio, A_0/A, of interest. In this example, we next use the species-level geographic abundance distributions for arbitrary scale ratios, A/A_0, to up-or down-scale. We begin by defining the downscaling problem. Assume we know that area A contains S(A) species and N(A) individuals and that we would like to get the average of the species richness values over a large number of plots of area A/2 nested inside A. Not that a plot of area A/2 does not have to be the left or right, or top or bottom, half of A. Because the Lagrange multiplier, β, will be evaluated at many scales in this section and the following, we express it as $\beta(A)$ to make the scale at which it is evaluated easily. By substituting $\Pi(n|A_0/2, n_0, A_0)$ into Eq. 2.3 using Eq. 2.49, we can link $\bar{S}(A/2)$ to S(A) and N(A):

$$\bar{S}(A/2) = \bar{S}(A) \sum_{n=1}^{N_0} \frac{n}{n+1} \frac{1}{log\frac{1}{\beta(A)}} \frac{e^{-\beta(A)n}}{n} \tag{2.50}$$

To keep things simple, the subscript from the summation variable n_0 was removed. Additionally, note that we have written 0 rather than S(A), even though we presume that S has a defined value at scale A. The reason for this is that we will shortly utilise this formula at arbitrary scale transitions, not simply those in which we have precise information at the bigger size. Only the average species richness at both the larger and smaller sizes is known in those instances. At each scale, we shall use the sign N(A) rather than $\bar{N}(A)$. After finding $\bar{S}(A/2)$, $\bar{S}(A/4)$ can be obtained by iterating the following equation.

$$\bar{S}(A/2) = \bar{S}(A)e^{\beta(A)} - N(A)\frac{1 - e^{-\beta(A)}}{e^{-\beta(A)(N(A)+1)}}(1 - e^{\frac{-\beta(A)(N(A)}{N(A)+1}}) \tag{2.51}$$

Calculating $\beta(A/2)$ is necessary since it is determined by the now estimated $\bar{S}(A/2)$ and N(A/2). N must scale linearly with the area, as the total of the abundances in the two parts of A must equal N(A). As a result, $N(A/2) = N(A)/2$. When $N >> \bar{S} >> 1$ is present, Eq. 2.51 can frequently be simplified since $1 >> \beta$ and $e^{-\beta N}$ are present. As a result, the right-hand side of the equation:

$$\bar{S}(A/2) \approx \bar{S}(A) - \frac{\bar{S}(A)}{log(1/\beta(A))} \tag{2.52}$$

is always $< \bar{S}(A)$ if $\beta < 1$. If we now represent the species-area connection as $\bar{S}(A) \equiv A^z$ but allow for scale dependence in z, we may write:

$$\bar{S}(A) = 2^{z(A)}\bar{S}(A/2) \tag{2.53}$$

Then, from Eq. 2.52, follows:

$$z(A) \approx \frac{log(\frac{\frac{1}{\beta(A)}}{log(\frac{1}{\beta(A)})-1})}{log(2)} \tag{2.54}$$

If β is sufficiently small so that $log(\frac{1}{\beta}) >> 1$, Eq. 2.54 can be reduced further:

$$z(A) \approx \frac{1}{log(2)log(1/\beta(A))} \tag{2.55}$$

As long while $S >> 1$ and $1 >> \beta$ are true as Eq. 2.51 is iterated to finer scales, Eq. 2.55 holds true and offers a generic formula for z's scale dependency. Because $\beta(A)$ is a function of solely the ratio $\frac{\bar{S}(A)}{N(A)}$ assuming the inequalities hold, Eq. 2.55 indicates that all species-area connections should collapse onto a universal curve when $log(\bar{S}(A))$ is plotted against the variable $log(\frac{N(A)}{S(A)})$ rather than the standard variable $log(A)$. In other words, METE predicts that the value of $\frac{N(A)}{S(A)}$ at a certain scale dictates the form of the SAR at bigger or smaller scales.

2.2.3 Summary of the Major Predictions of METE

This section will summarise the critical METE predictions.

The species-level spatial abundance

At the spatial scale of a cell bisection, the spatial abundance distribution of species is similar to the uniform distribution predicted by the HEAP:

$$\Pi(n|A = \frac{A_0}{2}, n_0, A_0) = (1 - n_0)^{-1} \tag{2.56}$$

METE predicts an exponential (Boltzmann) distribution at finer scales, or the HEAP distribution if the bisection result is iterated. The collector's curve is constructed from the abundance distribution: $S(N) = N$ and $S(N) \equiv log(N)$ respectively for $\frac{N}{N_0} << \beta$ and $beta < \frac{N}{N_0} < 1$.

Distribution of species abundance

The Fisher logseries distribution is estimated to be $\Phi(n)$:

$$\Phi(n|S_0, N_0) = (c/n)e^{-\beta n}.$$

Here, c is a normalisation constant, and β is a function of S_0 and N_0 defined by the precise solution to:

$$\frac{N_0}{S_0} \approx \frac{\sum_{n=1}^{N_0} e^{-\beta n}}{\frac{\sum_{n=1}^{N_0} e^{-\beta n}}{n}}$$

or by the solution to:

$$\frac{S_0}{N_0} = \beta log \frac{1}{\beta}$$

In most cases, the expected number of species with a single individual is βN_0.

Species–area relationship

If the SAR is expressed as $S(A) = cS^{z(A)}$, $z(A)$ is assumed to be dependent on the state variables at scale A, as stated in Eq.

$$z(A) \approx \frac{log(\frac{log(1/\beta(A))}{log1/\beta(A)-1})}{log(2)}.$$

Given that $N(A)$ is proportional to A, the SAR takes on a universal shape, with plots of $S(A)$ vs N/S exhibiting a scale collapse onto a universal curve.

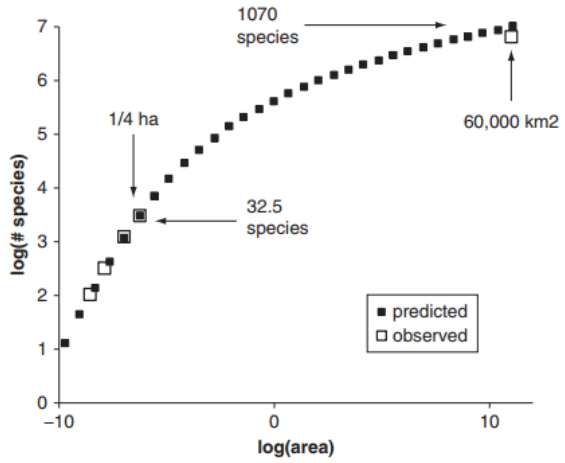

Figure 2.6: Test of upscaling and downscaling predictions for tree species' richness in the Western Ghats dataset. The input information for all the predicted values of species' richness shown in the graph are the averages of total abundance and species' richness [8].

Distributions of metabolic rates.

The following equation:

$$\epsilon_\Psi(r) = \frac{1}{\lambda_2} log(\frac{\beta N_0 + r + 1/2}{r - 1/2}) - \frac{\lambda_1}{\lambda_2}$$

predicts the rank–metabolism link for all individuals in a group. The distribution of metabolic rates inside each species is a Boltzmann distribution:

$$\Theta(\epsilon|n, S_0, N_0, E_0) \approx \lambda_2 n e^{-\lambda_2 n(\epsilon-1)}$$

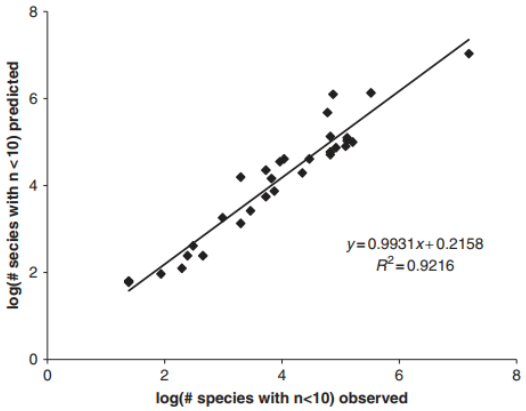

Figure 2.7: Test of the METE prediction for the number of rare species (here taken to be n 10) [8].

which declines monotonically with metabolic rate. By contrast, the distribution of intra-specifically averaged metabolic rates across species is unimodal:

$$\nu(\bar{\epsilon}|S_0, N_0, E_0) \approx \frac{1}{log(1/\beta)} \frac{e^{\frac{-\beta}{\lambda_2(\epsilon-1)}}}{(\bar{\epsilon}-1)}$$

The predicted mass distributions will vary according to the shape of the connection between mass and metabolic rate, $\epsilon(m)$.

Energy-equivalence principle.

The product of abundance times the average metabolic rate is projected to be independent of abundance. $n_0 < \frac{E_0 - N_0}{S_0}$. Communities of plants, animals, or birds with a high degree of size variation between species will contain species with a high degree of size variation between life stages.

2.2.4 Applications to Conservation Biology

Attempts to quantify the biological repercussions of human actions may frequently be reduced to a succession of smaller, or at least more concentrated, research subjects that conservation biologists deal with on a daily basis.
The topics covered may include the following: how to estimate species diversity at broad scales using small-scale census data, how to estimate the number of species at risk of extinction due to habitat degradation and how can we infer abundance from sparse presence/absence data.

Scaling up species' richness

A lot of research has been done by ecologists to answer the first question on this list. Knowing the form of the SAR at geographical scales ranging from tiny plots to entire biomes enables the calculation of biome-scale species richness using data from small

plots, and METE does exactly that. According to the theory, the slope z at each scale A within a biome is a universally decreasing function of the ratio N(A)/S(A), where N(A) is the total number of individuals in all species at that size and S(A) is the number of species at that scale. While more testing, particularly with animal data, is required, the theoretical prediction is consistent with observations over a wide range of habitats and geographical scales, from plots of a few square metres to vast expanses. There are several instances where this strategy will manifest a failure. The approach is incapable of predicting species richness in regions with a wide variety of habitats using data from tiny plots. To expand the theory to diverse biomes, data on species turnover as a function of the distance between tiny plots will need to be incorporated. However, when combined with data on arboreal arthropod diversity from tree-canopy fumigation, the proposed idea might be utilised to upscale the richness of arthropod species from the scale of each tree canopy to that of a broader region of a relatively similar environment.

Inferring abundance from presence-absence data

In conservation biology, inferring abundance from presence-absence data or from the findings of other incomplete census is critical. The fundamental concept behind any approach to this issue is as follows. For any imagined spatial abundance distribution at the species level, $\Pi(n|A, n_0, A_0)$, which is uniquely dependent on n_0, a known value of Π at any value of n determines n_0. With presence-absence data, in particular, a measured estimate of the proportion of cells in area A that are devoid of the species, $\Pi(0|A, n_0, A_0)$, suffices to determine n_0.

Estimating extinction under habitat loss

Thomas et al. (2004) developed a technique for calculating the number of species at risk of extinction as a result of habitat loss or degradation due to climate change or land-use patterns. They postulated that each species has a scaling formula for its chance of persistence as the amount of acceptable habitat for that species declines. Their recommended formula is as follows:

$$P_{after} = P_{before}(A_{after}/A_{before})^z \tag{2.57}$$

where P_{after} and P_{before} represent the chance of survival in the reduced habitat of area A_{after} and the likelihood of survival in the original habitat of area A_{before}. METE accomplishes the same purpose, but in order for the conclusion to be relevant to conservation biologists' concerns, certain explicit assumptions about the relationship between population size change and extinction risk must be made.

2.3 Testing METE

2.3.1 A General Perspective on Theory Evaluation

Evaluating a theory's "goodness" in absolute terms or compared to others is not a simple task to accomplish. Theories differ in terms of the number of changeable

parameters they include and, consequently, their ability to be modified flexibly to match empirical data. Additionally, they differ in their scope and the number of diverse phenomena they attempt to explain. As a result, comparing many hypotheses and determining which is the "best" one is not easy. There are statistical approaches for accounting for the number of fitting parameters to penalise heavily parameterised models or theories, but there is no indisputably optimum procedure. Furthermore, there are presently no formal processes for determining the best theory among a set of theories that predict the forms of a variable number of metrics with varying degrees of accuracy. Thus, there is no agreed-upon way of determining whether a theory that adequately predicts the form of two metrics or one that accurately predicts the form of five metrics is superior.

Finally, theory evaluation in ecology is complicated by the fact that the majority of datasets in macroecology contain poorly defined sources of uncertainty, resulting in ill-defined magnitudes of error. This is due to the following factors: the difficulty of truly replicating ecological phenomena, the inherent errors in census data collected by fallible observers, the stochasticity in the physical environment's influences on populations and the stochasticity in the demographics of those populations, even in the presence of a constant environment.

For the reasons stated before, the objective of testing METE is to determine the extent to which the theory captures the basic trends of macroecological empirical patterns.

It is critical to recognise that METE does not include any parameters for fitting. In other words, once the state variables S, N, and E are measured at some spatial scale A, all metrics (cell–occupancy distributions, species-area and endemics–area relationships, species–abundance distributions, and metabolic rate distributions across individuals and species) can be predicted at multiple spatial scales. Additionally, if the metabolic dependency on body mass is stated, the mass metrics are uniquely determined.

When comparing METE predictions to data, two difficult questions arise. The first is if the patterns are predicted accurately enough to be useful (for example, when extrapolating species' richness from small to large spatial scales). The second is there are systematic trends in the deviations between observation and prediction that may point to future refinements of the theory.

To validate METE's predictions, census data for plants, birds, arthropods, molluscs, and microbes were analysed. The data came from tropical and subtropical moist and dry forests, subalpine meadows, serpentine grasslands, deserts, temperate forest understory, and savannah. Most of the datasets analysed were from relatively undisturbed locations. Further tests of theory in highly disturbed environments, such as those following wildfire or avalanche (when a fast ecological recovery toward a pre-disturbed state takes place), were recently done and helped with the dynamic reformulation of METE.

2.3.2 Comparisons of the Predicted Distributions with Data

The species-level spatial abundance distribution

The predicted species-level spatial abundance distribution $\Pi(n|A, n_0, A_0)$ may be considered as METE's most precise forecasts. The latter refers to the distribution of individuals within a species over the two halves of a plot or to the distribution of individuals within a species across the two halves of a plot. METE forecasts that all possible allocations are equally likely within a plot's two halves.
To test the prediction, it is possible to check the proportion of each species' individuals located in the left-hand half of the plot and the fraction located in the upper half of the plot. If the hypothesis is correct, a plot of all these fractions should demonstrate that they all have an equal probability.
A practical approach to visualise these fractions is with rank–fraction graphs. If the fraction of individuals in the left- or top-half of all species with $n_0 > 1$ in A_0 is rank-ordered, with rank 1 corresponding to a fraction equal to 1 and the highest rank corresponding to a fraction equal to 0, then if the hypothesis is correct, a graph of observed fraction versus rank, with each data point representing a species, should be a straight line declining from 1 at rank 1 to 0 at the highest rank. According to the equal allocation prediction, a straight-line rank–fraction graph indicates that the probability distribution of the fractions is constant.
In comparison, if the distribution of individuals is randomly chosen from a binomial distribution, species are most likely to have roughly equal numbers of individuals in each half of the plot, and the majority of data points on a rank–fraction graph occur at fraction = 0.5, resulting in a nearly horizontal line over the majority of rank values, with an upturn at low rank and a downturn at high rank.
The iterated form of METE, which is identical to the HEAP model, predicts that this pattern will remain true at any spatial scale. For example, if a species is located in the top half of one of the plots and has an abundance of four, then all three distributions of its individuals between the top-left and top-right quadrants should be equally likely. Thus, when the fractions of each species in the upper-left quadrant of A_0 are rank-ordered and displayed as a rank–fraction graph, the same straight line should arise. Finally, the data seem to lie between the HEAP and MaxEnt predictions, with the more numerous species following the non-iterated MaxEnt forecast more closely.
There is strong but not substantial agreement between census data and METE predictions for species-level geographic abundance distributions. While statistics from a variety of sites appear to follow the equal allocation assumption, certain sites deviate significantly from the forecast. The projected link between cell occupancy and species–abundance is very variable around the line of a perfect agreement but is often relatively accurate.

The community-level species abundance distribution

Rank–variable graphs are frequently used to compare expected probability distributions to observed distributions. When plotted, log(abundance) vs rank distribution,

the expected rank–abundance distribution is a straight line for high rank but with an upturn for low rank. The magnitude of the expected upturn varies considerably, ranging from hardly discernible to fairly evident. The explanation for the variation in the degree of the upturn is that the measured value of the ratio, S_0/N_0, differs per location. The greater that ratio, the greater is β, the sum of the Lagrange multipliers appearing in the exponent of the anticipated log series distribution. And the greater the value of β is, the greater the upward trend on a log(abundance) vs rank graph. Indeed, if the value of log(abundance) is $\beta = 0$, the graph of log(abundance) vs rank is a straight line.
The agreement between the METE forecast and the data represented in the graphs is typically good. However, a few instances of considerable variance can be noted.
In conservation biology, one of the most critical characteristics to know of an ecosystem is the number of uncommon species, as they are the ones most likely to face extinction. The estimated number of species demonstrates METE's capacity to forecast the number of uncommon species, defined here as those with less than ten individuals. Thus METE successfully predicts the populations of uncommon species.
METE can also forecast the abundance of an ecosystem's most abundant species, and it was tested that (J. Harte et al., 2008) the prediction captures the majority of the variation in the data.

The species-area and endemics area relationships

Another noteworthy prediction of METE is that all species-area curves collapse into a universal curve when data are suitably rescaled. More precisely, METE argues that at any scale, A, the local slope of the SAR is a universal function of the ratio N(A)/S.
The more practical significance of the application of METE is to upscale species richness from small plots with accessible data to much larger sizes. And it is probable that the disparities between anticipated and observed slopes, z, of the SAR will accumulate to provide significantly erroneous estimates for large-scale species richness.

The distribution of metabolic rates

METE predicts the distribution of metabolic rates across all individuals, $\Psi(n)$, the distribution of metabolic rates across all individuals within a known abundance species, $\theta(\epsilon|n)$, and the distribution of the average metabolic rate of individuals within a species across species, $\nu(\epsilon)$. However, testing these assumptions is not easy since individual metabolic rates, and hence the overall metabolic rate,E_0, are rarely directly recorded in the kind of censuses that also yield values for our other state variables, S_0 and N_0. To validate metabolic rate distribution predictions, we must make one or both two assumptions: a metabolic scaling rule and allometry.
Assuming the metabolic scaling rule is accurate, it is possible to estimate metabolic rates using body mass data, which are easier to collect than metabolic rate measurements. However, research suggests that the power scaling rule is not strictly applicable throughout the whole range of natural body mass variance. It is unclear what the appropriate number to use for individual mass is for trees in particular. Ad-

ditionally, direct body mass measurements are unavailable in many circumstances, particularly with plants. Often, the basal area or diameter at breast height of trees is measured, from which the body mass of the tree may be determined, provided the plant's allometry is understood. However, such allometries are contentious. While simple laws such as the metabolic rate of an individual plant being proportionate to its total leaf area can be invoked, the corpus of an empirical study on plant allometry reveals major deviations.

2.3.3 Patterns in The Failures of METE

There are two plausible scenarios in which METE forecasts will fail. To begin, systems with very fast-changing state variables may not be properly characterised by a theory based on a static conception of state variables. As a result, it is easy to seek for failures in systems that are rapidly diversifying, degrading, or succession in the aftermath of disturbance.
Second, systems with highly variable habitat features across wide geographical scales are unlikely to meet the METE species richness scale-up prediction. In other words, attempting to scale up species richness using data from tiny plots within a single habitat type would likely underestimate species richness at big scales, as the species lists from the many habitats all add up to the large-scale species list.
Both of the preceding generalisations are supported by empirical data from METE testing. A site of intermediate age was analysed and resulted as the one that most radically deviated from the METE forecasts. Perhaps that location was the where species diversify most rapidly, as would be the case if species richness follows a logistic-type curve beginning with the formation of a colonisable, originally barren site. Beyond such speculation, there is evidence from moth censuses at various plots at Rothhamstead (Kempton and Taylor, 1974) that the log series species–abundance distribution more accurately describes the data in general, except for plots known to be undergoing rapid change in the aftermath of disturbance. METE also fails when used to elevate species richness in diverse regions.
Kunin et al. (2018) demonstrated that METE significantly underestimates the total number of plant species in the whole United Kingdom when the average S and N values from several plots are used as input data. As a result, the second of the two proposed scenarios for METE's failure is supported. This is unsurprising, given that the plots cover a diverse range of unique ecosystems with essentially non-overlapping species lists.
Erica A. Newman's research (2022) on macroecological patterns in a fire-dependent Bishop pine forest suggests that METE's predictions are more robust in late-successional, slowly changing, or steady-state systems than those undergoing rapid change in terms of species composition, abundance, and organism size. In contrast to a control site that has not burnt in decades, the SAR in a successional post-fire ecosystem deviates significantly from the METE forecast. Such shifts are also occurring in much longer time periods. For example, at younger sites in the Hawaiian Islands, where arthropod diversity is occurring more rapidly, the SAD and MRDI deviate from static theory predictions, in contrast to older sites on the islands.
Carey et al. (2006) demonstrated that the form of the SAR in recovered subalpine

vegetation plots following both the Mount St. Helens eruption and a hillslope-erosion event differed significantly from that reported in neighbouring undisturbed comparison plots.
At the Barro Colorado Island site in Panama, consistent divergences from MaxEnt predictions were noticed across the Smithsonian forest plots. In that location, the state variables S and N have decreased during the last 30 years, possibly as a result of a combination of local disturbance and the development of Gatun Lake, which resulted in the constructed island becoming semi-isolated from its metacommunity. At the moment, the shape of the SAD at BCI is intermediate between the log-series predicted by METE and the lognormal, with proportionally more intermediate-abundance species than observed in less disturbed Smithsonian forest plots, such as Cocoli and Bukit Timah, which are more in agreement with the log-series SAD predicted by METE.
The recent publication of John Harte et al. (2021) proposed a new extended macroecological theory from static to dynamic, DynaMETE. This theory will be discussed in greater detail in the following chapter.

Chapter 3

DynaMETE: A Candidate Dynamic Theory of Macroecology in The Anthropocene

3.1 The DynaMETE Theory's Predictions on Patterns Shifts in Perturbed Ecosystems

"It is not enough to change the world. We also have to interpret this change. And precisely in order to change it."

G. Anders, *The Obsolescence of Man*

Using restrictions imposed by static state variables, the Maximum Entropy Theory of Ecology (METE) predicts the forms of macroecological measures across geographical scales, taxonomic groups, and habitats. However, in disturbed ecosystems with time-varying state variables, its predictions often turn out to be inaccurate. By integrating the MaxEnt inference technique with explicit mechanisms driving disturbance, the macroecological theory is extended from static to dynamic. The resultant theory, DynaMETE, reduces to METE in the static limit but also predicts a novel scaling relationship for static state variables. DynaMETE predicts the time trajectories of state variables as well as the time-varying shapes of macroecological metrics such as the species abundance distribution and the distribution of metabolic rates across individuals in the presence of disturbances (expressed as shifts in demographic, ontogenic, or migration rates). An iterative approach for solving the dynamic version of the theory will be detailed in the following section. Finally, by combining both MaxEnt inference and explicit dynamical mechanisms of disturbance, DynaMETE becomes a potential macroecology theory for ecosystems reacting to anthropogenic or natural disturbances.

3.1.1 An Introduction and a Recall of METE

While the study of dynamic ecosystems is a growing field of research in ecology, the macroecological theory has largely ignored systems experiencing fast succession,

diversification, or collapse.
However, empirical evidence is increasing that dynamic and static ecosystems exhibit distinct and reoccurring macroecological patterns. In this part of the dissertation, the DynaMETE theory will be presented, and its applications for predicting macroecological patterns in dynamic systems will be explored [19]. The static theory (METE), based on the maximum entropy (MaxEnt) principle, offers a good starting point [20].
In order to make this chapter independent from the rest of the dissertation, it will be summarised very briefly what has been explained previously. Additionally, a glossary (Table 3.1) will be provided to ensure that all symbols used throughout the dissertation are comprehended.

Macrolevel state variables	
S	Total # species in community
N	Total # individuals in community
E	Total metabolic rate of community
B	Total biomass of community
P	Total productivity of community
S_m	Total # species in metacommunity
Microlevel-independent variables	
n	Abundance of a randomly selected species
ε	Metabolic rate of a randomly selected individual
m	Mass of an individual
Probability distributions	
$R(n,\varepsilon)$	Ecological structure function
$\phi(n)$	Distribution of abundances over species
$\psi(\varepsilon)$	Distribution of metabolic rates over individuals
Lagrange multipliers and functions thereof	
λ_i	Index i runs from 1 to 5
β	$\lambda_1 + \lambda_2$
β_m	β for the metacommunity
Z	Normalisation constant for R
$\gamma(\varepsilon)$	$\lambda_1 + \lambda_2\varepsilon$
Transition rate functions	
f	Governs the time rate of change of abundance
g, h	Governs the time rate of change of metabolic rates of individuals, species
q	Governs the time rate of change of species richness
Transition rate parameters	
b_0	A birth rate constant
d_0	A death rate constant
m_0	Immigration rate constant
w_0, w_1	Ontogenic growth rate constants
w_{10}	$w_1/\ln^{2/3}(1/\beta)$
E_C	Metabolic carrying capacity of ecosystem
μ	$\ln(1/\beta_m)/S_m$
σ_1, σ_2 speciation rate constants	
K	speciation saturation constant
Mathematical quantities	
γ	Euler's constant (~0.577)
$\delta_{n,1}$	Kronecker delta function (=1 if $n = 1$; = 0 otherwise)

Table 3.1: Glossary of symbols. [19]

MaxEnt chooses the flattest, hence least informative, probability distributions consistent with prior knowledge restrictions. Thus, bias is eliminated in the form of unsupported assumptions about the distribution (Jaynes 1957). Under imposed

limitations, a probability distribution, p(n), is obtained by maximising its Shannon information entropy (Shannon 1948).
The MaxEnt Theory of Ecology (METE) presupposes prior information in the form of static state variables characterising a taxonomic group (plants, for example) in a given region.
The original form of the theory includes four state variables: the ecosystem's size, A, the total number of species, S (within the taxonomic group of that specific ecosystem), the total number of individuals, N, within those species, and the total metabolic rate, E, of those individuals.
The predicted macroecological patterns include a log-series species abundance distribution (SAD) (Harte et al. 2008), a species-area relationship (SAR), and a metabolic rate distribution over individuals (MRDI). An extension of the original theory predicts species distribution over wider taxonomic categories and the dependency of the abundance–metabolism connection on the taxonomic tree structure (Harte et al., 2015).
METE's forecasts frequently fail in ecosystems that are experiencing fast change. When state variables change because of succession or anthropogenic disturbance, their values at any point in time no longer reliably predict the forms of macroecological metrics at that point in time.
There are several examples of systematic macroecological patterns in disturbed ecosystems. Some studies indicate a log-series SAD (as METE predicts) in less disturbed areas and a lognormal SAD in more disturbed areas, with fewer unusual species. Others demonstrate that when state factors (species richness and total abundance) in small-mammal groups are adjusted experimentally, the functional form of the SAD changes. Franzman et al. (2021) demonstrate that throughout several years of drought stress, both the SAR and SAD deviate increasingly from METE projections in an alpine plant community. Macroecological patterns also shift when systems are recovering from a perturbation.
The pattern of macroecological measures deviating from METE projections varies significantly among damaged ecosystems.
Whereas the SAD tends toward a lognormal distribution in certain disturbed sites, it tends toward a geometric distribution with a shortened tail at small n in others (alpine plant community). In certain disturbance sites (post-burn Bishop pine forest), the SAR deviates from the METE forecast toward a power-law behaviour, but in others, it deviates more from power-law behaviour (alpine plant community).
This wide range of macroecological pattern reactions to disturbances compels the scientific community to develop a theory that anticipates and interprets the links. This is to predict the possible threats from altered ecosystems under anthropogenic disturbance.
It will be demonstrated that DynaMETE predicts deviations from steady-state macroecological distributions depending on the type of disturbance. Additionally, it could forecast the future trajectories of state variables associated with damaged ecosystems.
METE makes the assumption that state variables vary slowly enough that their instantaneous values are sufficient to build macroecological distributions. The static METE theory becomes inadequate in a dynamic environment with fast-changing

state variables. In thermodynamics, if the macroscopic state variables are pressure, volume, and temperature, the Boltzmann distribution of molecule kinetic energy may be calculated using MaxEnt (Jaynes 1957, 1982). The instantaneous averaged values of pressure, volume, and temperature no longer define the instantaneous molecular energy distribution in an out-of-steady-state 'disturbed' gas, such as one with inhomogeneously varying temperature. In DynaMETE, the constraints imposed are added by the first-order derivatives of the state variables S, N, and E.
The MaxEnt approach for obtaining the least biased probability distributions is then combined with explicit processes that move the system away from a steady state. Due to the fact that the dynamics are dependent on time-dependent state variables, an iterative technique is proposed for updating both constraints and macroecological distributions.
The next subsection reviews METE and introduce the theoretical background for DynaMETE, including how explicit processes are included and upscaled from individuals to communities, as well as an iterative approach for producing predictions. After that, projected scaling connections between state variables in DynaMETE's static limit will be analysed. Then, the theory's dynamic predictions toward a steady state will be evaluated. In order to get projected trajectories for these variables under various perturbations, the coupled time-differential equations for the state variables will be solved (eqns 3.27–3.29). Additionally, it will be demonstrated the expected deviations in abundance and metabolic rate distributions under a range of perturbations using a first-order iteration of the entire theory. METE is based on a time-independent structure-function, where R is a joint conditional distribution over a species' abundance, n, and an individual's metabolic rate, $Rd\epsilon$ is the probability that a species was randomly chosen from the species pool, and that an individual randomly chosen from the species with abundance n has a metabolic rate in the interval $\epsilon + d\epsilon$.
A discrete notation for all variables n, ϵ, S, N, E is employed, with summation rather than integral signs, and follows the units convention that the smallest value for the metabolic rate is ϵ, the metabolic rate of the smallest organism. The static structure-function is subject to the following strict constraints:

$$\frac{N}{S} = \sum_{n,\epsilon} nR(n, \epsilon|S, N, E) \tag{3.1}$$

and

$$\frac{E}{S} = \sum_{n,\epsilon} n\epsilon R(n, \epsilon|S, N, E) \tag{3.2}$$

The MaxEnt solution for $R(n, \epsilon|S, N, E)$ is:

$$R(n, \epsilon|S, N, E) = \frac{e^{-\lambda_1 n - \lambda_2 n\epsilon}}{Z} \tag{3.3}$$

where Z^{-1} is a normalisation constant (see below). The λ's are Lagrange multipliers calculated using the values of S, N, and E. The number Z^{-1} is calculated as follows:

$$\frac{S}{N} \sum_{n=1}^{N} e^{-\beta n} = \sum_{n=1}^{N} \frac{e^{-\beta n}}{n} \tag{3.4}$$

The Lagrange multiplier, λ_2, is calculated as follows:

$$\lambda_2 = \frac{S}{E - N} \tag{3.5}$$

In general, state variables obey inequalities$E >> N >> S$, in which case $1 >> \beta$ and the answer to Eqn 3.4 are, approximately,

$$\frac{S}{N} \approx \beta ln(\frac{1}{1 - e^{-\beta}}) \approx \beta ln(\frac{1}{\beta}) \tag{3.6}$$

Additionally, within that range of approximation,

$$Z \approx \frac{ln(\frac{1}{\beta})}{\lambda_2} \tag{3.7}$$

The validity of these approximations will be assumed, and therefore we will write equations with the equal and not approximation sign. The species abundance distribution (SAD), $\Phi(n)$, obtained by summing R over metabolic rate, is the log-series distribution:

$$\Phi(n) = \frac{e^{-\beta n}}{n ln(\frac{1}{\beta})} \tag{3.8}$$

and the metabolic rate distribution over individuals (MRDI), obtained by summing $\frac{nRS}{N}$ overabundance, n, is the log-series distribution:

$$\Psi = \frac{\beta \lambda_2 e^{\gamma(\epsilon)}}{(1 - e^{-\gamma(\epsilon)})^2} \tag{3.9}$$

where

$$\gamma(\epsilon) = \lambda_1 + \lambda_2 \epsilon. \tag{3.10}$$

METE also incorporates an explicit spatial component. However, in order to concentrate on the fundamental principles behind DynaMETE, the spatial dimension will be omitted.

3.1.2 Architecture of DynaMETE

DynaMETE is a hybrid theory based on both the MaxEnt inference's logic and specific assumptions about the changement drivers. The structure-function, a dynamic generalisation of Eqn. 3.3 plays a critical role in connecting the microlevel, as defined by the independent variables n and ϵ, and the macrolevel, as defined by state variables. It can be used to derive dynamic macroecological metrics such as a time-dependent SAD.
The DynaMETE's structure is a collection of transition functions that characterise the rates of demographic, ontogenic, migratory, extinction, and speciation. They are derived from individual and population analysis and thus rely on n and ϵ.
To upscale from the time derivatives of the micro-level variables n and ϵ to the time derivatives of the macrolevel state variables S, N, and E, it is not possible simply

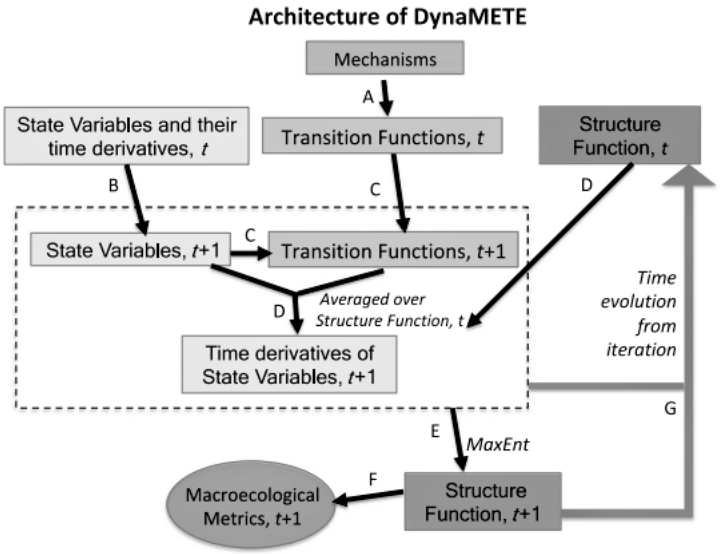

Figure 3.1: DynaMETE's architecture. (a) Transition functions contain selected mechanisms. (b) State variables' temporal derivatives are updated. (c) Transition functions that are state-dependent are modified. (d) To update the state variables' time derivatives, the updated state variables and transition functions are averaged across the prior (time t) structure-function. (e) MaxEnt modifies the structure-function when the constraints and transition functions are altered (dashed box). (f) The macroecological metrics are changed as a result of the structure function being updated. (g) Steps B–F are iterated. [Source: J. Harte et al., 2021]

replace n with N and ϵ with E in the transition functions due to these functions' nonlinearity. Rather than that, the transition functions are averaged across the dynamic structure-function. This function is then computed iteratively using MaxEnt, given the limitations imposed by the perturbed state variables and their temporal derivatives. DynaMETE's recursive architecture is seen in Figure 3.13.1. Notably, our difference between "steady-state" and "dynamic" applies solely to state variables. In the steady state, individuals can grow or die, and species' abundances can increase or decrease at any point in time, as long as the state variables remain constant.

Constraints on the dynamic structural function, R, at every point in time include state variables and their first time derivatives. Two Lagrange multipliers, λ_1 and λ_2, correspond to the restrictions imposed on state variables by their ratios, N/S and E/S, respectively, as in METE. Three more Lagrange multipliers, λ_3, λ_4, and λ_5 correspond to the $\frac{(1/S)dN}{dt}$, $\frac{(1/S)dE}{dt}$, and $\frac{dS}{dt}$ restrictions, respectively.

Consider an ecosystem in a steady state until time $t = 0$. The state variables were constant, and the structure-function was defined by Eqn 3.3. These processes may include extinction, speciation, and immigration for S; birth, death, and immigration for N and ontogenic growth, individual death. And immigration for E. At time $t = 0$, a disturbance is applied, such as a decrease in immigration due to habitat fragmentation or a change in the rate of ontogenic growth or per capita death due to climatic change.

DynaMETE depicts the system's temporal history following the disturbance as an iterated series of steps (A-G) in Fig. 3.1 and more explicitly in Table 3.2.

Step	Known	Derived from known
Before the perturbation		
1. In the steady-state past, the static structure function is derived from static state variables; this step generates eqn 3.	$X_{\text{past}}; \left\{\frac{dX_{\text{past}}}{dt}\right\} = 0;$ $\lambda_{j,\text{past}} = 0 (j = 3, 4, 5)$	$\lambda_{1,\text{past}}; \lambda_{2,\text{past}}; R_{\text{past}}$
Initialising the system right after the perturbation is imposed at t = 0		
2. A perturbation is now imposed, expressed by a change in one or more of the parameters, $\{c\}$, in the transition functions, k ($\{X\},\{c\}$). The initial time derivatives of the state variables are calculated from eqns 21–23.	$\{X_0\} = \{X_{\text{past}}\}; \lambda_{j,0} = \lambda_{j,\text{past}};$ $R_0 = R_{\text{past}}$; perturbed transition functions	$\left\{\frac{dX_0}{dt}\right\} \neq 0$
After the system is initialised to the Perturbation		
3. The state variables are updated using their time derivatives using eqn 20.	$\{X_0\}; \left\{\frac{dX_0}{dt}\right\}$	$\{X_1\}$
4. The transition functions are updated by substituting updated state variables.	$\{k(\{X_0\},\{c_0\})\}$	$\{k(\{X_1\},\{c_1\})\}$
5. The time derivatives of the state variables are updated using eqns 21–23.	$\{k(\{X_1\},\{c_1\})\}; R_0$	$\left\{\frac{dX_1}{dt}\right\}$
6. The structure function is updated from the constraints derived above using eqns 14–18.	$\{X_1\}; \left\{\frac{dX_1}{dt}\right\}; \{k(\{X_1\},\{c_1\})\}$	$\lambda_{1,1}, .., \lambda_{5,1}, R_1$
Subsequent steps repeat steps 3–6. With each update of the structure function, the updated effects of the perturbation on abundance and metabolic rate distributions can be derived.		

Table 3.2: The inference dynamics. An iterative procedure for solving equations involving dynamic state variables. The subscript I denotes time. X_i denotes the set of state variables S_i, N_i, and E_i; dX_i/dt denotes the set of their time derivatives, and $k(X_i, c_i)$ denotes the set of dynamic transition functions f, h, and q. [19]

To convert Fig. 3.1 and Table 3.2 to equations, it is necessary to define the transition functions. We represent the population change rate of an arbitrary species as:

$$\frac{dn}{dt} = f(n, \epsilon, X, c) \tag{3.11}$$

X refers to the collection of state variables, whereas c refers to the set of factors governing changes in the species' abundances, such as migration rate or per capita birth and death rates. The assumption that f and the other transition functions are independent of the $\frac{dX}{dt}$ is made. A species' metabolic rate can alter in response to population size changes or to an individual's ontogenic growth within the population. The individual's metabolic rate is referred to as its rate of change as follows:

$$d\epsilon/dt = (n, \epsilon, X, c) \tag{3.12}$$

Then d is the metabolic rate of a species.

$$\frac{d(metabolic\ \ rate\ \ of\ \ a\ \ specie)}{dt} = h(n, \epsilon, X, c) \tag{3.13}$$

where h is formed from f and g. (see SI-C). The time derivatives of N and E are defined as the functions f and h multiplied by S and averaged across the structure-function (Eqns 3.16 and 3.17 below).
Finally, the transition function $q(n, \epsilon, fgX, c)$ denotes the mechanisms regulating changes in species richness, such as extinction, immigration, and speciation; when averaged across the structure function, it yields dS/dt (Eqn 3.18 below). To denote the iterative process, we add a discrete time-step index, the time-dependent state variables, their time derivatives, the Lagrange multipliers, the transition rate parameters, and the structure-function will be denoted, respectively, as X_i, dX_i/dt, λ_{ji}, c_i, and R_i. The index j denotes the Lagrange multipliers and ranges between 1 and 5. Consider once more a system that was in steady-state in the past ($i < 0$), with static state variables, the static structure-function defined by equation 3.3, and the Lagrange multipliers defined by equations 3.5 and 3.6. For($i < 0$), $\lambda_{3,i}$, $\lambda_{4,i}$, and $\lambda_{5,i}$, the state variables' time derivatives disappear. At $i = 0$, an imposed disturbance is expressed as a change in one or more of the transition functions' parameters, c. It might be a parameter modification that occurs over time or one that occurs only once.
Iteratively, three groups of equations are cycled through. To begin, at any point in time, the structure-function is generated using MaxEnt, taking into account the limitations imposed by the instantaneous values of the state variables and their temporal derivatives:

$$N_i = S_i \sum_{n,\epsilon} n R_i(n, \epsilon, X_i, c_i) \tag{3.14}$$

$$E_i = S_i \sum_{n,\epsilon} n\epsilon R_i(n, \epsilon, X_i, c_i) \tag{3.15}$$

$$\frac{dN_i}{dt} = S_i \sum_{n,\epsilon} f(n, \epsilon, X_i, c_i) R_i(n, \epsilon, X_i, c_i) \tag{3.16}$$

$$\frac{dE_i}{dt} = S_i \sum_{n,\epsilon} h(n, \epsilon, X_i, c_i) R_i(n, \epsilon, X_i, c_i) \tag{3.17}$$

$$\frac{dS_i}{dt} = \sum_{n,\epsilon} q(n, \epsilon, X_i, c_i) R_i(n, \epsilon, X_i, c_i) \tag{3.18}$$

Equations 3.14 and 3.15 impose the same limitations as Equations 3.1 and 3.2, whereas Equations 3.16 and 3.18 introduce new constraints. For notational simplicity, the structure function's conditionality on the time derivatives of the state variables is implicit in Eqns 3.14–3.18. Equations 3.14 and 3.18 correspond to steps E and 6 in Figure 3.1. The following ecological structure-function is obtained from these equations using the MaxEnt inference procedure:

$$R_i(n, \epsilon, X_i, c_i) = Z_i^{-1} e^{-\lambda_{1,i} n} e^{-\lambda_{2,i} n\epsilon} e^{-\lambda_{3,i} f(n,\epsilon,X_i,c_i)} e^{-\lambda_{4,i} h(n,\epsilon,X_i,c_i)} e^{-\lambda_{5,i} q(n,\epsilon,X_i,c_i)} \tag{3.19}$$

where Z_i denotes a normalisation factor that is dependent on j,i: We need to update the state variables before iterating the structure function:

$$X_{i+1} = X_i + \frac{dX_i}{dt} \Delta t \tag{3.20}$$

With $\Delta t = 1$ and i integer.
This corresponds to steps B and 3 in Fig.1.1 and Table 3.2 respectively. Equation 3.20 then enables us to update the transition functions directly (step C in Fig.1.1, step 4 in Table 3.2):
Finally, we update the time derivatives of the state variables from time step i to time step $i + 1$ by averaging the transition functions over the structure function, with the Lagrange multipliers determined by Eqns 3.14–3.18 fixed at time step i and the transition functions f, h, and q appearing in the exponents of Eqn 3.19 evaluated at the $X_i + 1$:

$$\frac{dN_{i+1}}{dt} = S_{i+1} \sum_{n,\epsilon} f(n, \epsilon, X_{i+1}, c_{i+1}) R_i(n, \epsilon, X_{i+1}, c_{i+1}) \tag{3.21}$$

$$\frac{dE_i + 1}{dt} = S_{i+1} \sum_{n,\epsilon} h(n, \epsilon, X_{i+1}, c_{i+1}) R_i(n, \epsilon, X_{i+1}, c_{i+1}) \tag{3.22}$$

$$\frac{dS_{i+1}}{dt} = \sum_{n,\epsilon} q(n, \epsilon, X_{i+1}, c_{i+1}) R_i(n, \epsilon, X_{i+1}, c_{i+1}) \tag{3.23}$$

The subscript I indicates that the Lagrange multipliers in Eqns 3.21–3.23 are those at step i and so rely on X_i and dX_i/dt. Equations 3.21 and 3.23 correspond to steps D and 5 in Fig. 3.1.
DynaMETE consists of Equations 3.14 and 3.23. They can be iterated in order to determine the temporal evolution of both state variables and structural functions. The latter allows for the calculation of time-dependent SAD and MRDI (step F in Fig. 3.1).
We note that there is no mathematical or de facto connection between information entropy maximisation and equilibrium. At the conclusion of each entropy maximisation step, S, N, and E will typically have non-zero time derivatives, at least under disturbance, necessitating the need to update their values first, then their time derivatives, and finally their Lagrange multipliers in subsequent iterations. This process is continued until the system reaches an equilibrium point.
DynaMETE operates on a dual time scale. The rate constants in the transition functions will be expressed in inverse time units, and for practical reasons, this time scale may be readily expressed in years. The gap between iteration stages is another time scale. In general, increasing the rate of updating improves numerical accuracy, nevertheless, the ideal time intervals for the iteration process remain unknown.
The Supporting Information-A (SI-A) section discusses the justification for the term S by multiplying the summations in Eqns 3.16, 3.17, 3.21, and 3.22. SI-B section elaborates on the entire set of Eqns 3.14–3.23, proving their internal consistency.
Let's shift our attention to the hybrid theory's model-dependent, mechanistic parent: formulations for the transition functions f, h, and q.
A fairly broad theoretical framework was thus provided that may be applied to a wide range of dynamical systems. In order to proceed, specific model assumptions concerning mechanistic transition functions are made.
There is no agreed-upon collection of processes that determine the rates of change of n, nor is there an agreed-upon set of mathematical representations for selected processes. As is the case with any mechanistic model, the transition functions are

given in SI-C, with some extra mathematical information concerning diversification via immigration provided in SI-D. Alternatives to the transition functions specified here can easily be replaced.
In ecology, reasonable mathematical representations of extremely complicated and poorly understood systems are inherently simplified.
These decisions were made in accordance with metabolic theory conclusions (Brown et al. 2004) and with the scale-consistency constraints outlined below. The derivations from our selection of explicit functional forms for the transition function:

$$f(n,\epsilon) = (b_0 + d_0 E/E_c)\frac{n}{\epsilon^{1/3}} + m_0\frac{n}{N} \tag{3.24}$$

$$h(n,\epsilon) = w_0 n\epsilon^{2/3} - \frac{w_{10}}{ln^{2/3}(1/\beta)}n\epsilon - d_0 n\epsilon^{2/3}E/E_c + \frac{m_0 n}{N} \tag{3.25}$$

$$q(n,\epsilon) = \mu_0 e^{\mu-\gamma} + \frac{\sigma_1 KS}{K+S} + \frac{\sigma_2 b_0 nS}{\epsilon^{1/3}} - S\delta_{n,1}\frac{d_0 E/E_c}{\epsilon^{1/3}} \tag{3.26}$$

3.1.3 Summary of the Major Predictions of DynaMETE

To begin, we truncate the complete iteration procedure at step 2 of Table 3.2 and derive a set of coupled time-differential equations of motion (eqns 3.27–3.29) that predict relationships between state variables in steady-state and the dependence of state variable trajectories on the small perturbations to the transition function parameters. These conclusions should be considered approximations only for tiny deviations from steady-state, as they are derived from the static structure-function (Eqn 3.3) with a constant of one.
Then, in the first iteration of the whole theory (steps 3–6 in Table 3.2), eqns 3.14–3.23 are used to determine the lowest order effects on the structure function of various perturbations in the transition function rate constants. Next, the changed shapes for the abundance and metabolic rate distributions will be constructed using the perturbed structure function. These results may be significantly different from those achieved by higher-level repetitions.

Predicted properties of state variables near steady-state

We can obtain: Using eqns 3.21–3.23, transition functions stated in eqns 3.24–3.26, and R defined by eqn 3.3:

$$\frac{dN}{dt} = [b_0 - d_0(E/E_c)][\frac{1.21N^{4/3}ln^{1/3}(\frac{1}{\beta})(1+\frac{4Nln(1/\beta)}{3E})}{E^{1/3}} - \frac{3N^2ln(1/\beta)}{2E}] + m_0 \quad (3.27)$$

$$\frac{dE}{dt} = [w_0 - d_0(E/E_c)][\frac{2.42E^{2/3}N^{1/3}}{ln^{2/3}} - \frac{2.26E^{2/3}S^{1/3}}{ln(1/\beta)}] - \frac{w_{10}E}{ln^{2/3}(1/\beta)} + m_0 \quad (3.28)$$

In general, when it comes to immigration and both speciation and we have systems in place, in addition to extinction:

$$\frac{dS}{dt} = m_0e^{-\mu S-\gamma} + \sigma_1\frac{KS}{K+S} + \sigma_2b_0\frac{1.21N^{4/3}ln^{1/3}(\frac{1}{\beta})}{E^{1/3}} \quad (3.29)$$

$$(1+\frac{(4Nln(\frac{1}{\beta}))}{3E}) - \frac{3N^2ln(1/\beta)}{2E} - \frac{1.35d_0}{E_c}\frac{S^{4/3}E^{2/3}}{ln(1/\beta)})$$

Steady states

By zeroing out the temporal derivatives in eqns 3.27–3.29, we find the following connections between the static values of the state variables and the dynamic parameters. Using Eqn 3.27:

$$E = E_c\frac{b_0}{d_0}(1+\delta_E) \quad (3.30)$$

We can also derive that:

$$N = [\frac{0.41w_{10}}{w_0 - d_0(E/E_c)}]^3E(1-\delta_N) \quad (3.31)$$

For the immigration-only case $\sigma_1 = \sigma_2 = 0$, use eqn 3.29.
We obtain:

$$Se^{3\mu S/4} = [\frac{0.41m_0ln(1/\beta)}{d_0(E/E_c)}]E^{1/4} \quad (3.32)$$

Regarding cases $m_0 = \sigma_2 = 0$ and $S >> K$,

$$S = [\frac{0.35\sigma_1ln(1/\beta)}{d_0(E/E_c)}]^{3/4}E^{1/4} \quad (3.33)$$

If $S << K$, then:

$$S = [\frac{0.35\sigma_0ln(1/\beta)}{d_0(E/E_c)}]^3E \quad (3.34)$$

Finally, for the instance $m_0 = \sigma_1 = 0$:

$$S = [\frac{0.9\sigma_2b_0}{d_0(E/E_c)}]^{3/4}ln(1/\beta)E \quad (3.35)$$

The Species–Area Relationship in a Steady State (SAR)

We can obtain nested SARs from eqns 3.32–35 since E_c, E, and N grow linearly with area in a layered design. Taking the logarithm of Eqn 3.32 in the immigration-only model yields:

$$S = \frac{ln(E)}{3\mu} + \frac{ln(m_0)}{\mu} - \frac{4ln(S)}{3\mu} + \frac{ln(ln(1/\beta))}{\mu} + ln(\frac{0.41E_c}{d_0E}) \tag{3.36}$$

E_c, E, and N scale linearly with area in a layered SAR architecture, and in general, $E >> m_0$. Thus, S scales logarithmically with the area, with the third and fourth terms (see Eqn 3.6) on the right-hand side of Eqn 3.36 providing $ln(ln(area))$ corrections. If m_0 is a power of the area, the second term also produces a $ln(area)$.
The METE SAR was constructed using species abundance and spatial occupancy patterns at the species level. The DynaMETE forecast is not dependent on a spatial distribution function but on the processes governing the transition functions f, h, and q that resulted in Eqn 3.30. METE and the static limit of DynaMETE, however, predict comparable functional forms for the SAR in the migration model: $S \approx ln(area)$ with $ln(ln(area))$adjustments. Beyond this functional resemblance, numerical simulations for several state variables demonstrate that they predict almost overlapping SARs (see, e.g. Fig. 3.2). In the first speciation model, a quarter-power scaling of species richness with E (up to a correction of $ln(1/\beta)$) is obtained and hence with area from Eqn 3.33 with $S >> K$. S scales linearly with area in that model, with 3.29 and for any S in the second speciation model, up to a 3.30 correction. With a tiny saturation term K compared to the steady-state species richness, the first model produces a more realistic species-area relationship.
A connection exists between productivity, biomass, diversity, and abundance at a steady state.
Individual mass m is linked to individual metabolism by $m(\epsilon) = m(1)\epsilon^{4/3}$. To increase the magnitude of this expression from individual mass, m, to total community biomass, B, we must once again add the structure.
As calculated in SI-E, total biomass, B, is as follows:

$$B = m(1)S\sum_{n,\epsilon}\epsilon^{4/3}nR(n,\epsilon|N,S,E) = m(1)\frac{4.17E^{4/3}}{S^{1/3}ln(1/\beta)} \tag{3.37}$$

Thus, the link between community mass and metabolism includes both species richness and overall abundance via the $ln(1/\beta)$ term.
Interpreting the state variable E as the community's total net productivity P, Eqn 3.37 yields the following relationship between productivity, biomass, species richness, and abundance:

$$P = 0.343B^{3/4}S^{1/4}ln^{3/4}(1/\beta) \tag{3.38}$$

Where B and P are quantified in such a way that $m(\epsilon = 1) = 1$.
Because Eqn 3.29 was not used in its derivation, equation 3.38 does not depend on whether migration, speciation, or a combination of the two contributes to diversification. Nor is it dependent on the shapes of the transition functions, which can vary by habitat. Taking into account the different scaling exponents for the contributions

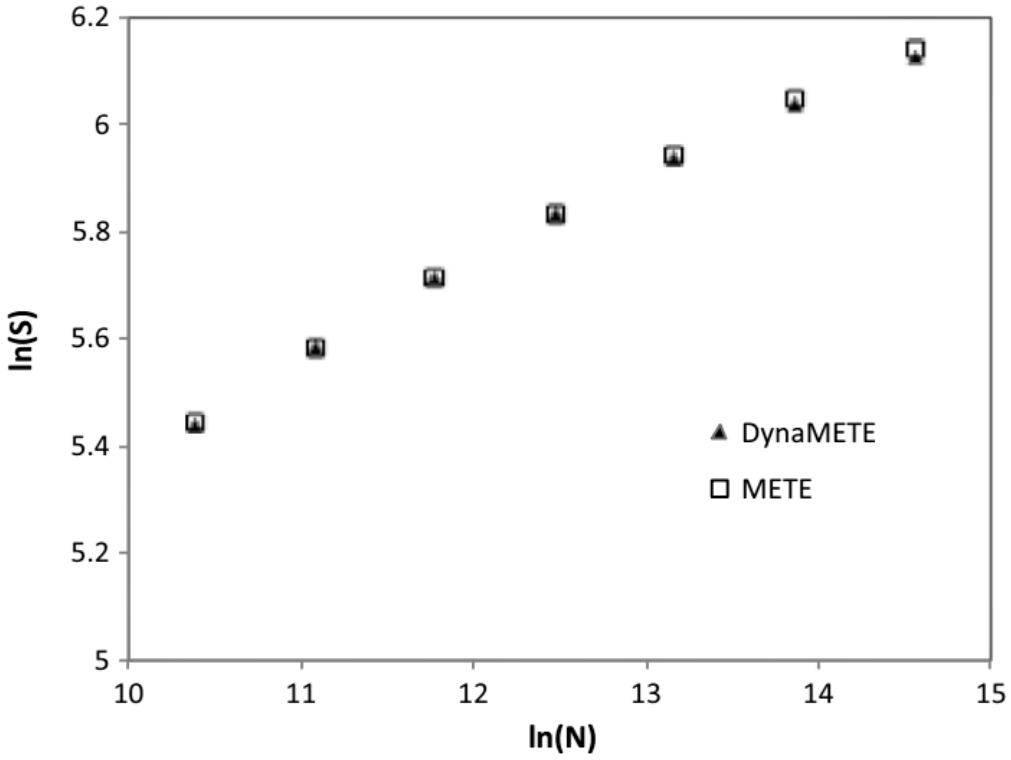

Figure 3.2: Comparing up- and down-scaled species richness using METE and DynaMETE, starting with the same species richness and abundance at the medium scale. The values of N, a scale factor used to represent the area, span a scale range of 2^7. For the medium scale, the transition function parameters and S and N values are taken from Table 3.3. Ec and m_0 are assumed to scale linearly with area for larger or smaller sizes, while the other parameters remain constant.[Source: J. Harte et al., 2021]

Parameter	Value
b_0	0.2
d_0	0.2
m_0	500
w_0	1.0
w_{10}	0.4096
E_c	2×10^7
$\mu = S_{meta}^{-1} \ln(1/\beta_{meta})$	0.0219
State variables	
S	320
N	230 000
E	2.04×10^7

Table 3.3: Parameter values for transition functions and state variables in a BCI-like forest ecosystem where diversification is solely facilitated by immigration. [19]

of biomass and species richness to P and the fact that $ln(1/\beta)$ varies approximately as $ln(N) - ln(S)$, the influence of biomass on productivity is significantly greater than that of species richness, which in turn is greater than that of abundance, which enters only via the $ln(1/\beta)$ term. Furthermore, while productivity and abundance are constant, total biomass fluctuates as $S^{1/3}$. Empirical surveys of the link between productivity, biomass, richness, and abundance are generally compatible with these findings, but additional analysis will be necessary to test Eqn 3.38. Equation 3.38 is an "ideal biodiversity law" a thermodynamic state variable relationship analogous to the ideal gas law.
Since this equation was calculated using the steady-state structure-function in Eqn 3.3, likely, it will no longer hold true when the state variables are rapidly varying. Following the disturbance, the whole structural function (Eqn 3.19) is required to determine the link between productivity–biomass–abundance–species richness, which will then rely on the nature of the disturbance process.
We now divert our attention away from DynaMETE's static limit and toward its dynamic predictions, analysing both state variable dynamics and the form of the SAD and MRDI when they are not in a steady-state.

Near-steady state dynamics of state variables

The time trajectories of the state variables approaching steady-state are deduced from eqns 3.27–29. The first-order reactions of state variables to various types of disturbances were analysed, as reflected by changing transition rate parameters and the recovery to steady-state following a perturbed state.
The transition rate parameters are provided for a forest approximating the BCI tropical forest plot in these dynamical simulations. Table 3.3 contains approximate transition rate constants for this location. Figures 3.3a–d exhibit the reactions of the state variables over 100 years to various disturbances indicated by modifying the values of the transition function's rate parameters.
Certain basic patterns appear regardless of the extent of these parameters' changes. Reduced immigration rate constants, for example, result in a linear reduction in S at small t, a weak, damped oscillatory response of N and an almost undetectable change in E. (Fig. 3.3a). Increased mortality (Fig. 3.3b) results in a moderate drop in S, a substantial initial decline in N, and a smaller initial decline in E, followed by damped oscillatory behaviour. When the ontogenic development rate is decreased (Fig. 3.3c), a practically indiscernible increase in S occurs, as does a substantial damped oscillatory initial rise in N and a mild damped oscillatory initial reduction in E.
Figure 3.3d illustrates the effect of combining perturbations in migration, mortality, and growth rates on state variable trajectories. A detailed comparison with real data will be not given here due to the first-order approximation used to obtain these theoretical curves, but it is positive that the time trajectories of the BCI state variables from 1985 to 2015 (inset in Fig. 3.3d) also exhibit a steady decline in S, a decline and then partial recovery in N, and very little variability in E. In the immigration-only model, if the transition rate parameters are left the same (Table 3.3) and first lower, the state variables by twenty per cent.

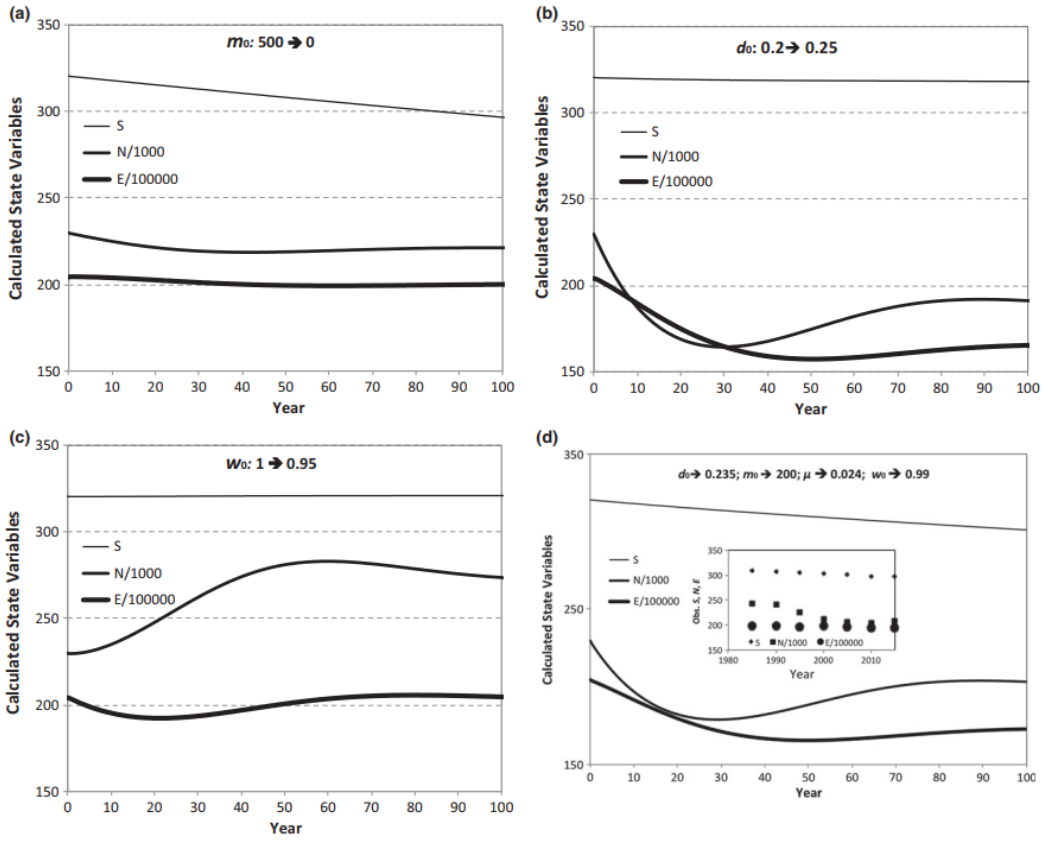

Figure 3.3: State variable responses to perturbations simulated using Eqns 3.27–29. (a) a decrease in the rate of immigration, m_0. (b) an increase in the mortality rate, d0. (c) a decrease in growth rate, w_0. (d) an increase in mortality and a decrease in immigration and ontogenic growth. The inset in 3d depicts the state variable trajectories in the BCI tropical forest plot from 1985 to 2015. Condit (2019) and Hubbell et al. (2005). The inset assumes that an individual's metabolic rate scales linearly with the basal area.[Source: J. Harte et al., 2021]

From their steady-state values, their return to steady-state is seen in Fig. 3.4. Notable features include S's monotonic recovery over centuries, N's massive overshoot and subsequent decrease to a steady state, and E's much lesser overshoot and decline.

If speciation is the primary engine of diversity, the pattern of species richness recovery is significantly different. These equations ran out to 3.48 and took the values of 3.49 and 3.50 as constraints in eqns 3.14–18 to calculate using MaxEnt, a perturbed structure function. S recovers to 3.45 of steady-state after around 4000 years in the second speciation scenario. N and E exhibit virtually identical recovery trajectories in both speciation models and are comparable to those seen in the immigration-only situation (Fig. 3.4).

DynaMETE's altered abundance and metabolic rate distributions

It is analysed, in a first approximation to a fully iterated solution, how different sorts of disturbances cause distinctive deviations from the steady-state form of the SAD, $\Phi(n)$, and the MRDI, $\Psi(\epsilon)$. Many steps from the iteration approach will be

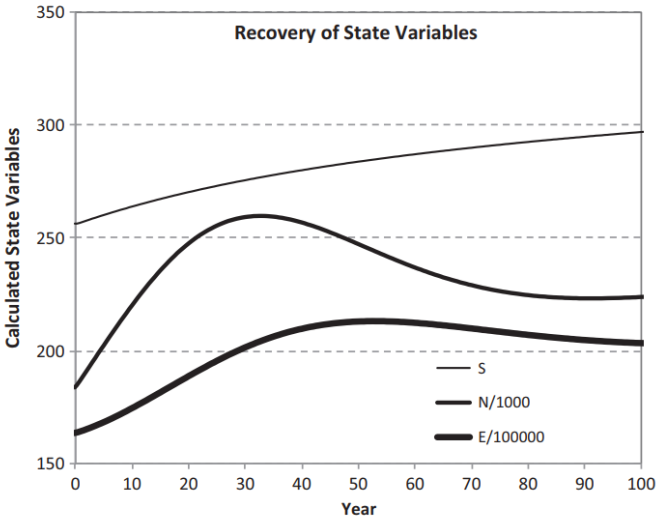

Figure 3.4: Illustrates the predicted recovery of state variables to their steady-state values, as predicted by Eqns 3.27–29, using steady-state parameters and initial state variables equal to 80 per cent of their steady-state values. The monotonic rise to steady-state in S and the large overshoot and subsequent damped oscillation in N, and the smaller overshoot and subsequent damped oscillation in E occur for a wide variety of initial depleted state variables, steady-state variables, and parameter choices.[Source: J. Harte et al., 2021]

omitted, most notably step 6 in Table 3.2. However, a single iteration at a one-year time step results in changes in the structure-function that are too modest to demonstrate meaningful divergences from the steady state. Thus a time step of 25 years is employed to provide a noticeable impact for a single iteration. To be more precise, the static structure-function is assumed, with Lagrange multipliers "frozen" at their static numerical values specified in eqns 3.21–23, perturb the transition functions by varying one or more rate constants, and then derive a set of time-differential equations for the state variables from eqns 3.21–23. These equations differ from eqns 3.27–29 in that the latter was calculated by periodically updating the Lagrange multipliers. Then these equations are extended to $t = 25$ and are used the values of $X(25)$ and $dX(25)/dt$ as constraints in eqns 3.14–18 to compute a perturbed structure-function using MaxEnt. This function will take the form of 3.19, and it will be used to generate perturbed variants of the species abundance distribution (SAD) and the metabolic rate distribution across individuals (MRDI), using the same summations as in eqns 3.8–9.

Fig. 3.5 illustrates the results. Table 3.4 contains the five calculated Lagrange multipliers. In this initial iteration of the entire structure-function, changing the immigration rate constant, m_0, to zero has a negligible effect on the SAD and MRDI (Fig. 5a and b). A 25-per cent rise in the mortality rate constant, d_0, causes the SAD to assume a lognormal form at intermediate abundances, as seen by the curving rank-log(abundance) graph (Fig. 3.5c). The rank-log(metabolism) graph becomes more complex, weaving around the METE prediction and predicting an increase in the number of the very smallest trees ($\epsilon = 1$), fewer individuals with low ($\epsilon = 2 - 100$) metabolism, and an increase in the number of trees with relatively high ($\epsilon = 100 - 100000$) metabolism, as well as a decrease in the sizes of the very

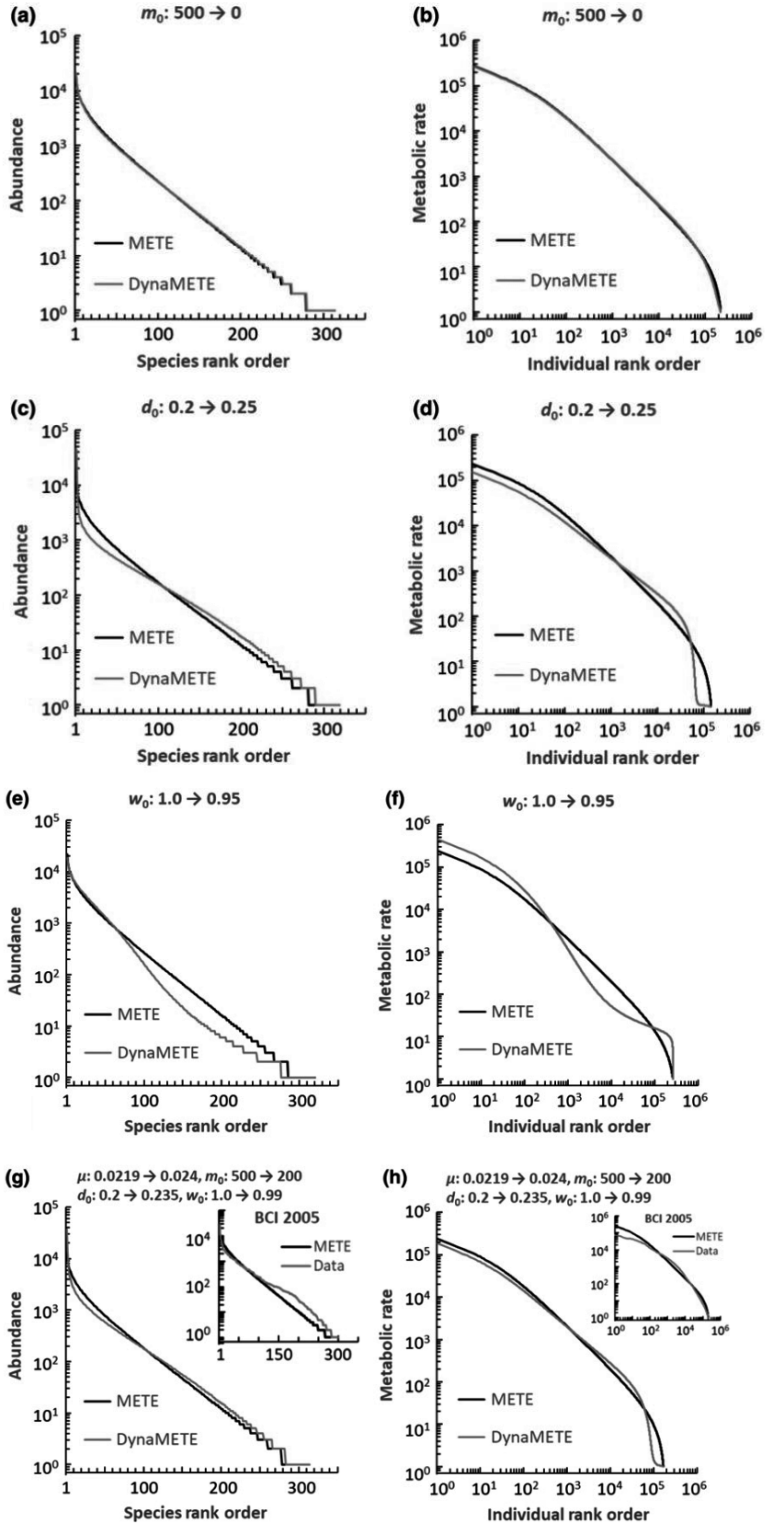

Figure 3.5: The effect of perturbations on the species abundance distribution (SAD) and the individual-level distribution of metabolic rates (MRDI). [Source: J. Harte et al., 2021]

largest individuals (Fig. 3.5d). Individuals' growth rates w_0 are reduced by 5-per cent, resulting in a nearly mirror-image shift in the SAD relative to an increase in

the mortality rate. The resulting SAD is essentially represented by an exponential distribution or an inverse power function with exponent>1 (Fig. 3.5e). Similarly, the change in the MRDI caused by a drop in growth rate is nearly identical to the change caused by an increase in mortality rate (Fig. 3.5f).
Figures 3.5g and h illustrate the effect of the identical combination of constant rate modifications as generated in Fig. 3.3d. We will not undertake a complete comparison with actual data in this section because of the first-order approximation utilised to create these theoretical curves. Still, we will remark on their approximate closeness to the empirical SAD and MRDI at BCI (see insets in Figs 3.5g and h).
It should be emphasised that solving eqns 3.14–23 fully iteratively in 25 one-year time steps over a period of 25 years may produce output that differs from the truncated solutions in Fig. 3.5 due to nonlinearities in the transition functions.
The results in Fig. 3.5 are analogous to a Taylor's series's first-order term. The iteration at a higher level is required to extend the predictions further into the future.

Discussion

DynaMETE was created to compensate for METE's inability to anticipate macroecological events in damaged, dynamic ecosystems. Because DynaMETE combines mechanism and MaxEnt, the theory's predictions diverge from METE in a manner dependent on the mechanism of the perturbation.
Within the limits of metabolic scaling theory, DynaMETE dynamics are characterised by processes dictating the microscale level of individuals and communities. Averaging the transition functions across the structural function derived from MaxEnt allows the upscaling to the macrolevel of communities.
This naturally leads to an iterative method, which is summarised in Fig. 3.1 and Table 3.2 and which is clearly expressed in eqns 3.14–23.
It has to be determined if this strategy, or alternatives such as the use of master equations to create stochastic realisations of population models, will lead to more accurate predictions.

A summary of the most relevant predictions

DynaMETE refinds the static METE predictions for the abundance distributions across species and metabolic rates across individuals in its static limit but also provides additional predictions. To begin, there is a scaling connection in steady-state between productivity, biomass, species richness, and abundance (Eqn 3.38). However, this relationship has yet to be confirmed. Second, in the version of DynaMETE in which only immigration, rather than speciation, contributes to diversity, DynaMETE predicts a static limit SAR growing to around $ln(A)$, with a $ln(ln(A))$ adjustment, which is quite near to the static SAR predicted by METE (Fig. 3.2). If speciation, rather than immigration, is considered to drive diversification, the SAR predicted by DynaMETE is highly dependent on the shape of the speciation rate's dependency on the variables S, N, n, and ϵ. If steady-state is obtained using $S >> K$ in the saturation model, we obtain a more realistic SAR (Eqn 3.33).

	$m_0 = 500 \rightarrow 0$	$d_0 = 0.2 \rightarrow 0.25$	$w_0 = 1.0 \rightarrow 0.95$	$\mu = 0.0219 \rightarrow 0.024$ $m_0 = 500 \rightarrow 200$ $d_0 = 0.2 \rightarrow 0.235$ $w_0 = 1.0 \rightarrow 0.99$
Figure	5a, 5b	5c, 5d	5e, 5f	5g, 5h
State variables and their rates of change used for constraints				
S	314.2	319.6	320.8	314.9
N	217 962	144 430	262 537	166 984
E	2.0380×10^7	1.7331×10^7	1.8280×10^7	1.7822×10^7
dS/dt	−0.242	−0.009	0.0246	−0.196
dN/dt	−418	−1052	2350	−758
dE/dt	−4349	−112262	−48162	−88709
Lagrange multipliers				
λ_1	0.00037020	0.0023398	−0.0073972	0.0014027
λ_2	0.000014717	9.6690×10^{-6}	0.000054585	0.000012665
λ_3	0.074392	0.16739	0.58409	0.16072
λ_4	−0.000015435	−0.00019515	0.00050473	−0.00010897
λ_5	−0.0049918	−0.015078	−0.27931	−0.0091964

Table 3.4: Figures 3.5a–h were generated using perturbations, constraints, and the resulting Lagrange multipliers. The text discusses the process by which the constraints are derived.

However, $S >> K$ contradicts the initial purpose for S-dependent speciation. DynaMETE provides a testable alternative: speciation is logarithmically dependent on species richness. This results in the probable SAR:

$$\frac{S}{ln^{3/4}(S)} \approx A^{1/4} ln^{3/4}(1/\beta) \tag{3.39}$$

Dynamics

By assuming a static structure-function (Eqn 3.3) in the theory's lowest order solution, eqns 3.27–29 predict time trajectories of the state variables for various sorts of perturbations to the transition function rate constants (Figs 3.3). For example, reduced immigration and growth rates combined with an elevated mortality rate produce trajectories similar to those reported in the BCI tropical forest study (see inset in Fig. 3.3d). Since these model simulations are dependent on extending the first-order iteration of the whole theory out in time, they are just indicative. Empirical testing will require additional iteration of eqns 3.14–23.

Additionally, DynaMETE forecasts state variable trajectories throughout an ecosystem's recovery from a perturbed condition. The predicted overshoot of N and subsequent decline to steady-state (Fig. 3.4) suggests the "dog tail" stage of forest succession, in which the abundance of small trees increases rapidly following a fire or other disturbance, E/N decreases. Then it self-restores the system to a quasi-steady state until the next disturbance.

In addition, DynaMETE predicts that different sorts of perturbations result in distinct patterns of divergence from static METE predictions (Fig. 3.5) for both species-level abundance distributions and individual-level metabolic rates.

These distinctive patterns may be used to characterise the mechanisms that drive ecosystem change in the presence of natural or human disturbance.

The SAD in the BCI tropical forest plot deviates from the log-series distribution anticipated by METE but matches the DynaMETE forecast when death, growth, and migration rates are perturbed together. The same perturbation leads to an MRDI that outperforms the METE prediction for individuals with a high metabolic

rate (big size) but over-predicts the number of individuals with a low metabolic rate. Further investigation of various parameter perturbations in conjunction with examining higher-order iterations of the dynamics is required.

3.1.4 Future Work

Flexibility of transition functions

Alternatives to the assumptions regarding the functional forms of transition functions can be considered. Additionally, a variety of alternatives exist for modelling the speciation rates' dependency on n and the state variables. When applied to forest census data that are restricted to trees with a certain minimum diameter-at-breast height, a tweak of the birth rate function can improve the realism of the transition functions.

Approaches to the higher-order iteration

Preliminary investigations of higher-order iterations in DynaMETE indicate that numerically solving the MaxEnt optimisation equations for the Lagrange multipliers can be very time-consuming. It is being assessed as a novel analytic technique for deriving and solving simultaneous linear differential equations for the Lagrange multipliers' time derivatives.

Traits

Individual metabolic rate (or body size) and species abundance are presently incorporated into DynaMETE. Other characteristics are overlooked or implicitly presumed to be distributed equally between species and individuals. METE predicts an inverse relationship between a species' abundance, n, and its average metabolic rate referred to as energy equivalence. METE, and DynaMETE may be expanded to incorporate more variables relating to other features or traits of individuals and species and analogues of energy equivalence for these. For instance, if one adds a new macro-level resource variable, W (for water availability), and an associated individual water uptake rate to the list of state variables, METE predicts a modified SAD, which has a higher degree of a rarity than the log-series distribution. If the transition functions are dependent on the individual water use efficiencies, the influence of water scarcity and the distribution of water use efficiencies on the SAD and MRDI should be examined.

Broader Issues

Both anthropogenic pressures and natural disturbances have the potential to induce fast changes in state variables, and hence systems suffering either form of disturbance may meet DynaMETE's requirement for a dynamic ecosystem. Although the data discussed at the beginning of the text indicates that systems subjected to either form of disturbance display macroecological patterns that depart from METE,

the applicability of DynaMETE to both anthropogenically and naturally disturbed ecosystems is still unknown. This is a high priority given the critical need to identify early warning signals which differentiate human impact on ecosystems from the effects of natural disturbance regimes. It was claimed that comparing patterns along disturbance gradients will yield no important new insights since the rules governing how process influences pattern will be consistent across all ecosystems. However, patterns do not depend on the process when the multiple mechanisms influencing ecosystems are in balance, resulting in static state variables. DynaMETE states that in disturbed systems with dynamic state variables, the underlying cause of disturbance controls macroecological patterns. In other words, the mechanisms have been altered as a result of the perturbation. It was argued that while physics maintains a clear distinction between the state of a physical system and the equations governing its time evolution, the successful biological theory will inevitably be self-referential or recursive in the sense that the state of the system will strongly influence the equations governing dynamics. This is also true for DynaMETE, and state variables are mentioned in the transition functions that drive state dynamics. Numerous academic fields seek to unify complex micro-and macro-level dynamics. It is speculated that the proposed iterative procedure at the heart of DynaMETE may find application in fields such as economics and statistical physics, where MaxEnt can capture static equilibrium patterns, but non-equilibrium dynamics remain elusive.

Conclusion

Even though ecosystems are dynamic and macroecological patterns change drastically in response to disturbance, dynamic macroecology has received insufficient attention. DynaMETE is a theory of dynamic macroecology which combines explicit processes of change with a powerful inference procedure called MaxEnt. By predicting how macroecological patterns will change in response to anthropogenic perturbations or natural successional and evolutionary forces, DynaMETE can contribute to a better understanding of disturbed ecosystems' fate, to the improvement of conservation and management strategies in ecology, to the development of early warning indicators for ecosystems in transition or at the edge of collapse, to the identification of specific processes driving ecological change and to understanding the roles of ecology and evolution in diversifying ecosystems. Thus, in the Anthropocene era, DynaMETE becomes a potential dynamical theory for macroecology.

3.2 Ecological Feedbacks to Global Warming: The Potential Threat from Altered Vegetation Communities

"We are rare and precious because we are alive because we can think. We are privileged to influence and perhaps control our future. We have an obligation to fight for life on Earth, not just for ourselves but for all those, humans and others, who came before us and to whom we are beholden, and for all those who, if we are wise enough, will come after. There is no cause more urgent than to survive to eliminate on a global basis the growing threats of nuclear war, environmental catastrophe, economic collapse and mass starvation. These problems were created by humans and can only be solved by humans."

C. Sagan, *Billions and Billions*

Over the last half-billion years, the evolution of land plants, carbon dioxide, and climate has kept atmospheric CO2 concentrations within finite limits, indicating the presence of an underlying complex network of geophysiological feedback.
However, continued increases in atmospheric carbon dioxide concentrations due to anthropogenic emissions are expected to result in significant climatic changes.
The ocean and forest ecosystems absorb approximately half of current emissions. Nonetheless, this absorption is affected by both climate and atmospheric carbon dioxide levels, creating a feedback loop.
To avoid this, more research must be conducted on the subject, with the resulting conservation and management strategies being implemented.

3.2.1 The Current State of the Climate

"We run carelessly over the precipice after having put something in front of us to prevent us from seeing it."

B. Pascal, *Thoughts*

There is a widespread scientific consensus that human activity has warmed the atmosphere, oceans, and land [21]. In only two centuries, there have been extended and rapid changes in the atmosphere, ocean, cryosphere, and biosphere. The magnitude of recent changes across the climate system as a whole and the present status of many aspects of the climate system is unprecedented in many hundreds to thousands of years (as can be seen in Fig. 3.6).
The anthropogenic climate change is already affecting a wide variety of weather and climate extremes in every region of the world. The evidence can be seen in the fast rise in extreme events such as heatwaves, heavy precipitation, droughts, and tropical cyclones, most of which are associated with human activities.

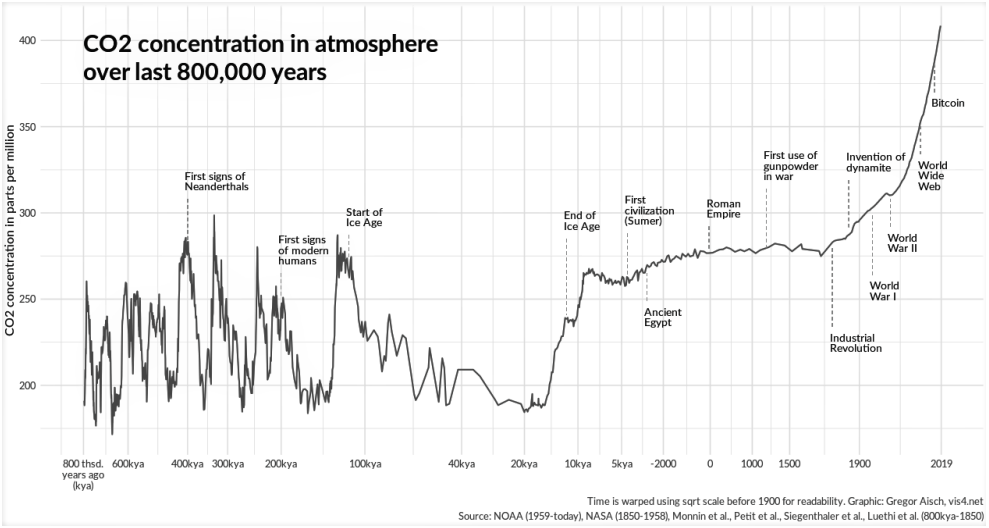

Figure 3.6: CO2 concentration in the atmosphere over the last 800,000 years. Time is warped using the sqrt scale before 1900 for readability. Graphic: Gregor Aisch, vis4.net. Source: NOAA (1959-2019), NASA (1850-1958), Monnin et al., Petit et al., Siegenthaler et al., Luethi et al. (800kya-1850).

Under all emission scenarios analysed, global surface temperature will continue to rise until at least the mid-century. The global warming of 1.5°C and 2°C will be exceeded during the twenty-first century unless significant reductions in carbon dioxide (CO2) and other greenhouse gas emissions will occur in the following decades.

Numerous changes in the climate system become more pronounced as global warming progresses. They include an increase in the frequency and intensity of hot extremes, marine heatwaves, heavy precipitation, droughts, and the proportion of powerful tropical cyclones, as well as decreases in Arctic Sea ice, snow cover, and permafrost. Global warming is also expected to further affect the worldwide water cycle, including its variability, global monsoon precipitation, and the intensity of long-lasting wet and dry periods.

In addition, ocean and terrestrial carbon sinks are expected to be less efficient at diminishing the accumulation of CO2 in the atmosphere under scenarios with increasing CO2 emissions.

Another aspect to point out is that any of these changes caused by past and future greenhouse gas emissions are irreversible, thus predestined to reverberate through the earth's ecosystems for centuries to millennia. This is particularly true for changes in the ocean, ice sheets, global sea level and vegetation.

Negative natural feedback and internal variability will partially mitigate human-caused damages, particularly at regional scales and in the short future, but will have little impact on the centennial global warming. These dynamics must be taken into account while considering and managing the whole spectrum of potential alterations of the climate.

In a scenario with prolonged global warming, each region is expected to face increasingly contemporaneous and numerous changes in the climatic effect drivers. Changes in several climate effect drivers would be more prevalent at 2°C global warming compared to 1.5°C global warming and would be much more extensive

and/or pronounced at higher warming levels.
Reducing human-induced global warming to a given level requires limiting cumulative CO2 emissions, achieving net-zero CO2 emissions before 2050, and significant reductions in other greenhouse gas emissions [22]. Significant, quick, and sustained reductions in CH4 emissions would also help to mitigate the warming effect of aerosol pollution and enhance air quality.

3.2.2 Carbon Cycle Feedbacks in a Changing Climate

O trees of life, when are you wintering?
Fused in harmonious unity we are not
like migratory birds, to the branches.
Overtaken constantly and too late,
we cross rapidly the winds,
and we fall into a stagnant lake.

R.M. Rilke, *Duino Elegies*

Despite such in-depth knowledge of the climate situation, we still know little about the ecological repercussions of this warming and even less about the extent to which ecosystem responses to warming will result in climatic feedback effects that either exacerbate (positive feedback) or mitigate (negative feedback) the warming thus worsening the state of the climate [23]. To reduce these uncertainties, many studies have been and should be undertaken. Among these researches, there is one which focuses on the carbon-cycle feedback.
The carbon cycle is the biogeochemical cycle that governs carbon exchange between the Earth's biosphere, geosphere, hydrosphere, and atmosphere. Carbon is the primary component of biological substances and a significant component of a variety of minerals, including limestone. Along with the nitrogen and water cycles, the carbon cycle is a series of processes that are necessary for the Earth to maintain life. It encompasses the recycling and reuse of carbon throughout the biosphere, as well as long-term processes of carbon sequestration in and release from carbon sinks.
As has been explained previously, continuous increases in the atmospheric concentration of carbon dioxide due to human-caused emissions are expected to result in substantial changes in the climate. Around half of the current emissions are absorbed by the ocean and land ecosystems, but this absorption is climate- and CO2-sensitive, producing a feedback loop [24]. According to a three-dimensional carbon-climate model, the carbon-cycle feedback has the potential to considerably accelerate climate change in the twenty-first century. It was discovered that in a "business as usual scenario", the terrestrial biosphere works as a net carbon sink until around 2050, but afterwards becomes a source [25]. At the current rate of deforestation and degradation (2022), tropical forests contribute nearly neutrally to the global carbon cycle, with intact and recovering forests absorbing as much carbon as is released through deforestation and degradation. However, tropical forests are likely to rapidly lose their ability to be carbon sinks due to ongoing vegetation loss

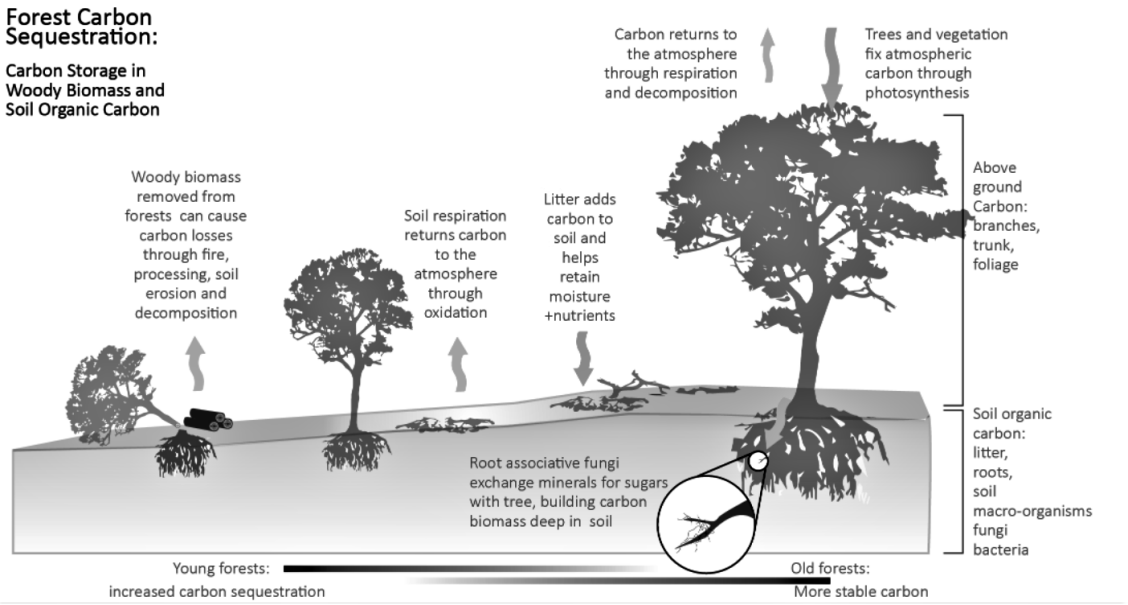

Figure 3.7: Forest carbon sequestration. The scheme illustrates how trees effectively capture carbon dioxide (CO2) and sequester it to reduce atmospheric CO2 concentrations. (Source: Board of Water and Soil Resources)

and the influence of climate change on the surviving trees' capacity to capture extra atmospheric carbon dioxide. As a result, this will make it more challenging to keep global warming below 2 degrees Celsius.
The following is an example of research on carbon-cycle feedback. Harte and colleagues have been studying the biogeochemical and vegetational consequences of heating a subalpine meadow since 1990 [23]. The heating was accomplished by overhead electric radiators that were programmed to continually imitate the model-predicted warmth. The plots feature habitats ranged from a mixed shrub-steppe and grassland vegetational community along a semi-arid ridge to a wet swale featuring a varied forb assemblage. The team has been monitoring soil temperature and moisture, floral productivity, phenology, and diversity, changes in net carbon storage above and below ground, mesofaunal soil biomass and species diversity, methane consumption rates, nitrogen pool sizes and turnover rates, and plant water stress. The major discoveries of the research group were the following:

- Heated-plot soils were, on average, 2°C hotter and 5–25 per cent drier than controls, with a strong diurnal cycle (up to 6°C warmer at midday) (Harte et al., 1995).
- In heated plots, the snow-free season was approximately one month longer.
- Heating promoted the growth of bushes such as sagebrush.
- Carbon capture was lost from heated plots in comparison to controls. This loss is attributed to a decrease in litter input to the soil rather than an increase in the rate of soil decomposition in heated plots (Saleska, Harte, and Torn, 1997).

- Heating increased mesofaunal diversity and biomass in cool, wet years but decreases them in hot, dry years (Harte, Rawa, and Price, 1996).
- Soil drying reduced methane consumption when the ambient soil was dry and increases it when the ambient soil was damp (Torn and Harte, 1996).

These findings indicate the possibility of numerous significant ecological feedback to climate change:

- A change in the rate at which soil bacteria consume methane as a result of climate change will alter the atmospheric concentration of this greenhouse gas. The results reveal that depending on the ambient soil moisture levels, this feedback can be either positive or negative.
- Because the albedo of vegetation varies between species and between forbs and shrubs, the observed shift toward sagebrush dominance will alter surface albedo. Radiometric measurements at the site indicated that this will result in decreased albedo, implying that the climate-induced shift in the composition of the vegetation community will result in positive feedback to warming.
- The observed loss of carbon stored in the biosphere in the heated plots indicates positive feedback to warming.

To further generalise these findings spatially and temporally, the essential issue of scale must be addressed. Simple multiplication by area is required for naive extrapolation from plot data to the landscape. This is unlikely to be attainable for one of two reasons: due to the small size of experimental plots, plot-scale data may be inapplicable to wider areas, and responses to climate change vary across the landscape. A viable strategy for optimising naive extrapolation is to use data on natural variation in ecosystem metrics along natural climate gradients. Assuming that ecological variation along natural temperature gradients reflects ecological responses to altered climate (i.e., variation in space is a proxy for variation in time), data from large-scale gradients can be used to forecast large-scale ecological reactions to warming. This, too, may fail due to a mismatch between the time scales for responding to relatively rapid anthropogenic climate change and adapting to slower natural climate variation along elevational gradients.
Another ongoing study on this subject is being conducted at the University of Bergen in Norway, where I did my internship. One of the main projects is called INCLINE, which stands for indirect climate change impacts on mountain plant communities. Their research is built on the evidence that climate change is already affecting plant communities in substantial ways, including range shifts to higher elevations and latitudes, as well as changes in biodiversity and ecosystem function. However, it is unknown to what extent these reactions reflect direct effects of altered climate or indirect effects mediated by altered species interactions. Unique interactions that occur because of species not migrating in unison could have a disproportionately big impact on species, community, and ecosystem responses to climate change, particularly if newly arrived species introduce novel functional features and trait combinations. Field experiments are done to explore and disentangle the consequences of climate warming's direct effects, indirect effects of changes in interactions between

already-existing species, and indirect effects of introducing novel species interactions. These studies, conducted in Western Norway, are expected to improve our understanding of how climate change affects plant populations, plant communities, biodiversity, and ecosystem function directly, indirectly, and through novel interactions. For example, one of the major funding of the project is that the evident shrub expansion is projected to feedback into climate change via changes in ecosystem functions and processes. Additionally, they discovered biome-wide trends toward higher canopy height and maximum observed plant height for the majority of vascular growth types, as well as a rise in leaf size and the number of invasive species [26] [27]. In conclusion, as previously seen, perturbed ecosystems experience rapid and nonlinear changes, resulting in "regime shifts" to a completely altered ecological state [28].
At the moment, the need to understand the magnitude, origin, scale, and reversibility of these changes as a result of humans' enormous impact on the natural world is critical. Tim Newbold and colleagues modelled ecological changes in four terrestrial biomes due to human-caused plant biomass reduction, such as that associated with agricultural land-use change [29]. They did discover that irreversible, non-linear reactions frequently occur when vegetation is removed at a rate greater than 80 per cent which occurs across almost ten per cent of the Earth's land surface. Substantial, irreversible changes in ecosystem structure are predicted at levels of vegetation removal comparable to those found in the most intensively exploited ecosystems.
The findings indicated that the expected significant increase in agricultural land conversion in the twenty-first century might result in widespread trophic cascades and, in some cases, permanent alterations to ecosystem structure.
Finally, one of the results I felt able to extrapolate is that the ecosystems that are subject to an extremely unstable climate condition tend to foster the growth of the vegetation in the primary stage of the succession. In contrast, the vegetation of subsequent succession phases will typically be energetically disadvantaged. This can cause a continuous regression of the ecosystem itself without it being able to reach a state of equilibrium through successive successions. Indeed, the distinction between the first and the later successive stages is that the first grows rapidly and disperses a large number of seeds (birch, pine, etc.), whereas the second grows slowly and disperses a small number of seeds (yew, oak, etc.). As a result of the rapid ecosystem change, only plants from the first succession stage would be advantaged, but these plants store much less CO2 compared to the ones in the late stages of the succession.

3.2.3 Management Strategies and Future Perspectives

I sat upon the shore
Fishing, with the arid plain behind me
Shall I at least set my lands in order?

T. S. Eliot, *The Waste Land*

Biodiversity protection and vegetation management are critical for the survival of the Earth's life support system. Adopting land use regulations to ensure this protection is likely one of the largest environmental challenges that the world will face this century, as this problem is often invisible to the public and resistant to typical regulatory laws. Besides the fact that there are numerous practical and moral reasons to be concerned about the rapid loss of species and habitats, intrinsic characteristics of ecosystem degradation need environmental conservation [30].
The Earth has already experienced periods of high carbon dioxide concentration, and we have observed periods of higher temperatures than now. The problem is the rate at which this transformation has occurred during the previous two centuries. Ecosystems are unable to adapt to this very rapid change and hence tend to regress, resulting in positive feedback loops with unknown effects.
Society and policymakers should try at any cost to avoid this positive feedback loop that would result in vegetation retrogression, as has occurred in the past, for example, during glaciations. During that period, numerous plant species were unable to survive in Europe and Africa, separated by the Mediterranean Sea, due to their reduced migration capacity. Consequently, they were unable to migrate toward Africa or vice versa. As a result, species such as the red cedar (Sequoia sempervirens) became extinct in Europe but not in America, a continent with a continuous transition between cooler and warmer climates, resulting in a severe reduction of European tree species.
We could and should take action to encourage more adapted species to migrate from warmer, drier habitats to more northern and currently cooler locations.
The application of the DynaMETE modelling approach may facilitate these practical aspects of vegetation management by providing future scenarios with physical characteristics of changing ecosystems and the physiological requirements of plants. Therefore, ecosystems could adapt by the relocation of selected plant species and varieties to more suitable locations.
In this regard, DynaMETE can play a significant, practical role that other static, ecological niche-related models may be unable to carry out. In fact, to make informed choices about how to manage forests for climate change mitigation, such as whether to harvest or protect trees, we must first have a better understanding of the causes and future behaviour of these carbon sinks.
Valentin Bellassen and Sebastiaan Luyssaert [31] recommended that forest management should prioritise "win-win" solutions, those that improve both forest stock and wood collection through measures such as forest replacement. Secondly, they proposed that wood should be used in the most carbon-efficient manner possible. Increased timber harvesting may be a useful climate-change mitigation approach, particularly if the forest sink begins to decline, but it must be targeted to uses that save the greatest tonnes of CO2 per cubic metre harvested. For example, in buildings, wood can be used in place of steel or cement for studs or walls and subsequently recovered and recycled. Thirdly, they stated that it is critical to prioritise forest management approaches that improve both the amount of wood produced and the carbon stock kept in the forest. For example, when not in conflict with other forest uses, replacing dying or low-productivity stands, protecting young sprouts from damage following harvest, planting more resilient tree mixes, and optimising fer-

tiliser use and tree growth in afforestation projects all contribute to climate change mitigation, and regardless of how the global carbon sink evolves.
To reforest properly, it would also be necessary to enact a law allowing only plants from the first succession stage to be planted initially (after deforestation, wildfires, droughts, etc.), followed by plants from the second succession stage and so on, thus replicating the natural ecological succession in forests. Alternatively, towards the end of the first cycle, a mechanism for preserving the wood may be developed to prevent it from being re-converted to CO2 by microbial respiration during decomposition.
In conclusion, after hundreds of years of forcing ecosystems to alter and deteriorate, it is now up to us to ensure that they won't regress and continue to adapt and protect us through the carbon cycle.
Simply reforesting is no longer sufficient since potential carbon sinks may become a threat to the climate itself, as has been illustrated previously.
Forest management has become more of a gamble than a scientific discussion in modern times. We can gain time as we learn more by employing "no-regret" solutions. A politician tossing a coin should not decide the fate of the world's forests. On the contrary, the time has come when the scientific community's recommendations will finally be heeded.

Conclusions

"Everything is like an ocean, everything flows and intermingles, you have only to touch it in one place and it will reverberate in another part of the world. Granted, it may seem mad to ask birds for pardon, but how much better it would be for the birds and the child and every other creature around you now if you yourself preserved your human dignity, even a little."

F. M. Dostoevskij, *The Brothers Karamazov*

This dissertation reviewed a physical approach to the study of disturbed ecosystems, based on the principle of maximum entropy.
In the first chapter, the concept of entropy was traced through its historical development to better comprehend its meaning and applicability.
Entropy is definable on a specific set of probability distributions of a thermodynamic system at equilibrium and it is a particular case of Shannon's measure of information (SMI). Where SMI is a measure of uncertainty about the state of the system. For systems with any number of particles far from equilibrium, it is advisable to use SMI instead of entropy.
On a probabilistic level, the principle of maximum entropy (MaxEnt) was explained as the fact that a system will always tend toward equilibrium because the probability associated with this state is the highest. As a result, the information entropy will be maximal at equilibrium, since the uniform distribution maximises the uncertainty about the system's state. Consequently, the MaxEnt inference procedure can produce the least-biased predictions of the shapes of probability distributions consistent with the prior knowledge constraining them.
The first sections of chapter two explained how the study of complex systems could provide an effective framework for analysing ecological systems and successions.
Successively, it was illustrated how the "MaxEnt Theory of Ecology" (METE), assuming prior knowledge in the form of static state variables, could predict the shapes of macroecological metrics in relatively static ecosystems. It was also evidenced that its predictions tend to fail in disturbed ecosystems with state variables that vary rapidly over time. For this reason, the dynamic evolution of this theory, DynaMETE, was presented in the last chapter.
DynaMETE predicts that different types of perturbations will result in different deviation patterns from static METE predictions on the distributions of species abundances and individual metabolic rates.
Additionally, DynaMETE forecasts state variable trajectories throughout an ecosys-

tem's recovery from a perturbed condition. After a fire or another disturbance, it was shown that forests are predicted to decline to a steady state where the abundance of small trees increases rapidly and then it self-restores to a quasi-steady state until the next disturbance.
In the last part of the dissertation, it is proposed to follow this model in the reforestation management strategies. Therefore, it is suggested to gradually reforest following the natural post-disturbance ecological succession, prioritising plants from the first ecological succession at the beginning. This can make ecosystems more resilient and capable of mitigating global warming.
In conclusion, this discussion aimed to demonstrate how the theoretical framework provided by physics and the principle of maximum entropy, in particular, can lead to a better understanding of disturbed ecosystems, of which we ourselves are part and contribute significantly to their change.
As limited human beings faced with the tangle of the universe's problems, we may feel like the Newtonian picture of a man playing with little stones on the shore of a vast ocean. Nonetheless, if handled properly, this game could provide powerful explanatory knowledge that could be used to improve ourselves and, consequentially, our environment.
This is because: "We do not need other worlds. We need mirrors" [32].

Appendix A

Maximizing information entropy by the method of Lagrange multipliers

We are interested in obtaining the least biased estimate of the functional form of a probability distribution p(n) that is subject to a set of K constraints arising from prior information and given in the form of K equations:

$$\sum_n f_k(n)p(n) =< f_k > \tag{A.1}$$

The averages (over the distribution p) of the functions f_k are indicated by $< f_k >$. These are the restrictions whose values we know through past measurements or other sources of information. The normalisation condition is an extra constraint:

$$\sum_n p(n) = 1 \tag{A.2}$$

The independent variable n is summed across all of its potential values, and the index k is a positive integer between 1 and K. Jaynes (1982) has demonstrated that the function p(n) that maximises "information entropy" is the answer to this problem.

$$I_p = -\sum_n p(n)log(p(n)) \tag{A.3}$$

within those constraints. Maximization is accomplished using Lagrange multipliers. The maximising process results in the following:

$$p(n) = \frac{e^{-\sum_{k=1}^{K} \lambda_k f_k(n)}}{Z(\lambda_1, \lambda_{..}\lambda_k)} \tag{A.4}$$

where the K numbers l_k are referred to as Lagrange multipliers and Z denotes the partition function:

$$Z(\lambda_1, \lambda_{..}\lambda_k) = \sum_n e^{-\sum_{k=1}^{K} \lambda_k f_k(n)} \tag{A.5}$$

The l_k are defined explicitly by the solutions to the following problems:

$$\frac{\delta log(Z)}{\delta \lambda_k} = - < f_k > \tag{A.6}$$

Although, in reality, the Lagrange multipliers are commonly computed by starting with Eqs A.1 and A.5, substituting Eq. A.4 for p(n), and solving the resulting simultaneous equations algebraically or numerically. Eq. A.5's form assures that the form of p(n) in Eq. A.4 is appropriately normalised, as required by A.2. For a detailed explanation of why A.4 is the version of $p(n)$ that maximises information entropy see [33]. In this dissertation, an intuitive method of comprehending the solution will be provided. Consider only two constraints. The constraint on normalisation in A.2 and:

$$\sum_n f(n)p(n) =< f > \tag{A.7}$$

In A.3, the maximization of I_p is equivalent to the one of the expression:

$$W = -\sum_n p(n)log(p(n)) - \lambda_0(\sum_n p(n) - 1) - \lambda_1(\sum_n f(n)p(n) - < f >) \tag{A.8}$$

If both the normalising requirement and the constraint specified in A.7 are satisfied.

The critical aspect of the procedure is that we wish to determine the maximum value of W. To maximise a functional (a function of a function), W, of p(n), we must set the derivative of W concerning p equal to zero. The derivative is as follows for each value of n:

$$\frac{dW}{dp} = -log(p(n)) - 1 - \lambda_0 - \lambda_1 f(n) \tag{A.9}$$

and setting this to zero results in the following:

$$p(n) = ke^{-\lambda_1} f(n) \tag{A.10}$$

where:

$$k = e^{-(\lambda_0+1)} \equiv \frac{1}{Z} = \frac{1}{\sum_n e^{-\lambda_1 f(n)}} \tag{A.11}$$

denotes the normalisation factor. Equation 5.14 follows directly from the restriction itself. While our derivation was for a single constraint plus a normalisation condition, Eqs A.4-6 are valid for any number of constraints. Additionally, the derivations above are easily generalised to joint probability distributions $p(n, m, ...)$. Sums over n are substituted by integrals over the continuous variable, x, in the case of a continuous distribution, p(x). A more general technique in this circumstance is to maximise the expression:

$$I_p = -\int dx p(x) log[p(x)/q(x)] \tag{A.12}$$

Where $q(x)$ is a reference distribution.
Occasionally, certain circumstances justify imposing the requirement that the shape of the probability distribution is independent of the units used to denote numerical values of quantities. The unit-independence requirement imposes an extra restriction, which may be resolved using the reference distribution [33]. In this dissertation, it won't be needed to deal with reference distributions since our distributions are either discrete or, in the case of energy distribution, units-independent.

Acknowledgments

The woods are lovely, dark and deep,
But I have promises to keep,
And miles to go before I sleep,
And miles to go before I sleep.

R. Frost, *Stopping by Woods on a Snowy Evening*

I wish to thank every single person who has given me new perspectives.
Because every gift is also a sacrifice, and every gift contains both a promise and a responsibility that allow us to continue our path.

Ci tengo a ringraziare ogni singola persona che mi abbia donato delle nuove prospettive. Perché ogni dono fatto è anche un sacrificio, ed ogni dono contiene in sé una promessa e una responsabilità che ci permette di continuare il nostro cammino.

Bibliography

[1] I. Calvino and W. Weaver. *Invisible Cities*. Calvino invisible. Harcourt Brace Jovanovich, 1974.

[2] Ilya Prigogine and Dilip K Kondepudi. *Termodinamica: dalle macchine termiche alle strutture dissipative*. Bollati Boringhieri, 2002.

[3] Arieh Ben-Naim. "Information, Entropy, Life and the Universe". In: *What We Know and What We Do Not Know* (2015).

[4] Enrico Fermi. *Thermodynamics*. Dover Publications, 1956.

[5] Arieh Ben-Naim. *A farewell to entropy: Statistical thermodynamics based on information: S*. World Scientific, 2008.

[6] Carlo Rovelli. *The order of time*. Penguin, 2019.

[7] Walter T Grandy Jr. *Entropy and the time evolution of macroscopic systems*. Vol. 10. Oxford University Press on Demand, 2008.

[8] John Harte. *Maximum entropy and ecology: a theory of abundance, distribution, and energetics*. OUP Oxford, 2011.

[9] Olivier Rioul. "This is it: A primer on Shannon's entropy and information". In: *Information Theory*. Springer, 2021, pp. 49–86.

[10] Claude Elwood Shannon. "A mathematical theory of communication". In: *The Bell system technical journal* 27.3 (1948), pp. 379–423.

[11] Giorgio Parisi. "Complex systems: a physicist's viewpoint". In: *arXiv preprint cond-mat/0205297* (2002).

[12] Alberto Gandolfi. *Formicai, imperi, cervelli: introduzione alla scienza della complessità*. Edizioni Casagrande, 1999.

[13] Henri Poincaré. "Le hasard". In: *Revue du mois* 3 (1907), pp. 257–276.

[14] David Ruelle. "Chance and chaos". In: *Chance and Chaos*. Princeton University Press, 2020.

[15] D Bazeia et al. "Environment driven oscillation in an off-lattice May–Leonard model". In: *Scientific Reports* 11.1 (2021), pp. 1–8.

[16] Thierry Mora et al. "Local equilibrium in bird flocks". In: *Nature physics* 12.12 (2016), pp. 1153–1157.

[17] Nicholas B Davies, John R Krebs, and Stuart A West. *An introduction to behavioural ecology*. John Wiley & Sons, 2012.

[18] James Peter Kimmins. "Forest ecology". In: *Fishes and forestry: Worldwide watershed interactions and management* (2004), pp. 17–43.

[19] John Harte, Kaito Umemura, and Micah Brush. "DynaMETE: a hybrid MaxEnt-plus-mechanism theory of dynamic macroecology". In: *Ecology letters* 24.5 (2021), pp. 935–949.

[20] John Harte and Erica A Newman. "Maximum information entropy: a foundation for ecological theory". In: *Trends in ecology & evolution* 29.7 (2014), pp. 384–389.

[21] Richard P Allan et al. "IPCC, 2021: Summary for Policymakers". In: (2021).

[22] Hans O Pörtner et al. "Climate change 2022: impacts, adaptation and vulnerability". In: (2022).

[23] John Harte and Rebecca Shaw. "Shifting dominance within a montane vegetation community: results of a climate-warming experiment". In: *Science* 267.5199 (1995), pp. 876–880.

[24] Markus Reichstein et al. "Climate extremes and the carbon cycle". In: *Nature* 500.7462 (2013), pp. 287–295.

[25] Peter M Cox et al. "Acceleration of global warming due to carbon-cycle feedbacks in a coupled climate model". In: *Nature* 408.6809 (2000), pp. 184–187.

[26] Siri L Olsen et al. "From facilitation to competition: Temperature-driven shift in dominant plant interactions affects population dynamics in seminatural grasslands". In: *Global Change Biology* 22.5 (2016), pp. 1915–1926.

[27] Vigdis Vandvik and H John B Birks. "Partitioning floristic variance in Norwegian upland grasslands into within-site and between-site components: are the patterns determined by environment or by land-use?" In: *Plant ecology* 162.2 (2002), pp. 233–245.

[28] Mark Wilber Erica A. Newmann and John Harte. *Disturbance ecology meets macroecology: A new method for cross-system comparisons of ecosystems in transition.* Conference: 99th ESA Annual Convention, 2020.

[29] Tim Newbold et al. "Non-linear changes in modelled terrestrial ecosystems subjected to perturbations". In: *Scientific reports* 10.1 (2020), pp. 1–10.

[30] Corey JA Bradshaw et al. "Underestimating the challenges of avoiding a ghastly future". In: *Frontiers in Conservation Science* (2021), p. 9.

[31] Aerin L Jacob, Sarah Jane Wilson, and Simon L Lewis. "Forests are more than sticks of carbon". In: *Nature* 507.7492 (2014), p. 306.

[32] Andrei Tarkovsky and Stanislaw Lem. *Solaris.* Artificial Eye, 1972.

[33] Edwin T Jaynes. "Prior probabilities". In: *IEEE Transactions on systems science and cybernetics* 4.3 (1968), pp. 227–241.